



IntechOpen

Thermosoftening Plastics

*Edited by Gülşen Akın Evingür,
Önder Pekcan and Dimitris S. Achilias*



Thermosoftening Plastics

*Edited by Gülşen Akın Evingür,
Önder Pekcan and Dimitris S. Achilias*

Published in London, United Kingdom



IntechOpen





Supporting open minds since 2005



Thermosoftening Plastics

<http://dx.doi.org/10.5772/intechopen.83323>

Edited by Gülşen Akın Evingür, Önder Pekcan and Dimitris S. Achilias

Contributors

Taofik Azeez, Miguel Angel Hidalgo-Salazar, Juan Pablo Correa-Aguirre, Juan Manuel Montalvo-Navarrete, Diego Fernando Lopez-Rodriguez, Andrés Felipe Rojas-González, Elen Pacheco, Fernanda Santos, Leonardo Canto, Ana Silva, Leila Visconte, Javier Quagliano Amado, Feng Jiang, Chenqian Pan, Yanxiong Fang, Fenfen Wang, Ranran Jian, Weimin Yang, Hongbo Chen

© The Editor(s) and the Author(s) 2020

The rights of the editor(s) and the author(s) have been asserted in accordance with the Copyright, Designs and Patents Act 1988. All rights to the book as a whole are reserved by INTECHOPEN LIMITED. The book as a whole (compilation) cannot be reproduced, distributed or used for commercial or non-commercial purposes without INTECHOPEN LIMITED's written permission. Enquiries concerning the use of the book should be directed to INTECHOPEN LIMITED rights and permissions department (permissions@intechopen.com).

Violations are liable to prosecution under the governing Copyright Law.



Individual chapters of this publication are distributed under the terms of the Creative Commons Attribution 3.0 Unported License which permits commercial use, distribution and reproduction of the individual chapters, provided the original author(s) and source publication are appropriately acknowledged. If so indicated, certain images may not be included under the Creative Commons license. In such cases users will need to obtain permission from the license holder to reproduce the material. More details and guidelines concerning content reuse and adaptation can be found at <http://www.intechopen.com/copyright-policy.html>.

Notice

Statements and opinions expressed in the chapters are these of the individual contributors and not necessarily those of the editors or publisher. No responsibility is accepted for the accuracy of information contained in the published chapters. The publisher assumes no responsibility for any damage or injury to persons or property arising out of the use of any materials, instructions, methods or ideas contained in the book.

First published in London, United Kingdom, 2020 by IntechOpen

IntechOpen is the global imprint of INTECHOPEN LIMITED, registered in England and Wales, registration number: 11086078, 7th floor, 10 Lower Thames Street, London, EC3R 6AF, United Kingdom

Printed in Croatia

British Library Cataloguing-in-Publication Data

A catalogue record for this book is available from the British Library

Additional hard and PDF copies can be obtained from orders@intechopen.com

Thermosoftening Plastics

Edited by Gülşen Akın Evingür, Önder Pekcan and Dimitris S. Achilias
p. cm.

Print ISBN 978-1-83880-612-5

Online ISBN 978-1-83880-613-2

eBook (PDF) ISBN 978-1-83880-614-9

We are IntechOpen, the world's leading publisher of Open Access books Built by scientists, for scientists

4,600+

Open access books available

120,000+

International authors and editors

135M+

Downloads

151

Countries delivered to

Our authors are among the
Top 1%

most cited scientists

12.2%

Contributors from top 500 universities



WEB OF SCIENCE™

Selection of our books indexed in the Book Citation Index
in Web of Science™ Core Collection (BKCI)

Interested in publishing with us?
Contact book.department@intechopen.com

Numbers displayed above are based on latest data collected.
For more information visit www.intechopen.com



Meet the editors



Dr. Gülşen Akın Evingür, born in 1976, is currently working as Associate Professor at Pîrî Reis University, Istanbul, Turkey. She completed her BSc at Yildiz Technical University, Istanbul, Turkey and her PhD at Istanbul Technical University in 1996 and 2011, respectively. She has been engaged in various academic studies in the fields of composite gels and their optical, electrical, and mechanical properties. She has more than 40 SCI articles, 3 chapters, and 4 projects.



Professor Pekcan received his MSc degree in physics at the University of Chicago in June 1971. His PhD thesis was accepted in solid state physics at the University of Wyoming in 1974. He visited ICTP Trieste as a visiting scientist in 1980. He was a visiting scientist at the Technical University of Gdansk in Poland between 1980-1981. He worked as visiting professor at the University of Toronto, Department of Chemistry between 1981-1988. He was appointed as full Professor at the Istanbul Technical University in Department of Physics and worked there between 1988 and 2005. He is currently the Professor at Kadir Has University in the Department of Bioinformatics and Genetics. Since 2012, he has been a member of the Science Academy. He has more than 360 SCI articles, 25 chapters, and 10 projects.



Dr. Dimitris S. Achilias is a Professor of Polymer Chemistry and Technology, Director of the Lab Polymers and Dyes Chemistry and Technology, and Vice-Head of the Department of Chemistry, Aristotle University of Thessaloniki (AUTH), Greece. He completed his BSc and Ph.D. at the Chemical Engineering Department, AUTH in 1985 and 1991. From his research on the polymer thermo-chemical recycling, synthesis of polymer nanocomposites and polymerization or degradation kinetics, he has published over 145 research papers, with h-index 40 and more than 5000 citations (Scopus). He has been the editor of 2 books on recycling (IntechOpen) with over 120,000 downloads and is a member of the Editorial Board of Polymers (MDPI). He has participated in several research projects and holds 3 patents.

Contents

Preface	XIII
Chapter 1 Processing and Properties of Plastic Lumber <i>by Fernanda A. dos Santos, Leonardo B. Canto, Ana Lúcia N. da Silva, Leila Lea Yuan Visconte and Elen B. A. Vasques Pacheco</i>	1
Chapter 2 Multi-Field Synergy Process for Polymer Plasticization: A Novel Design Concept for Screw to Facilitate Phase-to-Phase Thermal and Molecular Mobility <i>by Ranran Jian, Hongbo Chen and Weimin Yang</i>	17
Chapter 3 Cellulose-Based Thermoplastics and Elastomers via Controlled Radical Polymerization <i>by Feng Jiang, Fenfen Wang, Chenqian Pan and Yanxiong Fang</i>	35
Chapter 4 Thermoplastic Recycling: Properties, Modifications, and Applications <i>by Taofik Oladimeji Azeez</i>	53
Chapter 5 Thermal Resistance Properties of Polyurethanes and Its Composites <i>by Javier Carlos Quagliano Amado</i>	73
Chapter 6 Recycled Polypropylene-Coffee Husk and Coir Coconut Biocomposites: Morphological, Mechanical, Thermal and Environmental Studies <i>by Miguel Ángel Hidalgo-Salazar, Juan Pablo Correa-Aguirre, Juan Manuel Montalvo-Navarrete, Diego Fernando Lopez-Rodriguez and Andrés Felipe Rojas-González</i>	87

Preface

Thermosoftening Plastics are polymers that can be manipulated into different shapes when they are hot, and the shape sets when it cools. If we were to reheat the polymer again, we could re-shape it once again. Modern thermosoftening plastics soften at temperatures anywhere between 65°C and 200°C. In this state, they can be moulded in a number of ways. They differ from thermoset plastics in that they can be returned to this plastic state by reheating. They are then fully recyclable because thermosoftening plastics do not have covalent bonds between neighbouring polymer molecules. Methods of shaping the softened plastic include: injection moulding, rotational moulding, extrusion, vacuum forming, and compression moulding.

Additionally, the large amount of plastics produced and consumed in several areas of everyday life, together with their low biodegradability and short use have resulted in enormous waste amounts of these materials. Thus, **polymer recycling** is more than imperative. Several recycling methods have been presented in literature, aiming for the recovery of monomers or other secondary value-added materials as well as for converting polymeric wastes into fuels or energy. Therefore, in this book, methods for recycling of thermoplastic polymers are included, together with potential uses of the recycled materials.

This book shows three areas of thermosoftening plastics, thermoplastic materials, and the characterization of them, as well as some elements of recycling thermoplastics, together with their applications.

This book comprises six chapters. First chapter covers composition and processing conditions of plastic lumber and their characterizations. The second chapter shows a new screw design to facilitate phase to phase thermal and molecular mobility for polymer plasticization. The third chapter describes the controlled radical polymerization for cellulose based thermoplastics and elastomers. The fourth chapter presents the properties, modifications, and applications of thermoplastic recycling. The fifth chapter highlights thermal resistance properties of polyurethanes and its composites. The final chapter shows the morphological, mechanical, thermal and environmental studies of recycled polypropylene-coffee husk and coir coconut biocomposites.

We would like to take this opportunity to thank all the researchers who have made direct contributions to the writing of this book. Also, we would like to thank all the editorial members of IntechOpen, in particular, Mrs. Dajana Pamac, author service manager, for her effective editing and support during different stages of the production of this book.

Gülşen Akın Evingür
Faculty of Engineering,
Pîrî Reis University,
Tuzla, İstanbul, Turkey

Önder Pekcan
Faculty of Engineering and Natural Sciences,
Kadir Has University,
Cibali, İstanbul, Turkey

Dimitris S. Achilias
Department of Chemistry,
Aristotle University of Thessaloniki,
Thessaloniki, Greece

Processing and Properties of Plastic Lumber

*Fernanda A. dos Santos, Leonardo B. Canto,
Ana Lúcia N. da Silva, Leila Lea Yuan Visconte
and Elen B. A. Vasques Pacheco*

Abstract

Plastic residue can be processed into composites using wood flour, mineral fillers, plant or synthetic fibers to obtain plastic lumber, a substitute material for natural wood. The composition and processing conditions are largely responsible for the final characteristics of the plastic lumber. Factors such as density, particle size and moisture content in the material to be processed require extruders with specific technical characteristics, in order to reduce the residence time of the plastic inside the equipment, maintain a constant feed rate and ensure good degassing and homogenization of the components. The composites can be manufactured using single-screw, co- or counter-rotating conical or parallel twin-screw extruders. Plastic lumber exhibits different physical and mechanical properties from natural wood, including lower stiffness (elastic modulus) and superior weathering resistance.

Keywords: recycling, plastic lumber, plastic, reprocessing, property

1. Introduction

The increasing generation of plastic waste by industry and in urban areas in recent years has prompted concern in society and efforts to recycle discarded and unused plastic materials [1–3]. Among the alternatives to minimize plastic waste accumulation is using postconsumer plastics to produce plastic lumber as a substitute for natural wood [4, 5].

According to the American Society for Testing and Materials (ASTM) [4, 5], the term plastic lumber applies to products made primarily from plastic (with or without additives), with a rectangular cross-section and size typical of wood products used for building. However, plastic lumber products can also exhibit a circular cross-section, as well as other shapes, with applications such as furniture and farming, among others.

Most plastic lumber products on the market are made from polyethylene, particularly high-density polyethylene (HDPE), but can be obtained using polymers, such as polypropylene (PP), polystyrene (PS) and polyvinyl chloride (PVC), or mixtures of different plastic wastes [6]. Additionally, fillers and additives, such as natural fibers, sawdust [7–9], mineral fillers and glass fiber, can be added to plastic lumber formulations [10, 11].

Both composition and processing conditions are largely responsible for the final characteristics of plastic lumber products. Research and patents demonstrate that



Figure 1.
Examples of different plastic lumber profiles.

different processes and recycling equipment are used to produce plastic lumber [12–15]. Factors such as the properties of the material to be processed, how plastic waste reaches the processing stage, the presence of additives and the moisture content of the material require extruders with specific technical characteristics when compared to processing virgin plastic [12]. These characteristics include shortening the residence time of the plastic inside the equipment, maintaining a constant feed rate inside the extruder and good degassing and homogenization of the material.

Due to their natural origin, wood-based products may exhibit a series of structural defects, such as knots, cracks, warping, wormholes and fungal damage, as well as low-dimensional stability and other imperfections resulting from varying moisture content and drying, which significantly influence the final strength of products and are difficult to control [16].

Plastic lumber has several advantages over natural wood in a number of applications and can be made from used plastics such as bottles, cups, packing and other products with a short useful life, thereby minimizing the accumulation of plastic material in the environment. It can be worked using conventional carpentry tools and planed, sawn, drilled and nailed in the same way as natural wood [6]. The advantages of plastic lumber over natural wood include being waterproof, resistant to weathering, mold and borers, and not requiring regular painting or maintenance, meaning it can be used in environments that natural wood would be unable to withstand for long periods. These include wet or underwater structures such as sea dikes in coastal areas [17, 18]. Plastic lumber can also be used to protect forests by preventing new trees from being felled to make furniture, decking, fencing and piers [6]. Different plastic lumber profiles are shown in **Figure 1**.

2. Background

The oldest records of plastic lumber date back to the early 1970s, when processing techniques for the material were developed in Europe and Japan. The resulting plastic lumber consisted primarily of post-industrial plastic scrap, which was the only source of low-cost plastic available at the time. Nevertheless, the plastic lumber industry did not initially experience significant growth [17].

The Klobbie intrusion system was developed in the 1970s and is based on a combination of conventional extrusion and injection processes. It consists of an extruder coupled to several rotating molds and a tank of cooling water. The plastic material is mixed and melted in the extruder and then forced into one of the molds. Once the

mold is filled, the carousel rotates to allow another mold to be filled. The filled mold is then cooled by passing it through the tank of chilled water before ejecting it. The process is capable of producing thick wall moldings and linear profiles [13, 17, 19].

Technologies developed from the 1980s onwards include Advanced Recycling Technology (Belgium), Hammer's Plastic Recycling (United States) and Superwood (Ireland). The equipment developed by Advanced Recycling Technology, denominated ET/1 (Extruder Technology 1), is an adiabatic extruder capable of processing mixed waste plastics with different densities to produce posts, rods, stakes, boards, etc. The process used by Hammer's Plastic Recycling differs somewhat from the Klobbie system and generates thick wall parts such as pallets, animal feeders and bench brackets, as well as linear profiles such as planks [19].

Other processes have been developed for the continuous extrusion of profiles under cooling, such as Mitsubishi Petrochemical's Reverzer process to manufacture large cross-section products. There have also been historical experiments with compression molding, such as the Recycloplast process developed in Germany [17, 19] to produce thick wall parts such as pallets, benches and grates.

Following the abovementioned efforts in equipment design, attention turned to the composition of plastic lumber, and wood-plastic composites (WPC) emerged in the 1990s to replace wood with recycled plastic lumber in decking and fencing [16, 18]. Also in the 1990s, pioneering studies on plastic recycling for the development of plastic lumber began at the Institute of Macromolecules of the Federal University of Rio de Janeiro, under the supervision of Professor Eloisa Biasotto Mano, the first line of research in the area at university level. In 2009, at the same institute, a laboratory scale plastic recycling machine and pilot scale equipment were developed at the Center of Excellence in Recycling and Sustainable Development (NERDES).

Despite the development of technology to obtain recycled PL, lack of standardization prevented its use by the construction industry in the early 1990s, particularly in structural applications. The Plastic Lumber Trade Association worked to establish a set of ASTM standards initially applicable to plastic lumber made from high-density polyethylene (HDPE) [16, 20].

Wood-plastic composites (WPC) are an important segment of the plastic lumber market [16, 21].

In addition to their application in decking, American manufacturers use WPC to replace plywood in fencing, windows and panels [22], and the composites are also being considered in the production of roofing and cladding [6, 23, 24].

Plastic lumber has been used in marine environments as a replacement for natural wood treated with chromated copper arsenate (CCA) due to its rot resistance and high durability, as well as the environmental preservation it provides because no harmful chemicals are used in its manufacture [25, 26]. Recent studies have shown that copper, chromium and arsenic are continuously released by CCA-treated wood in marine environments [18, 27–29]. By contrast, the disposal of metal and organic contaminants from plastic lumber in river or seawater is low and no highly toxic compounds have been identified [30].

The timber market and industry are searching for more sustainable products, and plastic lumber is a viable alternative in railway tie manufacturing, for example [31].

3. Processing

Although the composition of plastic lumber varies, the market consists primarily of companies that manufacture HDPE-based plastic lumber and those that use plastic composites and wood waste [16]. This has contributed to greater interest in the search for wood-plastic composite (WPC) processing technologies.

Composite	Type of screw extrusion	Tensile strength (MPa)	Izod impact strength (kJ/m ²)—unnotched
PP/wood flour: 70/30 wt%	Single-screw	25	7
	Twin-screw	28	10

Table 1. Mechanical properties of polypropylene (PP) composites filled with wood flour made using different manufacturing processes [33].

In general, WPC are manufactured by extrusion, whereby the molten material is forced through a matrix and formed into a continuous profile in the desired shape. Extrusion is a process whereby plastic and other additives are melted, mixed, homogenized and formed into long continuous profiles typical of construction materials [21], in either simple solid shapes or complex hollow structures [6, 22, 32].

Wood-plastic composites can be produced in single-screw, co- or counter-rotating conical or parallel twin-screw extruders or piggyback extruders [21, 32]. Manufacturing companies use different types of extruders and processing strategies [21], with some employing a single-screw extruder for the final shaping process [21], or use a twin-screw extruder for mixing and mold the final artifact in another extruder. Other manufacturing companies use a range of piggyback extruders, one to homogenize the mixture and others for shaping [21]. The screws are specifically designed to bind the wood residue to the polymer matrix in order to evenly disperse it in the polymer [24].

Various types of extruders used lead to significant differences in the properties of plastic lumber. Yang et al. [33] studied the properties of WPC and polypropylene (PP) composites filled with rice husk flour (RHF) made using different manufacturing processes. The authors used single- and twin-screw extrusion systems and found that WPC processed in a twin-screw extruder exhibited better mechanical properties when compared to the composite obtained by single-screw extrusion, attributing these results to better wood dispersion in the former process (Table 1). They also observed that the presence of a maleic anhydride-grafted polypropylene (MAPP) compatibilizer [34, 35] improved the mechanical properties of the RHF-filled PP composite when compared to the composite without the compatibilizing agent [33].

In addition to extrusion, processing technologies such as injection and compression molding can also be used to produce WPC [36], with the composite formulation adjusted according to processing requirements. For example, the low viscosity needed for injection molding may limit the wood residue content in the formulation [21]. Experts from the WPC industry claim that injection molding has significant potential, with the ability to produce complex shapes, whose growing number of applications includes products such as tiles and cladding [9, 37].

A number of aspects should be considered when processing WPC. Moisture content and particle size should be tightly controlled to prevent discontinuities and parts with defects due to the presence of bubbles or stains caused by thermo-oxidative processes [34, 38]. Thus, as a primary requirement, wood waste must be pre-dried, and degassing zones must be used to remove residual moisture during processing. One of the factors directly affected by the moisture content of the lignocellulosic reinforcement is the output of the extrusion line: the higher the moisture content of the particles, the lower the throughput due to the longer residence time needed to devolatilize the composite [39, 40]. As such, the longer the material remains inside the extruder, the more susceptible it is to thermomechanical degradation.

Additionally, the low thermal stability of cellulose (200–220°C) is a limiting factor in the process, except when residence times are minimal. Exposing wood waste

to temperatures above this range releases volatile compounds, causing discoloration and odor and making the composite brittle [36]. This has restricted the use of thermoplastics in WPCs to major commercial resins such as polyolefins (PE and PP), styrenics (PS, HIPS and ABS) and polyvinyl chloride (PVC), which can be processed at temperatures below cellulose degradation [9, 21].

Another factor that hampers WPC processing is the low density of wood waste, which makes it difficult for the residue to pass through the small openings typical of plastic processing equipment, leading to a decline in throughput [41].

Processing WPC can be classified into four distinct categories. In pre-drying and premixing, wood waste is pre-dried at moisture levels below 1% and the material is fed into a counter-rotating twin-screw extruder along with the polymer, usually in the form of a powder. The dry blend of polymer, wood and additives is prepared in high-intensity Henschel mixers before being fed into the extruder [42]. The dry blend is then fed into the extruder using a Crammer feeder. Given the narrow residence time distribution of the material in the system and limited thermal energy generation, counter-rotating twin-screw extruders are used primarily for PVC conversion due to its thermal instability [12, 40].

Pre-drying wood and feeding the polymer and wood residue into the extruder separately (pre-dry; split feed) allow better control of the residence time of the wood filler during processing [42]. High capacity twin-screw extruders with side feeders are generally used in this type of process, where the residue is mixed with the molten polymer, passing through distributive mixing and degassing zones.

A third process involves feeding wet wood residue into the extruder first, followed by the molten polymer (wood first; melt feed). Two simultaneously operating extruders are needed, the first to dry the wood and a second smaller extruder to plasticize the polymer and additives [42]. An example of this type of system is the WoodTruder[®], equipped with a counter-rotating twin-screw extruder designed to remove moisture from wood fiber even at high levels (1–8% moisture content). The process includes a primary counter-rotating parallel twin-screw extruder (L/D 28:1) and a satellite extruder with either one or two screws depending on the polymer used. The primary extruder dries the wood fiber and then mixes it with the polymer, while the satellite extruder melts the polymer and returns it to the primary extruder [32].

In many ways, processing wood waste in parallel twin-screw extruders is similar to processing neat polymers [32]. Although standard feeders are generally used for polymers, gravimetric ones are needed to feed the wood waste into the twin-screw extruder. The feed rate is automatically adjusted by the controller to increase feeding efficiency, circumventing the problems caused by wood fiber bulk density fluctuation. The screws drive the residue forward as the heat from the barrel and screws is transferred to the material, heating both the wood and the water in the wood fibers and releasing moisture.

The WoodTruder system uses a set of two extruders. The wood fibers enter the feeding zone of a counter-rotating parallel twin-screw extruder with a special venting section to draw moisture, while the molten polymer is added in sequence via a side mounted, single-screw extruder. The mixture then enters the compression section of the primary extruder to more easily blend the two components [32, 42]. Degassing occurs after compression in order to remove volatile components from the polymer or residual moisture from the wood fiber. The completely dried homogenized mixture then moves into a different zone to increase the pressure flow through the head. Melting temperatures are typically between 170 and 185°C. Temperatures above 200°C should be avoided in order to reduce wood degradation. In addition to wood fibers, the WoodTruder system can also process rice hulls, sisal, peanut shells and a range of other materials [32].

The fourth WPC production process uses wet wood and separate feeding of the polymers and additives (wood first, split feed), whereby the wet wood residue is fed into the extruder first and the polymer and additive are subsequently introduced into the barrel via a side feeder. However, this process typically requires longer extruders (L/D 44 or 48:1) with degassing zones located close to the feeding zone to remove moisture from the wood, which is not always possible [42].

Changes in moisture can lead to melt consistency problems in processes where an extruder is used to dry the wood fiber, making pre-dried wood a safer alternative.

4. Properties

The physical and mechanical properties of plastic lumber differ from natural wood parts with the same dimensions [6, 16, 17]. One of the most significant differences is the lower stiffness (modulus of elasticity) of plastic lumber. Pine and oak typically have a modulus of at least 6.9 GPa, which is higher than that of plastic lumber without a filler.

Mechanical properties of polymers depend on the time and temperature at which stress is applied. Plastic lumber is subject to permanent deformation (creep) under long-term loads [17, 18]. The strain rate depends on the amount and duration of the stress applied, as well as temperature. Moreover, changes in size as a result of temperature are more marked in plastic lumber than natural wood [8].

Drawbacks of plastic lumber include its low resistance to heat and flame in relation to the slow burn of natural wood, intense heating when exposed to direct sunlight and slow cooling. These problems can be mitigated by placing a small opening between adjacent planks, allowing air to flow around them and generating a cooling effect [17] or by producing hollow or foamed profiles.

These differences mean plastic lumber is generally unsuitable as a direct replacement for natural wood of a similar shape and size, since the resulting structures may exhibit unacceptable deformation under load or buckle over time due to their own weight [17, 43].

The abovementioned features limit the use of plastic lumber in structural applications such as support posts for decks. Most plastic lumber in decks is used as flooring, where the flexural modulus is less critical. The properties of this synthetic material change with the addition of fillers or compatibilizers or by promoting crosslinking of the base polymer [32].

Different compositions have been used to modify the physical and mechanical properties of plastic lumber and thereby ensure a larger number of applications with better results, the most noteworthy being those containing wood waste. One of the benefits of wood-plastic composites (WPC) is that they provide an alternative for waste from the lumber industry, which requires special attention as a low density material that needs a significant amount of storage space. Furthermore, using plant fibers in polymer composites improves the mechanical performance of conventional plastics, reduces environmental impacts, ensures recyclability and lowers costs [9, 44].

Wood fillers also increase the stiffness of composites, improve their machinability and are less expensive than polymer resin. Given the increasing use and importance of WPC, different authors have studied the effects of adding wood fiber on the mechanical properties of plastic lumber [7, 9, 43, 45–47]. **Table 2** shows flexural modulus results of three composites made with the same filler, however in three different polymer matrices.

Research by Solís and Lisperguer [48] indicates that adding wood waste reduced the impact strength of WPC (**Table 3**).

Type of polymeric matrix in composite	Flexural modulus (GPa)
Polyethylene	1.7
Polypropylene	2.1
Polystyrene	4.9

Table 2.
Flexural modulus values as a function of plastic matrix in lumber samples with 25 wt% of wood flour [27].

Amount of wood flour (wt%)	Impact strength (kJ/m ²)
0	10.0
20	2.3
10	1.9

Table 3.
Impact strength of HDPE and wood flour composite [48].

Carroll et al. [43] evaluated the shear strength of Duraboard[®] plastic lumber planks made from a compound of recycled plastic and sawdust under load and high temperatures. Mechanical tests were also conducted simulating winter (−23.3°C) and summer conditions (40.6°C). The results under winter temperatures showed that plastic lumber exhibits tension, compression and flexure properties comparable to those of natural wood, but lower strength under simulated summer conditions, albeit with acceptable values. The findings demonstrate that plastic lumber pieces should be larger than their natural wood counterparts to compensate for these differences. The high temperature modulus of the plastic lumber was lower than that of natural wood, which increases structural deformation when submitted to loading. This behavior is evident in a number of decking applications. The low stiffness of plastic lumber planks makes them prone to buckling under their own weight. In the case of long plastic lumber planks, the distance between the support posts should be smaller and/or thicker planks should be used when compared to natural wood decking [17, 18, 43].

Glass fiber has also been used as a filler to reinforce WPC, which can significantly increase the elastic modulus and stiffness of PL, albeit not to the extent of natural wood [10, 11].

Breslin et al. [27] studied long-term variations in the mechanical properties of recycled plastic lumber made from HDPE with 20% fiberglass used to build a pier. The results of dimensional stability assessment indicated no significant variation in sample dimensions. Additionally, hardness showed no significant change over time.

However, individual hardness measurements of the exposed cross-section varied considerably along the surface (22 ± 16–36 ± 9 units on the Shore D scale). The authors attributed this result to the porous internal structure of the plastic lumber, making it denser closer to the surface. As such, since the properties of the porous core differ from those at the outer surface, plastic lumber should always be tested at different internal and external points in order to obtain conclusive results [43]. There was no significant difference in compressive strength until the nineteenth month of exposure to extreme weather conditions. The flexural modulus showed a high degree of variation between duplicate samples of plastic lumber profiles. Although the flexural modulus measured in the cross-sectional direction did not vary significantly between the first and nineteenth month of exposure, a substantial variation was measured over time, with the greatest change recorded in the summer months. According to the authors [43], varying cross-sectional bending

Composition (wt%)		Tensile modulus (MPa)
Glass fiber	Wood fiber	
0	0	810
25	0	2310
0	8	980
25	8	2900

Table 4.

Plastic lumber tensile modulus of HDPE reinforced with glass fiber and/or wood fiber [10].

modulus values may be due to the heterogeneity of the material. Significant bending modulus variations should be taken into account when designing plastic lumber structures.

George and Dillman [10] analyzed glass fiber filler used to reinforce plastic lumber made from recycled HDPE. Additionally, the authors tested different formulations containing wood fiber and compared the effect of the content of each filler on the mechanical properties of the composites. The results showed that glass fiber significantly improved stiffness and promoted a greater increase in tensile and flexural moduli when compared to wood fiber (**Table 4**).

In some cases, adding glass fiber to plastic lumber for applications that come into contact with the skin, such as benches and handrails, can cause skin irritation. Glass fiber is also associated with a disease that affects the lungs in a manner similar to asbestos [41]. As such, these types of applications should be avoided.

Ledur et al. [49] developed a plastic lumber made from a mixture of polyethylene (PE) urban waste and ethylene-vinyl acetate (EVA) copolymer industrial waste filled with calcium carbonate. It was compounded in a Drais batch mixer and hot compression molded as rectangular-shaped sheets. An urban trash container prototype was prepared from the plastic sheets and a hundred trash containers passed a pilot test.

Other types of fillers have been studied for use in plastic composites, particularly natural components such as sisal, jute, hemp and coconut fiber [9, 11, 50, 51]. Wambua et al. [11] produced polypropylene composites reinforced with lignocellulosic fibers and found mechanical property values similar to those reported in the literature for glass fiber-reinforced PP composites.

Natural fibers offer a number of advantages over mineral or synthetic fillers as reinforcement in polymer composites, including less equipment abrasion, lower density of the final product, low cost and greater abundance.

One of the difficulties encountered in plastic lumber technology is the wide range of raw polymers, whose composition is beyond industrial control. This diversity results in polymer blends with coarse phase separated morphologies, which inevitably lead to incompatibility of properties. Possible solutions include adding a compatibilizer to the polymer blend or generating in situ molecular changes in the components through reactive extrusion to allow bonds to form between the polymer chains of the different phases [34].

Wood fiber/polyolefin composites widely used to obtain plastic lumber are incompatible because the thermoplastic material is nonpolar, while cellulose is polar, thereby requiring compatibilization using coupling or interfacial adhesion agents. Processing aspects, compatibilization and properties have been investigated by several authors [34, 42, 47].

Initially, the compatibilizer or coupling agent in contact with the filler surface should interact strongly with the fibers through strong covalent bonds, acid-base

interactions or hydrogen bonds. The compatibilizing agent should contain a sufficient number of functional groups to allow reaction with cellulose hydroxyl groups. Another aspect to consider is the length of compatibilizer chains, which should be long enough to allow molecular entanglement with the polymer matrix in the interphase through mechanical anchoring [42]. Some authors [34, 52] have reported surface treatment of the fiber as a means of optimizing the compatibilization process.

Studies demonstrate that the modulus values of WPC increase slightly in relation to neat polymers, but with no statistically significant differences. However, there is almost no variation in tensile strength between neat HDPE and maleinized-polypropylene (MAPP) composites, although the former exhibited lower impact strength in relation to the other samples. This result is attributed to better adhesion between the fiber and polymer matrix, allowing better stress transfer to the fiber [9, 34, 50–52].

In addition to compatibilizers, other additives are used to improve the properties and appearance of the final product, such as impact modifiers, colorants, flame retardants, antioxidants, UV stabilizers, lubricants, stabilizers and biocides.

One way of altering the properties of plastic lumber is by modifying the molecular structure of one or more component polymers through exposure to ionizing radiation. Irradiation has the advantage of being a clean, continuous easy-to-control process [53–56]. It promotes the formation of crosslinks parallel to chain scission as well as double bonds. Crosslinking causes an increase in molecular weight, which typically improves properties, whereas chain scission reduces molecular weight and decreases properties in general [54].

Martins et al. [54] assessed the effects of ionizing radiation on IMAWOOD[®] plastic lumber made from recycled polyethylene (around 75% low-density polyethylene—LDPE and 25% HDPE), using irradiation produced by industrial equipment with a ⁶⁰Co source. The specimens received total doses of 10, 500, 1000 and 2000 kGy. The authors concluded that irradiation in air increased the tensile strength of IMAWOOD[®], although a decrease in elongation at break was observed with ductile-brittle transition. Additionally, from an engineering standpoint, IMAWOOD[®] offers the best conditions for certain applications after irradiation because it is less brittle.

One alternative to improve the mechanical properties of wood fiber-reinforced plastic lumber is through crosslinking using silane [57–60].

Studies have shown that crosslinked composites obtained by addition of silane display greater toughness, impact strength and interfacial adhesion than composites without silane [57, 58]. Additionally, the formation of crosslinks in the polymer matrix reduces buckling when the material is overloaded [57].

Bengtsson and Oksman [58] analyzed the effects of silane on the mechanical properties of wood-HDPE composites. The silane-grafted composites were stored at different moisture levels (in a sauna and temperature chamber) to determine how this parameter affects the degree of crosslinking in the composites. Experiments conducted with different amounts of vinyltrimethoxysilane in the presence of small amounts of peroxide indicated that the samples stored in the sauna showed the highest degree of crosslinking, which was calculated by measuring the gel content and swelling ratio. The results demonstrated that the samples exposed to the highest moisture level exhibited a higher degree of crosslinking. Water was responsible for the hydrolysis of methoxy groups to silanol, increasing the degree of crosslinking in the material stored in the sauna. The flexural modulus and flexural strength of neat HDPE were higher than those of the silane-grafted composites. In contrast to

neat plastics, the crosslinked composites showed better flexural strength than the material without silane.

The improved flexural strength is likely due to greater wood-polymer adhesion, enabling stress transfer from the polymer matrix to the wood fibers when the material is overloaded. The authors [58] attributed the superior adhesion to the covalent bond between wood and polyethylene to condensation or free-radical reactions. Furthermore, hydrogen bonding between the silanol groups grafted onto polyethylene and the hydroxyl groups of wood, as well as van de Waals forces between condensed silane in the wood and the polyethylene matrix, can improve adhesion between phases.

Lower creep was observed in the crosslinked composites when compared to those without crosslinking. This behavior may be related to the reduced viscous flow in the matrix due to crosslinking and better adhesion between the polymer matrix and wood flour [57–60].

Bengtsson et al. [57] evaluated mechanical property variations in WPC treated with silane containing different wood fiber concentrations. The stress-strain curves of the silane-treated composites indicated increased stiffness of the material with the addition of wood flour, in addition to a decline in ultimate strength. There was a significant increase in tensile strength with a rise in wood flour concentration, in contrast to the behavior reported by other authors [33, 61], whereby tensile strength declined with an increase in wood flour content. The authors attributed this behavior to greater interfacial adhesion between the wood and plastic promoted by silane addition.

5. Final remarks

In addition to adding value to postconsumer plastic packaging waste and preventing deforestation, plastic lumber offers other significant benefits, including resistance to fungi and insects and eliminating the need for painting and maintenance.

Its easy processing and the possibility of obtaining different compositions demonstrate the wide variety of properties and applications of plastic lumber. However, when replacing a traditional material with another, it is important to consider the required performance of the product, the application and the cost-effectiveness of the replacement in order to prevent any technical problems related to the characteristics of the two materials and ensure successful usage.

Thus, research is needed to develop new technologies aimed at obtaining recycled material with superior properties at lower economic, environmental and social costs, in order to increase the number of applications for plastic lumber as a replacement for natural wood and help reduce plastic waste accumulation.

Author details

Fernanda A. dos Santos¹, Leonardo B. Canto², Ana Lúcia N. da Silva^{1,3},
Leila Lea Yuan Visconte^{1,3} and Elen B. A. Vasques Pacheco^{1,3*}

1 Professor Eloisa Mano Institute of Macromolecules, Federal University of Rio de Janeiro, Rio de Janeiro, Brazil

2 Department of Materials Engineering, Federal University of Sao Carlos, São Carlos, SP, Brazil

3 Environmental Engineering Program, Federal University of Rio de Janeiro, Rio de Janeiro, Brazil

*Address all correspondence to: elen@ima.ufrj.br

IntechOpen

© 2018 The Author(s). Licensee IntechOpen. This chapter is distributed under the terms of the Creative Commons Attribution License (<http://creativecommons.org/licenses/by/3.0>), which permits unrestricted use, distribution, and reproduction in any medium, provided the original work is properly cited. 

References

- [1] Bridgens B, Powell M, Farmer G, Walsh C, Reed E, Royapoor M, et al. Creative upcycling: Reconnecting people, materials and place through making. *Journal of Cleaner Production*. 2018;**189**:145-154. DOI: 10.1016/j.jclepro.2018.03.317
- [2] Ragaert K, Delva L, Geem KV. Mechanical and chemical recycling of solid plastic waste. *Waste Management*. 2017;**69**:24-58. DOI: 10.1016/j.wasman.2017.07.044
- [3] Al-Salem SM, Lettieri P, Baeyens J. Recycling and recovery routes of plastic solid waste (PSW): A review. *Waste Management*. 2009;**29**:2625-2643. DOI: 10.1016/j.wasman.2009.06.004
- [4] American Society for Testing and Materials—ASTMD6117—18. *Methods for Mechanical Fasteners in Plastic Lumber and Shapes*. USA; 2018
- [5] American Society for Testing and Materials—ASTMD66662—17. *Polyolefin-Based Plastic Lumber Decking Boards*. USA; 2017
- [6] Platt B, Lent T, Walsh B. *Guide to Plastic Lumber*. Healthy Building Network's. Washington: Institute for Local Self-Reliance. 2nd ed 2005. Available from: <https://www.greenbiz.com/sites/default/files/document/CustomO16C45F64528.pdf> [Accessed: 20-07-2018]
- [7] Turku I, Keskiäsaari A, Kärki T, Puurtinen A, Marttila P. Characterization of wood plastic composites manufactured from recycled plastic blends. *Composite Structures*. 2017;**161**:469-476. DOI: 10.1016/j.compstruct.2016.11.073
- [8] Chen C-W, Salim H, Bowders JJ, Loehr JE, Owen J. Creep behavior of recycled plastic lumber in slope stabilization applications. *Journal of Materials in Civil Engineering*. 2007;**19**(2):130-138. DOI: 10.1061/_ASCE_0899-1561
- [9] Najafi SK. Use of recycled plastics in wood plastic composites—A review. *Waste Management*. 2013;**33**(9):1898-1905. DOI: 10.1016/j.wasman.2013.05.017
- [10] George SD, Dillman SH. Recycled fiberglass composite as a reinforcing filler in-post consumer recycled HDPE plastic lumber. In: ANTEC 2000, 58th Annual Technical Conference, Proceedings, Vol. 3, Orlando, US, May 7-11, 2000. pp. 2919-2921
- [11] Wambua P, Ivens J, Verpoest I. Natural fibres: Can they replace glass in fibre reinforced composites? *Composites Science and Technology*. 2003;**63**(9):1259-1263. DOI: 10.1016/S0266-3538(03)00096-4
- [12] Stasiak J. Extruders for recycling of waste thermoplastic materials. *International Polymer Science & Technology*. 1997;**24**(5):96-103
- [13] Klobbie EJG: Method and apparatus for producing synthetic plastics products, and product produced thereby. U.S. patent 4187352; 1978
- [14] Druschel TP. Extruded plastic lumber and method of manufacture. Patent US 6,616,391 B; 2003
- [15] Edgman TJ. Extruded plastic lumber and method of manufacture. Patent US 6,692,815 B2; 2004
- [16] Dias BZ, Alvarez CE. Mechanical properties: Wood lumber versus plastic lumber and thermoplastic composites. *Ambiente Construído*. 2017;**17**(2):201-219. DOI: 10.1590/s1678-86212017000200153

- [17] Lampo RG, Nosker TJ: Development and Testing of Plastic Lumber Materials for Construction Applications, USACERL Technical Report 97/95. Junho; 1997. Available from: https://books.google.com.br/books?id=W0kj2EKI_0AC&pg=PA17&hl=pt-BR&source=gbs_toc_r#v=onepage&q&f=false [Accessed: 18-07-2018]
- [18] Turku I, Kärki T, Puurtinen A. Durability of wood plastic composites manufactured from recycled plastic. *Heliyon*. 2018;**4**:e00559. DOI: 10.1016/j.heliyon.2018
- [19] Van Ness KE, Nosker TJ. Commingled plastic. Chapter 9. In: Ehrig RJ, editor. *Plastic Recycling: Products and Processing*. New York: Oxford University Press; 1992. pp. 187-229
- [20] Krishnaswamy P, Lampo R. Recycled-Plastic Lumber Standards: from Waste Plastics to Markets for Plastic Lumber Bridges. World Standards Day 2001 Paper Competition First Place Award Winner. Available from: <https://cdn.ymaws.com/www.ses-standards.org/resource/resmgr/imported/WSD%202001%20-%201%20-%20Krishnaswamy%20and%20Lampo.pdf> [Accessed: 17-07-2018]
- [21] Caulfield DF, Clemons C, Jacobson RE, Rowell RM. Wood thermoplastic composites. Chapter 13. In: Rowell RM, editor. *Handbook of Wood Chemistry and Wood Composites*. Boca Raton, FL: CRC Press, Taylor & Francis Group; 2005. Available from: http://www.fpl.fs.fed.us/documnts/pdf2005/fpl_2005_caulfield001.pdf [Accessed: 17-07-2018]
- [22] Martins G, Antunes F, Mateus A, Malça C. Optimization of a wood plastic composite for architectural applications. *Procedia Manufacturing*. 2017;**12**:203-220. DOI: 10.1016/j.promfg.2017.08.025
- [23] Markarian J. Wood-plastic composites: Current trends in materials and processing. *Plastics, Additives and Compounding*. 2005;**7**(5):20-26. DOI: 10.1016/S1464-391X(05)70453-0
- [24] Migneault S, Koubaa A, Erchiqui F, Chaala A, Englund K, Wolcott MP. Effects of processing method and fiber size on the structure and properties of wood-plastic composites. *Composites Part A: Applied Science and Manufacturing*. 2009;**40**(1):80-85. DOI: 10.1016/j.compositesa.2008.10.004
- [25] Breslin VT, Adler-Ivanbrook L. Release of copper, chromium and arsenic from CCA-C treated lumber in estuaries. *Estuarine, Coastal and Shelf Science*. 1998;**46**(1):111-125. DOI: 10.1006/ecss.1997.0274
- [26] Platten WE III, Sylvest N, Warren C, Arambewela M, Harmon S, Bradham K, et al. Estimating dermal transfer of copper particles from the surfaces of pressure-treated lumber and implications for exposure. *Science of the Total Environment*. 2016;**548-549**:441-449. DOI: 10.1016/j.scitotenv.2015.12.108
- [27] Breslin VT, Senturk U, Berndt CC. Long-term engineering properties of recycled plastic lumber used in pier construction. *Resources, Conservation and Recycling*. 1998;**23**(4):243-258. DOI: 10.1016/S0921-3449(98)00024-X
- [28] Brooks KM. Evaluating the environmental risks associated with the use of chromated copper arsenate-treated wood products in aquatic environments. *Estuaries*. 1996;**19**(2):296-305. DOI: 10.2307/1352235
- [29] Hingston JA, Collins CD, Murphy RJ, Lester JN. Leaching of chromated copper arsenate wood preservatives: A review. *Environmental Pollution*. 2001;**111**:53-66. DOI: 10.1016/S0269-7491(00)00030-0

- [30] Xie KY, Locke DC, Habib D, Judge M, Kriss C. Environmental chemical impact of recycled plastic timbers used in the Tiffany Street Pier, South Bronx, New York. *Resources, Conservation and Recycling*. 1997;**21**(3):199-211. DOI: 10.1016/S0921-3449(97)00038-4
- [31] Salles ACN, Legey LFL, Rosa LP, Pacheco EBAV, Woidasky J. Comparative analysis of the carbon footprints of wood and plastic lumber railway sleepers in Brazil and Germany, Chapter 5. In: Garmson E, editor. *Plastics and the Environment*. United Kingdom: Smithers Rapra Publishing; 2010. pp. 59-80
- [32] Gardner DJ, Han Y, Wang L. Wood-plastic composite technology. *Current Forestry Reports*. 2015;**1**(3):139-150. DOI: 10.1007/s40725-015-0016-6
- [33] Yang H-S, Wolcott MP, Kim H-S, Kim S, Kim H-J. Properties of lignocellulosic material filled polypropylene bio-composites made with different manufacturing processes. *Polymer Testing*. 2006;**25**(5):668-676. DOI: 10.1016/j.polymertesting.2006.03.013
- [34] Soccalingame L, Bourmaud A, Perrin D, Bénézet J-C, Bergeret A. Reprocessing of wood flour reinforced polypropylene composites: Impact of particle size and coupling agent on composite and particle properties. *Polymer Degradation and Stability*. 2015;**113**:72-85. DOI: 10.1016/j.polymdegradstab. 2015.01.020
- [35] Ichazo MN, Albano C, González J, Perera R, Candal MV. Polypropylene/ wood flour composites: Treatments and properties. *Composite Structures*. 2001;**54**(2-3):207-214. DOI: 10.1016/S0263-8223(01)00089-7
- [36] English B, Clemons CM, Stark N, Schnieder JP. Waste-wood derived fillers for plastics. In: *General Technical Report FPL-GTR-91*. United States Department of Agriculture. Forest Products Laboratory; 1996. pp. 1-17. DOI: 10.2737/FPL-GTR-91
- [37] Markarian J. Material and processing developments drive wood-plastic composites forward. *Plastics, Additives and Compounding*. 2003;**5**(4):24-26. DOI: 10.1016/S1464-391X(03)00433-1
- [38] Stark NM, Berger MJ. Effect of particle size on properties of wood-flour reinforced composites. In: *The Fourth Conference on Woodfiber-Plastic Composites*. 1997. Available from: <http://www.fpl.fs.fed.us/documnts/pdf1997/stark97d.pdf> [Accessed: 19-07-2018]
- [39] Rodolfo A Jr, John VM. Development of PVC/wood composites for the replacement of conventional wood products. *Polímeros*. 2006;**16**(1):1-11. DOI: 10.1590/S0104-14282006000100005
- [40] Lewandowski K, Zajchowski S, Mirowski J, Kosciuszko A. Studies of processing properties of PVC/wood composites. *Chem*. 2011;**65**(4): 329-336. Available from: http://www.chemikinternational.com/pdf/2011/04_2011/CHEMIK%202011_65_4_329-336.pdf [Accessed: 20-07-2018]
- [41] English B, Clemons CM. Weight reduction: Wood versus mineral fillers in polypropylene. In: *Proceedings of the Fourth International Conference on Woodfiber-Plastic Composites*, Madison, Wisconsin, USA. 1997. pp. 237-244. Available from: <https://www.fpl.fs.fed.us/documnts/pdf1998/engli98a.pdf> [Accessed: 19-07-2018]
- [42] Correa CA, Fonseca CNP, Neves S, Razzino CA, Hage E Jr. Wood-plastic composites. *Polímeros*. 2003;**13**(3):

154-165. Available from: <http://revistapolimeros.org.br/files/v13n3/v13n3a03.pdf> [Accessed: 19-07-2018]

[43] Carroll DR, Stone RB, Sirignano AM, Saindon RM, Gose SC, Friedman MA. Structural properties of recycled plastic/sawdust lumber decking planks. *Resources, Conservation and Recycling*. 2001;**31**(3):241-251. DOI: 10.1016/S0921-3449(00)00081-1

[44] Thomas S. Environmental effects on the degradation behaviour of sisal fibre reinforced polypropylene composites. *Composites Science and Technology*. 2002;**62**:1357-1372. DOI: 10.1016/S0266-3538(02)00080-5

[45] Jayaraman K, Bhattacharyya D. Mechanical performance of woodfibre-waste plastic composite materials. *Resources, Conservation and Recycling*. 2004;**41**(4):307-319. DOI: 10.1016/j.resconrec.2003.12.001

[46] Yang H-S, Wolcott MP, Kim H-S, Kim H-J. Thermal properties of lignocellulosic filler-thermoplastic polymer bio-composites. *Journal of Thermal Analysis and Calorimetry*. 2005;**82**(1):157-160. DOI: 10.1007/s10973-005-0857-5

[47] Selke SE, Wichman I. Wood fiber/polyolefin composites. *Composites Part A: Applied Science and Manufacturing*. 2004;**35**(3):321-326. DOI: 10.1016/j.compositesa.2003.09.010

[48] Solís ME, Lisperguer JH: Impact and tensile strength of wood-plastic composites. *Información Tecnológica* 2005;**16**(6):21-25. DOI: 10.4067/S0718-07642005000600004

[49] Ledur JG, Guaresi S, Gonella LB, Bianchi O, Oliveira RVB, Canto LB, et al. Urban trash containers made of recycled plastic lumber. *Scientia cum Industria*. 2013;**1**(1):6-10. DOI: 10.18226/23185279.v1iss1p6

[50] Saba N, Paridah MT, Jawaid M. Mechanical properties of kenaf fibre reinforced polymer composite: A review. *Construction and Building Materials*. 2015;**76**:87-96. DOI: 10.1016/j.conbuildmat.2014.11.043

[51] Yan L, Chouw N, Jayaraman K. Flax fibre and its composites—A review. *Composites Part B: Engineering*. 2014;**56**:296-317. DOI: 10.1016/j.compositesb.2013.08.014

[52] Kazayawoko M, Balatinez JJ, Matuana LM. Surface modification and adhesion mechanisms in woodfibre-polypropylene composites. *Journal of Materials Science*. 1999;**34**(24):6189-6199. DOI: 10.1023/A:1004790409158

[53] Suarez JCM, Mano EB, Pereira RA. Thermal behavior of gamma-irradiated recycled polyethylene blends. *Polymer Degradation and Stability*. 2000;**69**(2):217-222. DOI: 10.1016/S0141-3910(00)00065-3

[54] Martins FA, Suarez JCM, Mano EB. Recycled polyolefin products with higher performance than the corresponding virgin materials. *Polímeros*. 1999;**9**(4):27-32. DOI: 10.1590/S0104-14281999000400005

[55] Suljovrujic E. Post-irradiation effects in polyethylenes irradiated under various atmospheres. *Radiation Physics and Chemistry*. 2013;**89**:43-50. DOI: 10.1016/j.radphyschem.2013.04.003

[56] Perez CJ, Vallés EM, Failla MD. The effect of post-irradiation annealing on the crosslinking of high-density polyethylene induced by gamma-radiation. *Radiation Physics and Chemistry*. 2010;**79**(6):710-717. DOI: 10.1016/j.radphyschem.2010.01.005

[57] Bengtsson M, Gatenholm P, Oksman K. The effect of crosslinking on the properties of polyethylene/wood flour composites. *Composites Science and*

Technology. 2005;**65**(10):1468-1479.
DOI: 10.1016/j.compscitech.2004.12.050

[58] Bengtsson M, Oksman K. Silane crosslinked wood plastic composites: Processing and properties. *Composites Science and Technology*. 2006;**66**(13):2177-2186. DOI: 10.1016/j.compscitech.2005.12.009

[59] Fang L, Chang L, W-j G, Chen Y, Wang Z. Influence of silane surface modification of veneer on interfacial adhesion of wood-plastic plywood. *Applied Surface Science*. 2014;**288**: 682-689. DOI: 10.1016/j.apsusc.2013.10.098

[60] Grubbström G, Oksman K. Influence of wood flour moisture content on the degree of silane-crosslinking and its relationship to structure-property relations of wood-thermoplastic composites. *Composites Science and Technology*. 2009;**69**(7-8): 1045-1050. DOI: 10.1016/j.compscitech.2009.01.021

[61] Lai S-M, Yeh F-C, Wang Y, Chan H-C, Shen H-F. Comparative study of maleated polyolefins as compatibilizers for polyethylene/wood flour composites. *Journal of Applied Polymer Science*. 2003;**87**(3):487-496. DOI: 10.1002/app.11419

Multi-Field Synergy Process for Polymer Plasticization: A Novel Design Concept for Screw to Facilitate Phase-to-Phase Thermal and Molecular Mobility

Ranran Jian, Hongbo Chen and Weimin Yang

Abstract

A novel concept of screw design has been proposed considering the multi-field synergy principle to facilitate phase-to-phase thermal and molecular mobility; subsequently, a torsion element has been designed. This new screw design allows an innovative and effective way to resolve a growing challenge in polymer process engineering, especially for nanocomposites or biopolymers, that is, an inadequate control of mass transfer and thermal management for multicomponent melt flows through narrow channels during extrusion or injection. The adaption of torsion element in the screw facilitated the plasticization mixing and thermal distribution in polymer melts, and the torsional flow induced by the torsion elements shows a synergistic effect on the melt-phase mass flow and the thermal flow field. The latter effect enhances the mass and heat transfer of heterogeneous polymer systems and realizes effective heat management to achieve properly uniform temperature field.

Keywords: multi-field coupling, polymer plasticization, field synergy, torsional flow, heat and mass transfer enhancement

1. Introduction

Polymer plasticization is a complex process with many uncertain variables, which involves phase transfer and viscoelastic behavior. The nonlinear effect of polymer plasticization is a multidisciplinary engineering science problem that includes heat transfer, rheology, and flow dynamics among others. The thermal homogeneity and stability of polymer melts in this plasticization process is the key to determine the quality of products, especially for biodegradable nanocomposites or microcellular foam materials.

In polymer processing, plasticization screw is an added unit operation that facilitates melting and homogenization of an initially heterogeneous physical system [1, 2]. In general, the temperature distribution is not uniform in the process of plasticization; this is due to significant friction heating and the low thermal conductivity of polymers. It is very important to optimize the structural parameters and working characteristics of the screw in order to enhance plasticization of

polymers. The effect of barrel configurations and screw designs on heat and mass transfer has been investigated in the past and proved unquestionably important attributes for determining temperature uniformity and mixing effectiveness in extrusion and injection molding processes [3–8]. Different from conventional screw, the new types of screw can be roughly divided into four categories: distribution screws, barrier screws, separator screws, and channel screws with variable sections. These reconfigured screws are stated to be better than a standard one. For example, Kelly et al. [6] developed a barrier-flighted screw with Maddock mixer to achieve good melting performance and low temperature and pressure fluctuations. Spalding [9] introduced a distributive melt-mixing type screw equipped with an Eagle mixer in injection molding process and obtained better melting capacity and higher mixing than a conventional screw. Shimbo et al. [10] disclosed a mixture system by combining Pin and Dulmage type screws and also reported their beneficial effect in kneading, homogenization, and ensuring stability of gas/polymer solution. Zitzenbacher et al. [11, 12] indicated that the shearing sections like axial and spiral Maddock elements and Z-elements are often used to improve the melt homogeneity by enhancing dispersive mixing. Rydzkowski [13] developed an autothermal screw-disc extruder to induce autothermal effect. Rauwendaal [4] noted a CRD mixing screw with wedge-shaped barrier region to generate elongational flow. In this way, the mixing ability improves under the condition of lower power consumption and viscous dissipation than shear flow. Also, the melt temperatures and pressure fluctuation reduce in the flow channel. Based on the elongational flow and volume transportation, Qu et al. [14, 15] proposed a novel vane plasticization system in place of screw one to create extensional stress. Their results showed that the plasticizing capacity improved with the decrease of power consumption in the vane extruder. Diekmann [16] analyzed the direct-drive single-screw extruders without gearing and results indicated that plasticization capacity increased in the direct-drive system. Besides, Jiang [17] introduced ultrasonic plasticizing in the extruder to achieve energy saving. And Qu et al. [18] introduced a vibrational force field in the screw plasticization system. Their results showed that mixing performance improved and extrusion pressure reduced.

These studies may focus on mixing and rheology. However, heat transfer also plays a significant role in plasticizing. In the past, researchers paid little attention to understand heat transfer in viscous fluid. Understanding the mass and heat transfer processes in a plasticization system as a function of screw configurations is essential to further develop a more effective screw design to overcome some of the existing challenges. The properties of composites in the plasticization process also depend on the control of the velocity, temperature, shear, and pressure fields. Therefore, it is worth investigating the synergetic relationship, if any, between various physical fields in order to maximize the efficiency of the plasticization effect.

Mixing a high-viscosity or high-molecular weight polymer melt leads to shear-induced overheating due to the large torque induced, required to unleash the polymer chain entanglements. The challenge in this case is to fabricate a screw configuration that facilitates polymer chain mobility in melt phase without inducing high shear and by facilitating effective transfer of the excess local heat out of the bulk of the polymer melt. Otherwise, the local overheating effect essentially results in unwanted heat loss and poor melt quality, subsequently, the polymer chains break down and thermosensitive polymers such as biopolymers may even be degraded.

In order to overcome the challenges of an inadequate control of flow-thermal management for multicomponent melt, we explore the synergistic relationship and interaction mechanism between various physical fields for non-Newtonian viscous liquids such as polymer melts, with special emphasis on higher molecular weight thermoplastic resins, subsequently a torsion screw has been designed.

2. Multi-field synergy theory

In order to find out relationships among the velocity, velocity gradient, and temperature gradient fields in the plasticization process of polymer, we presented the mathematical expressions for quantitative analysis of multi-field synergy based on momentum conservation equation and energy conservation equation.

2.1 Synergy between velocity and velocity gradient

From the knowledge of polymer rheology, we have obtained the Navier-Stokes equation derived from momentum conservation equation in the form of Eq. (1).

$$\rho \frac{D\vec{v}}{Dt} = \nabla \cdot \vec{\tau} - \nabla P + \rho g \quad (1)$$

Eq. (2) is obtained by further expansion.

$$\rho \left(\frac{\partial \vec{v}}{\partial t} + \vec{v} \cdot \nabla \vec{v} \right) = \nabla \cdot \vec{\tau} - \nabla P + \rho g \quad (2)$$

where ρ is the fluid density, v is the fluid velocity, t is the time, τ is the stress, P is the pressure, and g is the gravitational acceleration. The left-hand term of the equation is the inertia term, reflecting the increment of fluid momentum per unit volume in unit time. In the parentheses in Eq. (2), there is a dot product of velocity and velocity gradient, which can be expressed as

$$\vec{v} \cdot \nabla \vec{v} = |\vec{v}| \times |\nabla \vec{v}| \cos \alpha \quad (3)$$

where α is the intersection angle between the velocity gradient and the velocity vector, and can be calculated according to Eq. (4)

$$\alpha = \arccos \left(\frac{\vec{v} \cdot \nabla \vec{v}}{|\vec{v}| |\nabla \vec{v}|} \right) \quad (4)$$

Here defines the synergy angle α to represent the synergy between the velocity and the velocity gradient. In the range 0° – 90° , the dot product Eq. (3) increases with decreasing α , which leads to the increase in momentum and enhancement of mass transfer. This means the interaction of velocity and velocity gradient has an effect on the momentum of the system, that is, the increment of momentum depends not only on the magnitudes of velocity or velocity gradient, but also on the overall synergy between velocity and velocity gradient.

When the synergy angle α becomes zero, the flow is a pure elongational one, and if it becomes 90° , the flow is a pure shear one. Most notably, it is generally known that the effect of elongational flow on mixing is more strong than that of shear flow [19–24], which provides evidence for the feasibility of field synergy analysis. Therefore, the synergy relationship provides a new perspective to understand the polymer mixing.

From Eqs. (2) and (3), we can also conclude that the pressure gradient is affected by the synergy angle α when the stress and gravity terms are invariable. In other words, the synergistic effect of velocity and velocity gradient can reduce

pressure loss and energy consumption, which is of great significance in Newtonian fluid flow. However, for most polymers, which are non-Newtonian in nature, the pressure term has little effect on mechanical power and energy consumption due to its very high viscosity.

2.2 Synergy between velocity and temperature gradient

Almost all polymer processing unit operations require heat transfer processes such as energy exchange, heating, and cooling to facilitate phase-to-phase thermal and molecular mobility. Therefore, the study of energy balance and distribution has special significance in the process of melt flow. It is well known that the general energy conservation equation in the flow field can be represented in the form of Eq. (5).

$$\rho C_V \frac{DT}{Dt} = -\nabla \cdot \vec{q} - T \left(\frac{\partial P}{\partial T} \right)_p (\nabla \cdot \vec{v}) + (\vec{\tau} : \nabla \cdot \vec{v}) \quad (5)$$

By further expansion, we obtain Eq. (6) as follows.

$$\rho C_V \left(\frac{\partial T}{\partial t} + \vec{v} \cdot \nabla T \right) = -\nabla \cdot (-K \nabla T) - T \left(\frac{\partial P}{\partial T} \right)_p (\nabla \cdot \vec{v}) + (\vec{\tau} : \nabla \cdot \vec{v}) \quad (6)$$

where ρ is the fluid density, C_V is the constant-volume specific heat, T is the fluid temperature, v is the fluid velocity, t is the time, τ is the stress, P is the pressure, and K is the heat transfer coefficient. The left-hand term of the equation is the changing rate of internal energy, reflecting the change of heat caused by the temperature variation per unit time at a point in the flow field. Moreover, in the parentheses, there is also a dot product of velocity and temperature gradient. The latter term signifies the interaction between velocity and temperature gradient, and demonstrates that this interaction parameter has an effect on the thermal energy of the system, that is, the change of internal energy depends not only on the velocity field and temperature gradient field, but also on the overall synergy between the velocity field and the temperature gradient field. The dot product in the parentheses in Eq. (6) can be further expressed as

$$\vec{v} \cdot \nabla T = |\vec{v}| \times |\nabla T| \cos \beta \quad (7)$$

where β is the intersection angle between the temperature gradient and the velocity vector, and can be calculated according to Eq. (8)

$$\beta = \arccos \left(\frac{\vec{v} \cdot \nabla T}{|\vec{v}| |\nabla T|} \right) \quad (8)$$

Here is defined as the synergy angle $\alpha \beta$ representing the synergy between the velocity and the temperature gradient. In the range 0° – 90° , the dot product (Eq. (7)) increases with decreasing β . When the viscous dissipation power is constant, a small β contributes to a large heat transfer coefficient K , which leads to enhanced heat transfer and temperature uniformity.

In the case of the problem of a two-dimensional flat-plate steady-state boundary layer, Guo et al. [25, 26] have simplified the energy conservation equations into the dimensionless forms

$$Nu_l = Re_l Pr_l \int_0^{\delta_t} (\overline{U} \cdot \overline{\nabla T}) d\overline{y} \quad (9)$$

where \overline{U} is the velocity vector, $\overline{\nabla T}$ is the temperature gradient vector, Re_l is the l -component of the Reynolds number, Pr_l is the l -component of the Prandtl number, and Nu_l is the l -component of the Nusselt number. Re_l , Pr_l , and Nu_l are expressed as

$$Re_l = \frac{\rho v \delta_t}{\mu}, Pr_l = \frac{C_p \mu}{\lambda}, Nu_l = \frac{K \delta_t}{\lambda} \quad (10)$$

where μ is the fluid viscosity, C_p is the specific heat capacity at constant pressure, λ is the thermal conductivity, and δ_t is the characteristic dimension, which refers to the thickness of the thermal boundary layer. From Eqs. (9) and (10), we can notice that an increase in interaction between the temperature gradient and the velocity fields increases the Nusselt number and the coefficient of local heat transfer, and consequently enhances the overall heat transfer. These synergy equations suggest a new approach to enhance heat transfer of the polymers with poor heat conductivity, namely by increasing the dot product in the integral (Eq. 9).

3. Model design and description

By understanding the multi-field synergy effect in the heat and mass transfer process of polymer plasticization, we can construct a specific flow field so that the directions of velocity field and temperature gradient field are no longer perpendicular, and the flow field movement is more random. The schematic diagram is shown in **Figure 1**. In this way, it can facilitate phase-to-phase thermal and molecular mobility, so as to significantly improve heat transfer and molecular mixing, particularly for highly viscous multicomponent polymer melts with Bio or Nano filler. Based on this method, we can design a special screw configuration to divert the fluid particles and obtain the desired flow field. Here, we propose a new type of screw element, namely, torsion element, to stimulate the spiral or torsional flow, which is the most common way of disturbing or changing flow direction in nature.

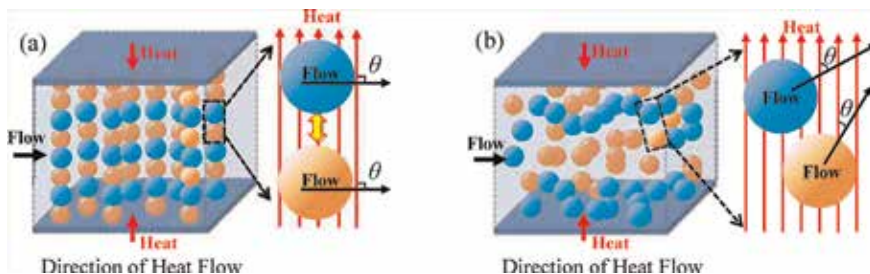


Figure 1. The synergy between velocity field and heat flow field: Parallel movement (a) and spiral movement (b).

4. Numerical analysis examples

In the following sections, we develop a novel torsion element-induced torsional flow into the flow field by adapting the field synergy principle. Then, we establish a three-dimensional physical and mathematical model with finite element method

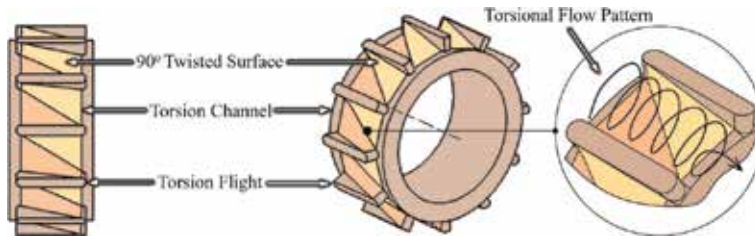


Figure 2.
The geometrical configuration and flow line of particles for a torsion element.

(FEM), and present results of computational fluid dynamics (CFD) simulations of the flow and heat transfer of a viscous polypropylene (PP) melt in the screw with torsion elements to confirm this field synergy method and compared them with the conventional screw in common use today.

The geometrical configuration of the proposed torsion element is shown in **Figure 2**. The torsion channels are divided into N parts along the circumferential direction by torsion flights. Between every two adjacent torsion flights, there are two surfaces twisted by 90° along the axial direction. When polymer flows over the torsion channel, it is expected to undergo a torsional rotation (tumbling) under the forces generated from viscous friction with barrel wall and with the steering between two 90° twisted surfaces. As a result, spiral-shaped or torsional-shaped flow may occur in the torsion channel. In consequence, the intersection angle between the velocity and the heat flux will decrease to less than 90° compared with that in the standard screw channel, and then the synergic effect between the velocity vector and the temperature gradient will be improved.

4.1 Geometrical configuration

Six screws with same length and diameter (designated by alphabetical A to F as shown in **Figure 3**) were employed in this work to verify the synergic effect of

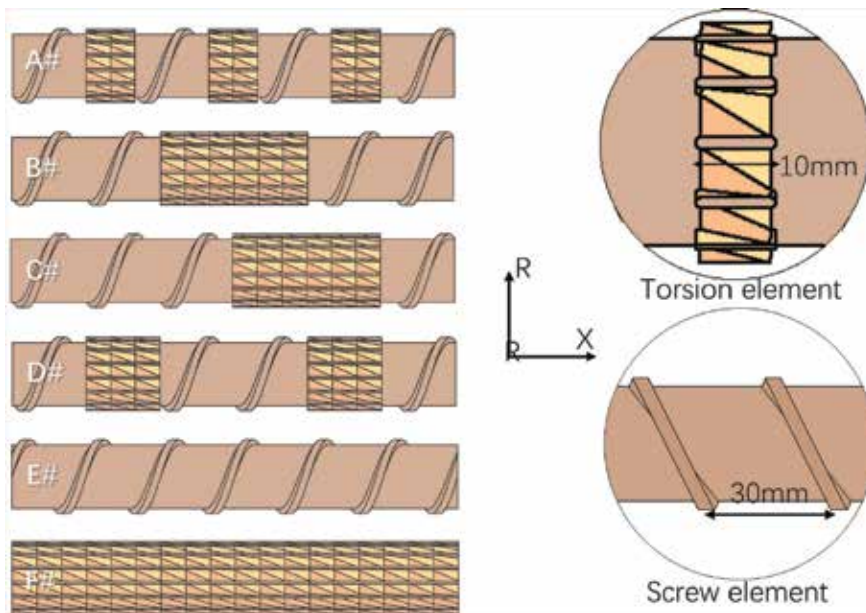


Figure 3.
The geometrical configuration of various screws (with screw elements and torsion elements).

Parameters	Dimensions (mm)
Length of screw	180
Diameter of screw	30
Diameter of barrel	30.4
Length of single torsion element	10
Lead of screw element	30
Inner diameter of screw	25.8

Table 1.
 Geometric parameters of simulation models.

torsion element. Screws were constructed of two kinds of polymer plasticization elements: the torsion element and the screw element. Screws A to D had six torsion elements with regular arrangement in different orders. As control subjects, screw E is a conventional screw without torsion element and screw F is a torsional screw without screw elements. **Table 1** presents a summary of the geometric parameters of simulation models.

4.2 Governing equations and boundary conditions

In this case, we assumed that the polymer fluid had non-isothermal transient laminar flow and was incompressible. No-slip conditions were adopted at the boundary. Polypropylene (PP) was chosen to be the model polymer due to its common use in polymer processing. Compared with viscous force, the inertial force can be neglected due to the high viscosity of PP. Therefore, the governing equations representing the flow field in this situation are shown in the form of Eqs. (11)–(13).

Continuity equation:

$$\frac{\partial u_i}{\partial x_i} = 0 \quad (11)$$

Momentum equation:

$$\rho \frac{\partial u_i}{\partial t} + \frac{\partial P}{\partial x_i} = \frac{\partial}{\partial x_j} \left(\eta \frac{\partial u_i}{\partial x_j} \right) \quad (12)$$

Energy equation:

$$\rho c_p \left(\frac{\partial T}{\partial t} + u_i \frac{\partial T}{\partial x_i} \right) = \lambda \frac{\partial^2 T}{\partial x_i^2} + \varphi \quad (13)$$

The apparent viscosity of PP was described by the Carreau-approximate Arrhenius model (Eq. 14), which match most polymers, to consider the factors of both temperature and shear.

$$\eta = \eta_0 (1 + t^2 \dot{\gamma}^2)^{(n-1)/2} \exp [-B(T - T_0)] \quad (14)$$

The physical characteristics of the PP and screw material are listed in **Tables 2** and **3**, respectively. The choice of the polymer affects only the constants in the constitutive equation (Eq. (14)). Moreover, the Carreau-approximate Arrhenius model has been already validated for most polymer melts (e.g., polystyrene,

polyethylene, and polyurethane.). Therefore, we assume modeling and simulated results based on the above conditions, which are generally applicable for most of the materials used in polymer processing.

In our work, ANSYS Polyflow 17.0 packaged software (ANSYS, Inc.) was adopted in the simulations. The 3D mesh systems for the screw and the fluid were created using the mesh superposition technique (MST). **Figure 4** shows the 3D model for screw E. The fluid model and screw model were implemented through mesh refinement by hexahedral and tetrahedral elements, respectively. In addition,

Density ρ	735 kg/m ³
Thermal conductivity λ	0.15 W/(m·K)
Specific heat capacity C_p	2100 J/(kg·K)
Zero shear viscosity η_0	26,470 Pa·s
Non-Newtonian index n	0.38
Natural time t	2.15 s
Coefficient of temperature sensibility B	0.02 K ⁻¹
Reference temperature T_0	513 K

Table 2.
Physical parameters of the PP.

Density ρ	8030 kg/m ³
Thermal conductivity λ	16.27 W/(m·K)
Specific heat capacity C_p	502.4 J/(kg·K)

Table 3.
Physical parameters of the screw.

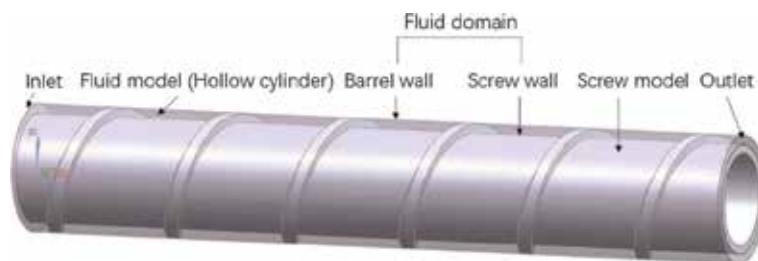


Figure 4.
Three-dimensional physical model of screw E.

Location	Flow boundary conditions	Thermal boundary conditions
Inlet	Setting zero pressure	513 K
Outlet	Setting zero pressure	Heat outlet
Barrel wall	No-slip wall	513 K
Screw wall	Screw speeds: 40,60,80,100,120 r/min	Free boundary

Table 4.
Boundary conditions.

progressively refined meshes for the screw and fluid models were constructed to ensure that the simulation results were mesh-independent. Different screws had the same mesh refinement setting and, with the same fluid model, simulation results were displayed in the grid of fluid domain. **Table 4** gives the flow and thermal boundary conditions used in this case.

5. Results and discussion

5.1 Temperature uniformity

Firstly, we investigated the axial melt temperature distribution by selecting different radial reference lines for these six screws as shown in **Figure 5**. From all the six screws, we can find that the temperature fluctuations decrease by the effect of torsion elements and the temperature difference between melt and barrel wall in the position of torsion elements is smaller than that of the position of screw elements. The reason for this phenomenon is heat transfer enhancement caused by the synergy effect between velocity and temperature gradient. We will prove this in the next section. **Figure 6** shows the radial melt temperature distribution for screw B in the position of torsion and screw elements. For the position of torsion element, almost all the fluid is in a high-temperature region, more than 500°C, while the radial temperature for most fluid in the screw channels is below 500°C. Results indicated that the radial temperature difference in the position of torsion element is much lower compared with that of the position of screw elements, no matter before

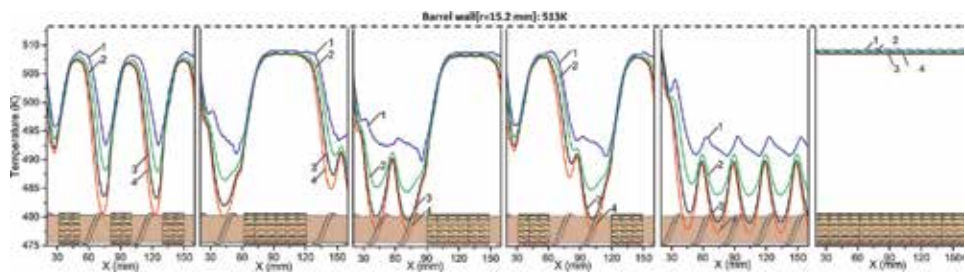


Figure 5. Radial and axial temperature distribution for the different screws at 40 r/min. (1) $r = 14.5$ mm; (2) $r = 14.0$ mm; (3) $r = 13.5$ mm; (4) $r = 13.0$ mm.

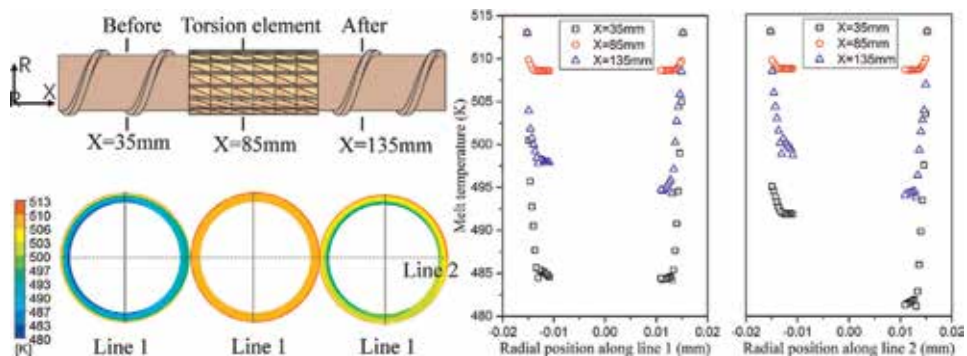


Figure 6. Temperature contours (left) and melt temperature profiles (right) across the melt flow with the magnitude of fluctuations for screw B at different x -positions at 40 r/min.

or after the torsion element. It can be concluded that the torsion element can achieve more uniform temperature distribution than the screw element.

5.2 Field synergy analysis

In order to verify the field synergy effect, we calculated the mean field synergy angle between temperature gradient and velocity fields and the Nusselt number at different screw speeds for these six screws as shown in **Figure 7**. It can be seen that the Nusselt number increases with screw speed, which is a well-known fact. Results also indicated that conventional screw E without torsion elements has the largest mean field synergy angle and smallest Nusselt number, while screw F without screw elements has the smallest mean field synergy angle and largest Nusselt number, which means the smaller the field synergy angle, the larger the Nusselt number. However, there are little difference of values in field synergy angle and Nusselt number for the screws A, B, C and D. This is because all these four screws have the same six torsion elements, which bring about almost the same influence on the variations of field synergy angle, that is, the arrangement of torsion elements in the screw has little effect on the field synergy angle. Therefore, it can be inferred that the screws equipped with torsion elements show better convective heat transfer capacity compared with the conventional screw, which then bring about a good melt temperature uniformity.

In addition, **Figure 8** shows the local field synergy angle and the local heat transfer coefficient at different cross sections for screw A. Results also indicated that the local regions with torsion elements have larger heat transfer coefficients and smaller field synergy angles than the local regions with screw elements. Besides, the local convective heat transfer was found to be inversely proportional to the local field synergy angle between velocity and temperature gradient.

The contours of the local field synergy angle at different positions further show that most of the local synergy angle distributions at the cross sections of torsion elements alternate between larger and smaller synergy angles, while those at the cross sections of screw elements are close to 90.0° .

Figure 9 shows the dependence of the Nusselt number on the field synergy angle for various screw speeds and shows that the Nusselt number increases with

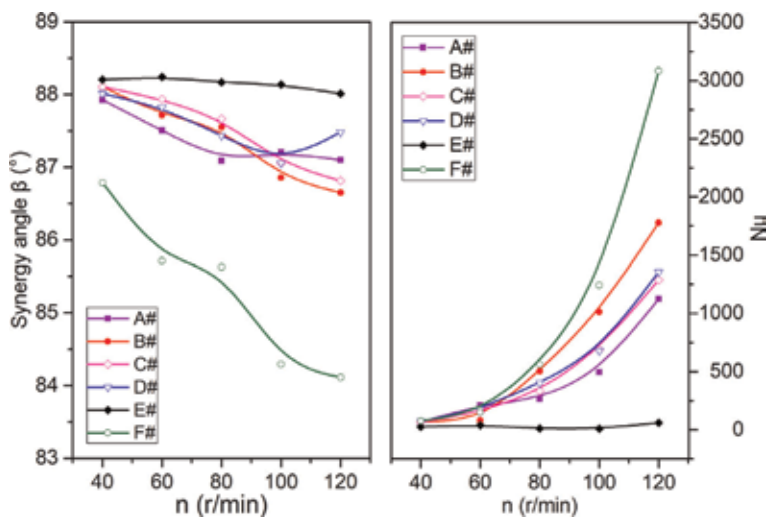


Figure 7. A plot of the mean field synergy angle (left) and Nusselt number (right) versus screw speed for various screws.

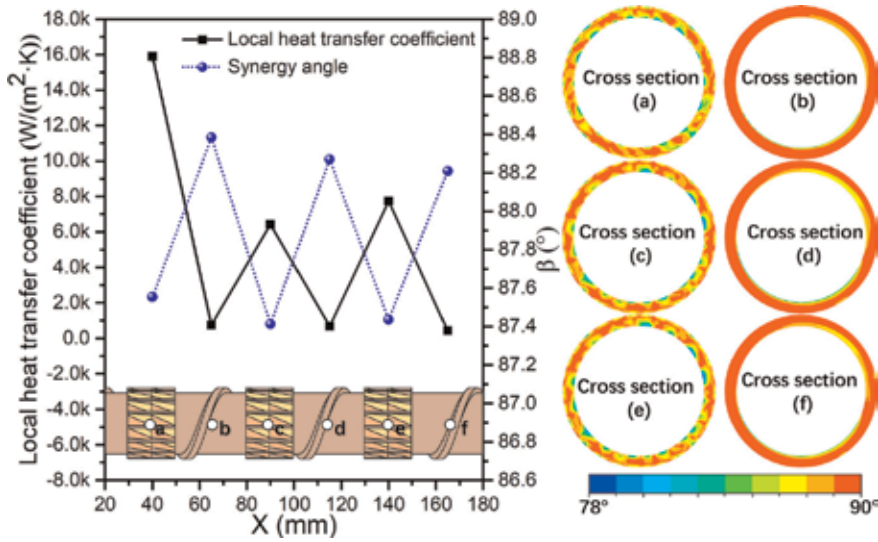


Figure 8.
 A plot of the local field synergy angle versus the local heat transfer coefficient (left) and the local field synergy angle contours at different cross sections (right) for screw A at a screw speed of 80 r/min.

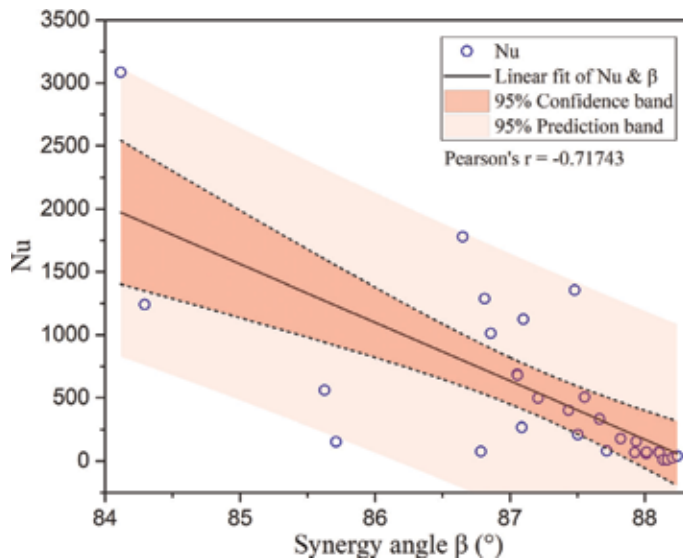


Figure 9.
 The dependence of the Nusselt number on the field synergy angle for various screw speeds. The inset is the Pearson correlation coefficient.

decreasing field synergy angle. It can be inferred that the Nusselt number is inversely interrelated with the synergy angle β . When the confidence level is 95%, its value is limited to a relatively narrow confidence band. Furthermore, the Pearson correlation coefficient is about -0.7 , which indicates a strong negative correlation. These results demonstrate that the coupling relationship between temperature gradient and velocity fields has a significant effect on the convective heat transfer of the polymer itself in a polymer plasticization process.

Accordingly, the field synergy principle is able to explain the enhancement of heat transfer brought about by the torsion elements.

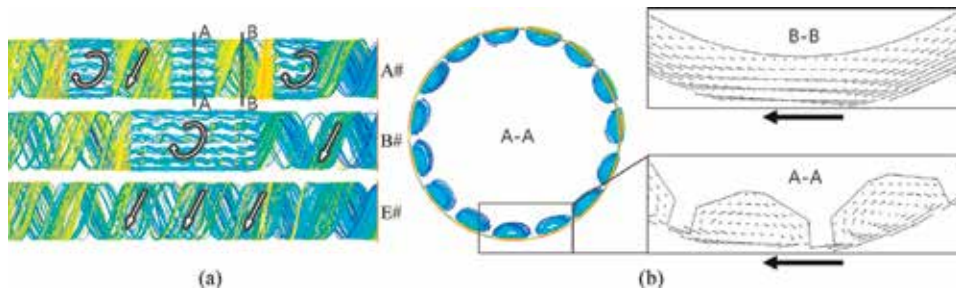


Figure 10. The streamline contours in screws A, B, and E at a screw speed of 40 r/min in the axial direction (a) and the cross section of the torsion element (b).

5.3 Fluid flow behavior

As stated previously, the synergy effect between velocity and temperature gradient in the torsion element is realized by constructing a spiral or torsional flow in the flow field. In order to verify the existence of torsional-spiral shaped flow, we investigated the fluid flow characteristics in the region of both torsion and screw elements as shown in **Figure 10**.

Figure 10(a) shows the streamline contours along the axial direction for screws A, B, and E. We can see that spiral-shaped flow occurs in the position of torsion elements for both screws A and B, which cannot be achieved in screw E. In this spiral-shaped flow, the velocity directions are changing along the flow direction and mass transfer is enhanced in the radial direction, that is, the synergy angles between velocity and thermal flow fields are no longer perpendicular to each other, which confirms the assumption shown in **Figures 1** and **2**. **Figure 10(b)** shows the cross sections in the torsion and screw elements. And results indicated that there are vortices in the torsion channel, while there are just plug flows without radial convection in the screw channel.

Therefore, it can be inferred that the torsion element improves the synergy between velocity and temperature gradient by inducing torsional flow, and then enhances heat transfer in the screw plasticization process.

6. Experimental validation

The performance of screw with torsion elements in the polymer plasticization process has been verified through numerical analysis. Furthermore, the mixing and heat transfer performances of the newly designed screw configuration based on field synergy principle were evaluated through extrusion runs and experimental data. Materials used were polypropylene (PP) and polystyrene (PS) bi-phase polymer composite mix.

Figure 11 shows the particle size distribution of PS (PP: PS = 100:10, % wt/wt) at the screw outlet; more specifically, **Figure 11(a)** is that of torsional screw with six torsion elements and **Figure 11(b)** is that of conventional screw without torsion element. The particle size distribution of PS fits Gaussian distribution. On the other hand, the relative frequencies of particle size in torsion screw are more concentrated in a narrow range [0–50 μm] than those in conventional screw. This can be further validated from the scanning electron microscope (SEM) pictures shown in **Figure 11(a)** and **Figure 11(b)**. SEM pictures clearly show that the particles of PS in torsional screw are finer and the particle sizes are smaller than those in conventional

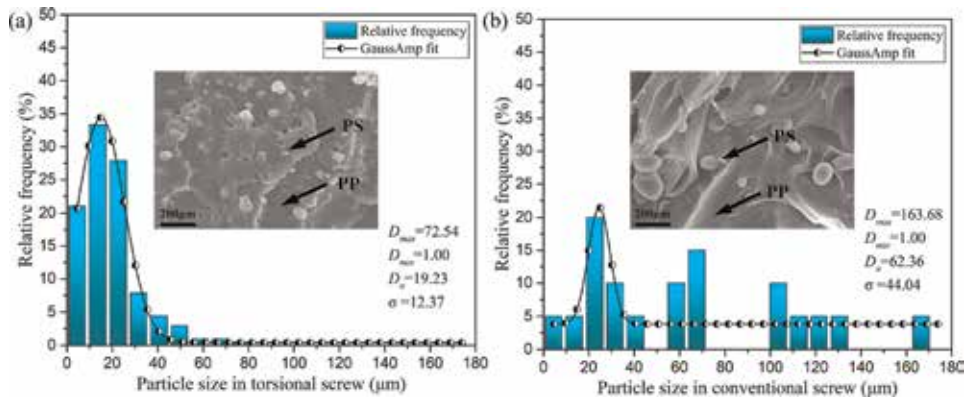


Figure 11. Particle size distribution in a PP/PS bi-phase composite in the outlet of the screws.

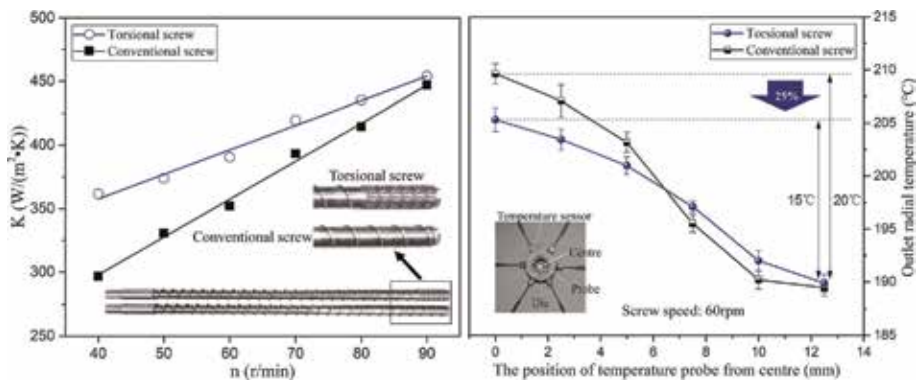


Figure 12. Heat transfer coefficient (left) and outlet radial temperature distribution (right) of the plasticization system for screws.

screw. Average particle size (D_n), the maximum value, minimum value, and standard deviation of particle size of PS are also calculated and summarized in **Figure 11**. Results indicate that the D_n , the standard deviation, and maximum value of particle size in torsional screw are much smaller than those in conventional screw. Therefore, the torsional screw with six torsion elements shows good mixing performance.

Figure 12 shows the variation of heat transfer coefficient K with screw speed and the outlet radial temperature distribution at 60 r/min for torsional screw and conventional screw. From the heat transfer coefficient K , we can see that the K value improves with screw speed, which is in agreement with **Figure 7**. More interestingly, the K value for torsional screw is higher than that for conventional screw, indicating that the torsional screw with six torsion elements shows better heat transfer capability than that of the conventional screw. Therefore, we can confirm that the configuration of torsion element designed based on field synergy principle can in fact enhance heat transfer, which is in agreement with the simulation results.

From the outlet radial temperature distribution, it can be found that the melt temperature in the center of die is higher than the temperature near the barrel walls, which is due to the viscous dissipation of polymers. Therefore, an effective heat transfer is needed in order to evenly distribute the thermal energy among the

polymer melt. In addition, the radial temperature difference of torsional screw is 15°C, whereas the radial temperature difference of conventional screw is 20°C, which is 25% higher than that of torsional screw. As the experiment data indicate that the radial temperature difference of melt decreases in the torsional configured screw, it can be concluded that the torsional configuration has a superior heat and mass transfer performance to achieve better temperature distribution than traditional screw, which is also in agreement with the simulation results.

7. Conclusions

One of the fundamental questions of non-uniform heat and mass transfer in viscous fluid was addressed by proposing a radial torsional flow pattern, by designing a torsion element and validating the same in a melt-phase polymer extrusion process. The synergistic interaction mechanisms between velocity and velocity gradient and velocity and temperature gradient have been investigated by considering theoretical and numerical aspects, which provides a new perspective to understand the polymer processing. Considering the multi-field synergy, a new design concept of torsion screw configuration has been proposed to facilitate phase-to-phase thermal and molecular mobility.

The spiral-shaped torsional flow induced by torsion configurations in a polymer channel changes the radial velocity direction, which in turn improves the interaction between velocity and temperature fields and helps to achieve good heat transfer and temperature homogeneity. The new torsion elements and their arrangement provide a novel pathway to achieve good thermal management of polymer melt by enhancing multi-field coupling. These results can be achieved to guide the screw design used for preparing high-performance composites, especially heat-sensible and biodegradable nanocomposites or microcellular foam controlled by temperature.

Acknowledgements

This work was supported by the National Natural Science Foundation of China (grant number 51576012). Support from China Scholarship Council is also gratefully acknowledged for Ranran Jian's joint PhD grant.

Appendices and Nomenclature

ρ	fluid density, kg/m ³
v	fluid velocity, m/s
τ	stress, Pa
P	pressure, Pa
C_V	constant-volume specific heat capacity, J/(kg·K)
C_p	constant-pressure specific heat capacity, J/(kg·K)
λ	thermal conductivity, W/(m·K)
T	fluid temperature, K
x, y, z	Cartesian coordinates, m
δ	velocity boundary layer thickness, m

δ_t	thermal boundary layer thickness, m
\bar{U}	velocity vector, m/s
$\nabla\bar{U}$	velocity gradient vector, s^{-1}
$\nabla\bar{T}$	temperature gradient vector, K/m
v_m	mean velocity of fluid, m/s
μ	fluid viscosity, Pa·s
K	heat transfer coefficient, W/(m ² ·K)
Re	Reynolds number
Eu	Euler number
Pr	Prandtl number
Nu	Nusselt number
α	synergy angle between the velocity gradient and the velocity, °
β	synergy angle between the temperature gradient and the velocity, °
P	pressure, Pa
η	apparent viscosity, Pa·s
η_0	zero shear viscosity, Pa·s
$\dot{\gamma}$	shear rate, s^{-1}
t	natural time, s
B	temperature sensibility coefficient, K^{-1}
n	non-Newtonian index
T_0	reference temperature, K

Author details

Ranran Jian^{1,2}, Hongbo Chen³ and Weimin Yang^{1*}

1 College of Mechanical and Electrical Engineering, Beijing University of Chemical Technology, Beijing, China

2 Centre for Biocomposites and Biomaterial Processing, Department of Mechanical and Industrial Engineering, University of Toronto, Toronto, ON, Canada

3 College of Electromechanical Engineering, Qingdao University of Science and Technology, Qingdao, China

*Address all correspondence to: yangwmmr@gmail.com

IntechOpen

© 2019 The Author(s). Licensee IntechOpen. This chapter is distributed under the terms of the Creative Commons Attribution License (<http://creativecommons.org/licenses/by/3.0>), which permits unrestricted use, distribution, and reproduction in any medium, provided the original work is properly cited. 

References

- [1] Deng J, Li K, Harkin-Jones E, Price M, Karnachi N, Kelly A, et al. Energy monitoring and quality control of a single screw extruder. *Applied Energy*. 2014;**113**:1775-1785
- [2] Abeykoon C, Martin PJ, Kelly AL, Li K, Brown EC, Coates PD. Investigation of the temperature homogeneity of die melt flows in polymer extrusion. *Polymer Engineering and Science*. 2014;**54**(10): 2430-2440
- [3] Tong FH, Shi DL, Qin JH. Single screw extruder characteristics on friction and heat generated with the barrel carved spiral groove. In: Wang CH, Ma LX, Yang W, editors. *Advanced Polymer Science and Engineering*. Stafa-Zurich: Trans Tech Publications Ltd; 2011. pp. 668-673
- [4] Rauwendaal C. New developments in mixing and screw design. *Plastics, Additives and Compounding*. 2008; **10**(6):32-36
- [5] Rauwendaal C. New screw design for cooling extruders. *Plastics, Rubber and Composites*. 2004;**33**(9-10):397-399
- [6] Kelly AL, Brown EC, Coates PD. The effect of screw geometry on melt temperature profile in single screw extrusion. *Polymer Engineering And Science*. 2006;**46**(12):1706-1714
- [7] Huang MS. Design analysis of a standard injection screw for plasticising polycarbonate resins. *Journal of Polymer Engineering*. 2016;**36**(5): 537-548
- [8] Abeykoon C, Kelly AL, Brown EC, Coates PD. The effect of materials, process settings and screw geometry on energy consumption and melt temperature in single screw extrusion. *Applied Energy*. 2016;**180**:880-894
- [9] Spalding MA, Kuhman JA, Kuhman J, Prettyman L, Larson D. Performance of a distributive melt-mixing screw with an advanced mixing tip. In: *Antec-Conference Proceedings*. Chicago; 2004. pp. 599-604
- [10] Shimbo M, Nishida K, Heraku T, Iijima K, Sekino T, Terayama T, et al. *Foam Processing Technology of Microcellular Plastics by Injection Mold Machine*. Brookfield Center: Soc Plastics Engineers; 1999
- [11] Potente H, Stenzel H. Computational design of spiral shearing sections. *Kunststoffe-German Plastics*. 1991; **81**(2):153-156
- [12] Zitzenbacher G, Karlbauer R, Thiel H. A new calculation model and optimization method for Maddock mixers in single screw plasticising technology. *International Polymer Processing*. 2007;**22**(1):73-81
- [13] Rydzkowski T. Plasticization degree of extrudate obtained during autothermal work of screw-disc extruder. *Polymers*. 2009;**54**(5):377-381
- [14] Qu JP, Zhao XQ, Li JB. Power consumption analysis of polymer solids discharging process in vane plasticization extruder. In: Chen WZ, Xu XP, Dai PQ, Chen YL, editors. *Advanced Manufacturing Technology, Pts 1-4*. Stafa-Zurich: Trans Tech Publications Ltd; 2012. pp. 1941-1944
- [15] Qu JP, Yang ZT, Yin XC, He HZ, Feng YH. Characteristics study of polymer melt conveying capacity in vane plasticization extruder. *Polymer-Plastics Technology and Engineering*. 2009;**48**(12):1269-1274
- [16] Diekmann C. Direct-drive singlescrew extruders. *Kunststoffe-Plast Europe*. 2004;**94**(9):243-245

- [17] Jiang BY, Peng HJ, Wu WQ, Jia YL, Zhang YP. Numerical Simulation and experimental investigation of the viscoelastic heating mechanism in ultrasonic plasticizing of amorphous polymers for micro injection molding. *Polymers*. 2016;**8**(5):199
- [18] Jinping Q, Baiping X, Gang J, Hezhi H, Xiangfang P. Performance of filled polymer systems under novel dynamic extrusion processing conditions. *Plastics, Rubber and Composites*. 2002;**31**(10):432-435
- [19] Yin XC, Li S, He GJ, Zhang GZ, Qu JP. Experimental study of the extrusion characteristic of a vane extruder based on extensional flow. *Advances in Polymer Technology*. 2016;**35**(2):215-220
- [20] Wen JS, Liang YH, Chen ZM. Numerical simulation of elongational flow in polymer vane extruder. In: Jiang ZY, Han JT, Liu XH, editors. *Advanced Design Technology*. Stafa-Zurich: Trans Tech Publications Ltd; 2012. pp. 415-418
- [21] Ragoubi M, Zouari R, Ben Abdeljawad M, Terrie C, Baffoun A, Alix S, et al. Design of doum palm fibers biocomposites by reactor/elongational flow MiXer: Evaluation of morphological, mechanical, and microstructural performances. *Polymer Composites*. 2018;**39**:519-530
- [22] Pierrot FX, Ibarra-Gomez R, Bouquey M, Muller R, Serra CA. In situ polymerization of styrene into a PMMA matrix by using an extensional flow mixing device: A new experimental approach to elaborate polymer blends. *Polymer*. 2017;**109**:160-169
- [23] Cao CL, Chen XC, Wang JX, Lin Y, Guo YY, Qian QR, et al. Structure and properties of ultrahigh molecular weight polyethylene processed under a consecutive elongational flow. *Journal of Polymer Research*. 2017;**25**(1):16
- [24] Bouquey M, Loux C, Muller R, Bouchet G. Morphological study of two-phase polymer blends during compounding in a novel compounder on the basis of elongational flows. *Journal of Applied Polymer Science*. 2011;**119**(1):482-490
- [25] Guo ZY, Li DY, Wang BX. A novel concept for convective heat transfer enhancement. *International Journal of Heat and Mass Transfer*. 1998;**41**(14): 2221-2225
- [26] Guo ZY, Tao WQ, Shah RK. The field synergy (coordination) principle and its applications in enhancing single phase convective heat transfer. *International Journal of Heat and Mass Transfer*. 2005;**48**(9):1797-1807

Cellulose-Based Thermoplastics and Elastomers via Controlled Radical Polymerization

Feng Jiang, Fenfen Wang, Chenqian Pan and Yanxiong Fang

Abstract

This chapter is concerned with the recent progress in cellulose-based thermoplastic plastics and elastomers via homogeneous controlled radical polymerizations (CRPs), including atom transfer radical polymerization (ATRP), reversible addition-fragmentation chain transfer (RAFT) polymerization, and nitroxide-mediated polymerization (NMP). The first section is a brief introduction of cellulose and cellulose graft copolymers. The second section is recent developments in cellulose graft copolymers synthesized by CRPs. The third part is a perspective on design and applications of novel cellulose-based materials. The combination of cellulose and CRPs can provide new opportunities for sustainable materials ranging from thermoplastics to elastomers, and these fascinating materials can find a pyramid of applications in our daily life in the near future.

Keywords: cellulose, graft copolymers, controlled radical polymerization, thermoplastics, elastomers

1. Introduction

As the most abundant biomaterial on earth, cellulose has received enormous attention due to its wide applications in different fields, such as packaging [1], drug delivery [2], cosmetics [3], textiles [4], membranes [5], bioengineering [6], and electronics [7]. Cellulose has some outstanding advantages, including low cost, non-toxicity, good mechanical properties, and excellent biodegradability and biocompatibility [8]. However, cellulose is lack of thermoplasticity and shows poor dimensional stability and crease resistance. Due to the high crystallinity and presence of a large amount of intra- and inter-molecular hydrogen bonding, cellulose is difficult to be dissolved in common solvents [9]. Different solvent systems have been proposed to dissolve cellulose, including *N,N*-dimethylacetamide (DMAc)/lithium chloride (LiCl) [10], dimethyl sulfoxide (DMSO)/tetrabutylammonium fluoride (TBAF) [11], *N,N*-dimethylformamide (DMF)/dinitrogen tetroxide (N_2O_4) [12], *N*-methyl morpholine-*N*-oxide (NMMO) [13], alkali/urea aqueous [14], and ionic liquids [15]. The existence of three hydroxyl groups in each anhydroglucose repeating unit makes cellulose an active material to develop various derivatives via etherification [16], esterification [17], amination [18], carboxylation [19], carbanilation [20], acetylation [21], grafting [22], sulfation [23], and silylation [24]. It is worth noting that the hydroxyl group in the 6 position of cellulose is most

reactive, followed by the hydroxyl groups at 2 and 3 positions. The degree of substitution (DS) indicated the substituted number of hydroxyl group in anhydroglucose unit (AGU).

Cellulose graft copolymers, which combine cellulose and grafted side chains in one macromolecule can open new opportunities toward developing novel bio-based materials with tunable properties. Cellulose graft copolymers can be achieved with grafting-to, grafting-through, and grafting-from strategies [25]. Among these methods, the grafting-from strategy is the most effective route for designing cellulose graft copolymers from thermoplastics to thermoplastic elastomers. Atom transfer radical polymerization (ATRP) [26, 27], reversible addition-fragmentation chain transfer (RAFT) [28, 29] polymerization, and nitroxide-mediated polymerization (NMP) [30, 31] are well-established controlled radical polymerizations (CRPs) that can be performed to prepare cellulose-based copolymers with well-defined structures and narrow molecular weight distributions in both heterogeneous and homogeneous conditions. This chapter summarizes recent advances that have been made in cellulose-based thermoplastics and elastomers from native cellulose via homogeneous CRPs.

2. Cellulose graft copolymers via homogeneous CRPs

2.1 Atom transfer radical polymerization (ATRP)

ATRP is the most used grafting method to prepare graft copolymers with cellulose-based macroinitiators and transition-metal catalysts. In general, the macroinitiators can be prepared by substituting the hydroxyl groups on cellulose backbone with chlorine or bromine-contained compounds. As shown in **Figure 1**, the macroinitiators, cellulose 2-bromopropionate (Cell-Bp), cellulose 2-bromoisobutyrylate (Cell-BiB), and cellulose chloroacetyl (Cell-ClAc) can be synthesized by reacting cellulose with 2-bromopropionyl bromide, 2-bromoisobutyryl bromide, and chloroacetyl chloride in 1-allyl-3-methylimidazolium chloride (AMIMCl),

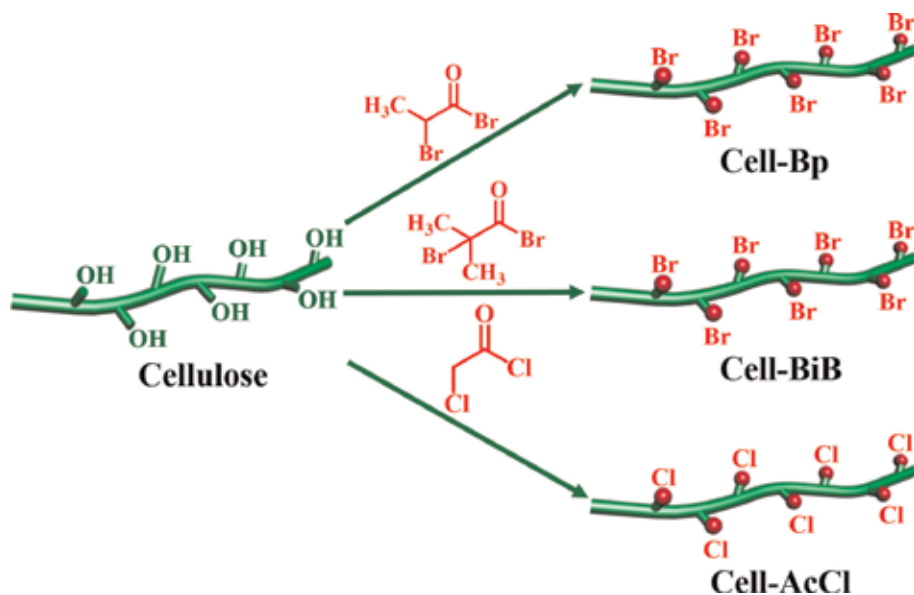


Figure 1.
Illustration for the synthesis of cellulose-based macroinitiators.

1-allyl-3-methylimidazolium chloride (BMIMCl) or DMAc/LiCl solution [32–37] under homogeneous conditions. The solubility of cellulose-based macroinitiator is strongly related to the DS of acylation, which can be adjusted by the molar ratio of acylating agent/AGU and reaction time [35, 38–40]. Therefore, it is flexible and convenient to prepare cellulose graft copolymers with controlled grafting density. Different solvents have been utilized as the media to synthesize cellulose graft copolymers via ATRP, including DMF, DMSO, 1,4-dioxane, AMIMCl, and BMIMCl. Moreover, varied catalyst systems, such as copper(I) chloride/2,2'-bipyridine (CuCl/bpy), CuCl/tris(2-(dimethylamino)ethyl)amine (CuCl/Me₆TREN), copper(I) bromide/bpy (CuBr/bpy), CuCl/*N,N,N',N''*-pentamethyldiethylenetriamine (CuCl/PMDETA), CuBr/PMDETA, CuBr/ethylenediamine, and CuBr/diethylenetriamine (CuBr/DETA), have been reported to control the grafting polymerization initiated by cellulose macroinitiator. During polymerization, the attached bromine or chlorine groups on cellulose macroinitiators can undergo a reversible redox process with metal catalysts and thus form active radicals to react and propagate with monomers. The active radicals can capture the halide ions from the oxidized metal complex to form activators and dormant halide species which can be reactivated. When polymerization is finished, the resultant cellulose graft copolymer can be obtained by removing the metal catalyst and precipitating into a poor solvent.

ATRP can be performed to synthesize different kinds of thermoplastics and elastomeric polymers due to its high tolerance. As displayed in **Figure 2**, a variety of vinyl and acrylate monomers, including methyl methacrylate (MMA) [33, 35, 37, 41–44], *N*-isopropylacrylamide (NIPAM) [45–48], 2-methacryloyloxyethyl phosphorylcholine (MPC) [32], styrene (St) [35, 42], *n*-butyl acrylate (BA) [44], *tert*-butyl acrylate (*t*BA) [49, 50], 4-vinylpyridine (4-VP) [49, 51], acrylamide (AM) [40], 3-ethyl-3-methacryloyloxy-methyloxetane (EMO) [12], *N*,

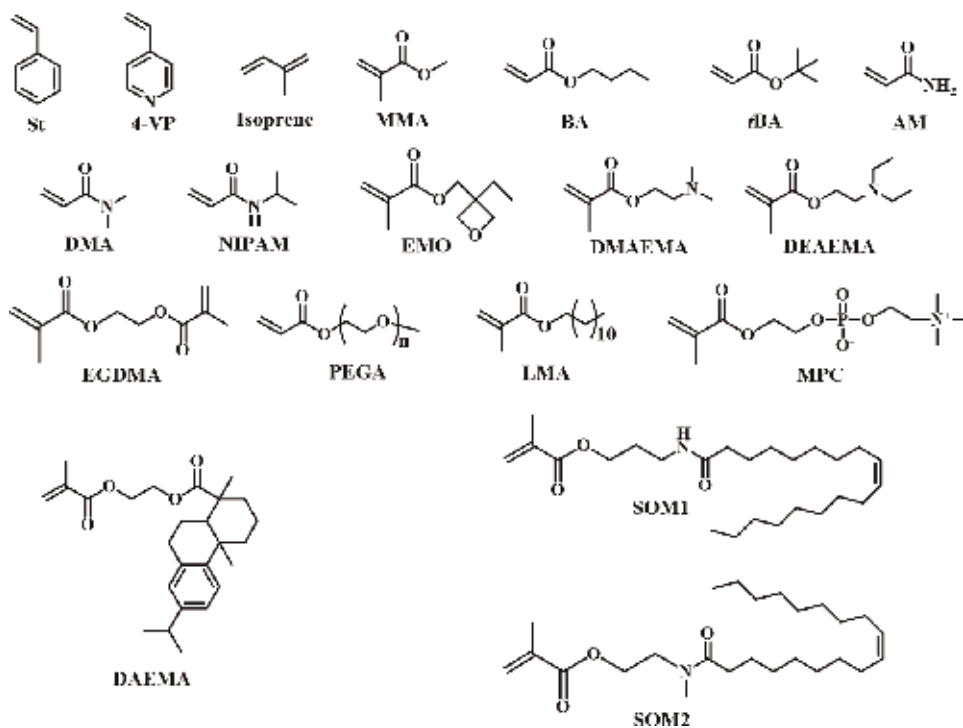


Figure 2. Monomers have been used to prepare cellulose graft copolymers via ATRP strategy in homogeneous conditions.

N-dimethylamino-2-ethyl methacrylate (DMAEMA) [34, 52], *N,N*-dimethylacrylamide (DMA) [40, 53–55], 2-(diethylamino)ethyl methacrylate (DEAEMA) [56], poly(ethylene glycol) methyl ether acrylate (PEGA) [57], isoprene [36, 58, 59], ethylene glycol dimethacrylate (EGDMA) [60], soybean oil-based methacrylates (SOM1 and SOM2) [61], lauryl methacrylate (LMA), and dehydroabiatic ethyl methacrylate (DAEMA) [62], have been grafted from cellulose via homogeneous ATRP to develop novel cellulose graft copolymers.

Thermoplastics and elastomers are essential polymeric materials in our daily life, and they are commercially available and can be used in diverse areas, such as household goods, clothing, packaging, auto parts, electronics, sensors, drug delivery, seals, foods, and tissue engineering [63–73]. Cellulose is an interesting natural polymeric material with high strength and durability. The marriage of cellulose and synthetic polymers can promote the development of novel thermoplastics and elastomers with excellent thermal and mechanical properties. Cellulose chains can be used as rigid backbones to design high-performance elastomers. As shown in **Figure 3**, Cell-*g*-P(BA-*co*-MMA) copolymer thermoplastic elastomers (TPEs) or cross-linked Cell-*g*-PI brush polymer elastomers (CBPs) were fabricated in our group via activators regenerated by electron transfer for atom transfer radical polymerization (ARGET ATRP) or combination of ARGET ATRP and activators regenerated by electron transfer for atom transfer radical coupling (ARGET ATRC)

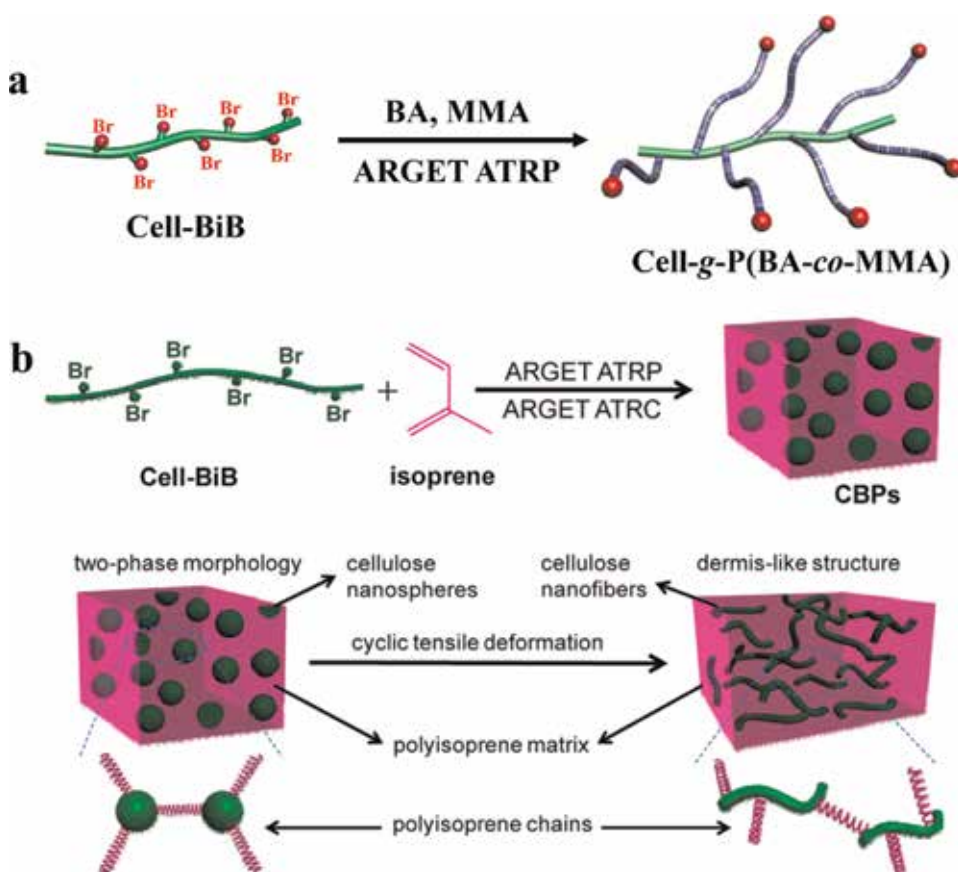


Figure 3. (a) Illustration for synthesis of Cell-*g*-P(BA-*co*-MMA) as TPEs via ARGET ATRP (adapted with permission from Ref. [44]). (b) Design concept of CBPs via ARGET ATRP and subsequent ARGET ATRC (adapted with permission from Ref. [58]).

[44, 58]. The design concept of cellulose graft elastomers is to graft soft rubbery random polymer matrixes from cellulose backbones, and these rigid backbones can act as minority physical cross-linking points to significantly enhance the macroscopic mechanical properties of resultant elastomer materials. The tensile strength, extensibility, and elasticity can be systematically tuned by adjusting the composition and molecular weight of the grafted side chains during polymerization. ARGET ATRP was selected because of the relatively low catalyst concentration and simple purification process. Such kind of multigraft architectures can bring up huge impacts on developing new-generation sustainable thermoplastics and elastomers by elaborate molecular design with renewable resource derived monomers [74, 75].

Novel renewable polymers derived from resources have opened the door for sustainable science and engineering. Plant oils, which can be produced from different plants, such as palm, coconut, sunflower, olive, soy, and peanut, are typical natural resources for the chemical industry [76]. By reacting with (meth)acryloyl chloride or methacrylate anhydride, plant oils can be transformed into polymerizable monomers for free radical polymerization. Recently, two soybean oil-based sustainable monomers, SOM1 and SOM2, were designed and used by Wang and coworkers to produce Cell-*g*-P(SOM1-*co*-SOM2) copolymers via ATRP [61]. By changing the molar ratios of SOM1/SOM2 during grafting polymerization, the glass transition temperatures (T_g s) of resultant cellulose graft copolymers varied from 40.7 to -0.7°C . For comparison purpose, they also synthesized linear P(SOM1-*co*-SOM2) copolymers as counterparts via free radical polymerization. However, the T_g values are located in the range from -6.9 to 30.6°C , which were much lower than the values of corresponding graft counterparts. In cellulose graft copolymers, the chain mobility of P(SOM1-*co*-SOM2) side chains was significantly reduced due to the presence of rigid cellulose backbones and hydrogen bonding formed by hydroxyl groups on cellulose and amide groups on side chains. These transparent Cell-*g*-P(SOM1-*co*-SOM2) films show different mechanical behaviors from thermoplastics to elastomers, depending on the composition of grafted chains and cellulose content. The incorporation of cellulose as the backbone in graft copolymers could significantly enhance the tensile strength and Young's modulus, since the corresponding linear counterparts showed much poorer mechanical properties. The combination of two kinds of distinct natural resources, cellulose and soy oils, is a promising area for developing fantastic biomaterials. Moreover, cellulose graft copolymers can also be used as templates for the synthesis of diverse one-dimensional (1D) nanocrystals with precisely controlled dimensions and compositions, including plain nanorods, core-shell nanorods, and nanotubes. In this work, cellulose-based bottlebrush-like block copolymers synthesized by sequential ATRP were applied as amphiphilic unimolecular nanoreactors to develop well-defined nanorod materials, which can find various applications in electronics, optics, sensors, optoelectronics, catalysis, and magnetic technologies [49].

It is convenient to graft polymers with apparently opposite physical properties by grafting from strategy via ATRP and thus to form self-induced nanostructures in bulk or in solutions. As shown in **Figure 4**, cellulose-*g*-polyisoprene (Cell-*g*-PI) composed of flexible and hydrophobic polyisoprene (PI) grafts and rigid and hydrophobic cellulose backbone synthesized via ATRP can be self-organized into core-shell nanostructures by a simple solvent-evaporation process [36]. In the past two decades, stimuli-responsive molecular brushes composed of a backbone and densely grafted side chains, which are sensitive to small external changes, such as pH, temperature, and ionic strength, have received increased attention due to their unique stimuli-responsive properties [77]. Cellulose-based polymeric micelles can be applied in drug deliveries by introducing functional polymers with good environmental sensitivities, hydrophilicity, and biocompatibility, such as poly

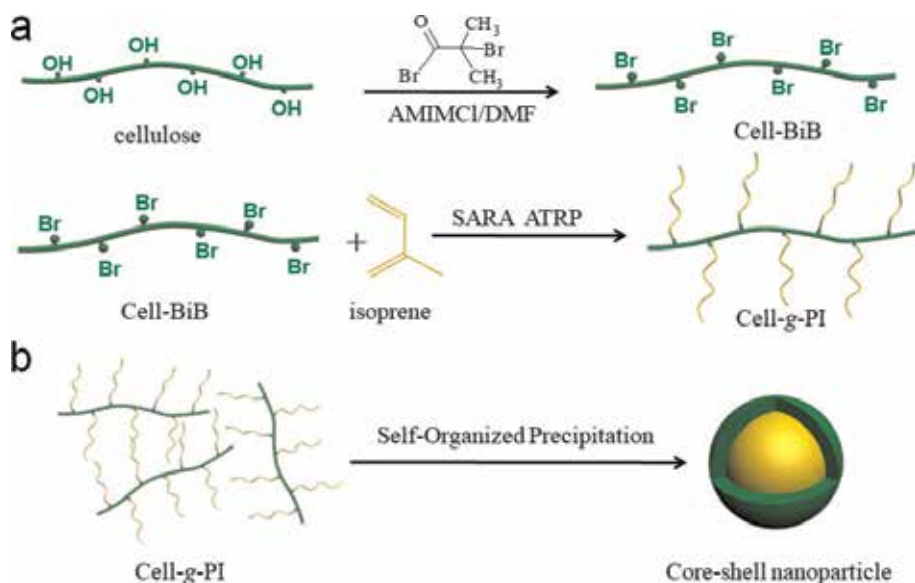


Figure 4. (a) Schematic illustration of the synthesis of Cell-g-PI by ATRP and (b) fabrication of Cell-g-PI core-shell nanoparticles with a PI core and cellulose shell (adapted with permission from Ref. [36]).

(*N*-isopropylacrylamide) (PNIPAM) [45–48], poly(4-vinylpyridine) (P4VP) [51], poly(*N,N*-dimethylamino-2-ethyl methacrylate) (PMDAEMA) [34], and poly(2-(diethylamino)ethyl methacrylate) (PDEAEMA) [56].

2.2 Reversible addition-fragmentation chain transfer (RAFT) polymerization

RAFT polymerization is an alternative method to synthesize well-defined and narrow distributed polymers with complex topological architectures by choosing a proper chain transfer agent (CTA). RAFT polymerization can be conducted without using any metal catalyst, and thus it is convenient and easy to purify the resultant polymers, which is the biggest advantage over ATRP. To date, only limited attention has been paid to cellulose graft copolymers through homogeneous RAFT polymerization in the literature [78–81]. The combination of cellulose and RAFT polymerization can provide new opportunities for graft copolymers, especially those that could not be synthesized directly via ATRP strategy. Recently, our group designed a novel cellulose-based macromolecular chain transfer agent by introducing a trithiocarbonate derivative with dodecyl as stabilizing group on cellulose backbone from Cell-BiB for the synthesis of Cell-g-P(BA-*co*-AM) copolymers as strong materials from thermoplastics to elastomers via RAFT polymerization [82]. As shown in **Figure 5**, the bromine groups on Cell-BiB can be substituted by reacting with 1-dodecanethiol, carbon disulfide (CS₂), and triethylamine (TEA) in DMSO. This Cell-CTA is versatile and suitable for a lot of monomers, and the DS of Cell-CTA can be manipulated by changing the molar ratios of above chemical reagents. AM and BA were chosen as the rigid and soft segments in the grafted side chains. PAM can provide reversible physical network structure in the cellulose graft copolymers. The N—H and C=O groups in AM units can form strong self-complementary hydrogen bonds, and they are distributed homogeneously in the polymer matrix, leading to the strong and tough elastomer materials. Inspired by this work, we propose that high-performance cellulose graft copolymer can be

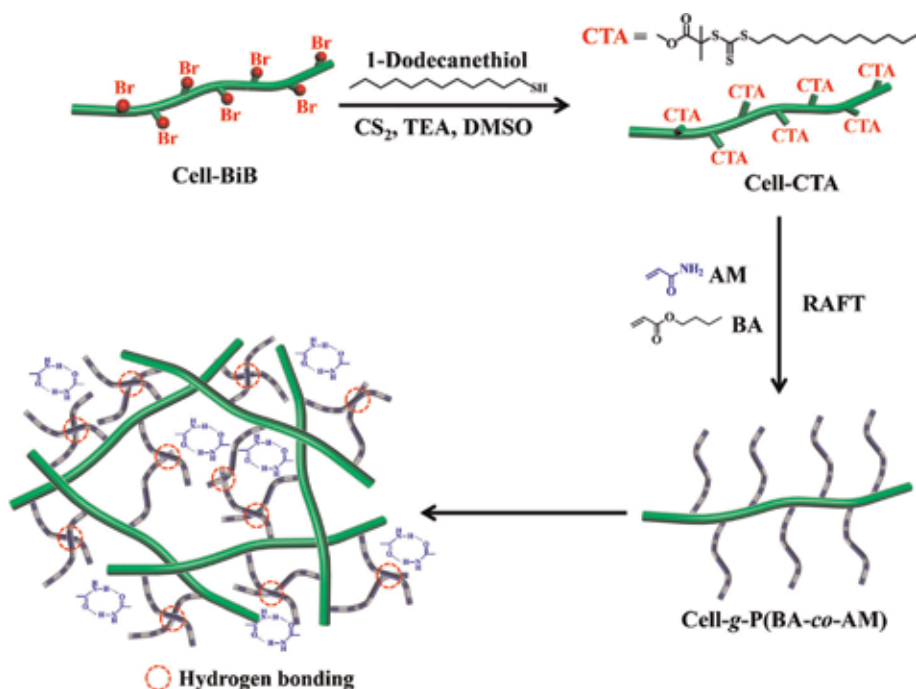


Figure 5. Illustrations for the synthesis of Cell-CTA, Cell-g-P(BA-co-AM) copolymer, and the self-complementary hydrogen bonding in the cellulose graft copolymer (adapted from Ref. [82]).

accessed by introducing other supramolecular interactions into the matrix as reversible physical networks, such as metal-ligand coordination, π - π stacking, and host-guest complexation.

2.3 Nitroxide-mediated polymerization (NMP)

NMP is the first and easiest CRP technology controlled by a reversible termination mechanism between the nitroxide moieties and growing propagating macroradicals. A wide range of monomers, including acrylates, styrene derivatives, vinylpyridines, acrylonitrile, acryl acid, acrylamide derivatives, cyclic ketene acetals, and miscellaneous, can be polymerized via NMP to develop well-defined polymers [31]. The primary advantage of NMP is the absence of post-treatment since no catalyst or bimolecular exchange is needed during the polymerization. However, the higher polymerization temperatures and lower polymerization rates limit the wide applications of NMP. To the best of our knowledge, only one study reported the synthesis of cellulose graft copolymers through homogeneous NMP strategy started from microcrystalline cellulose [83]. In this work, pretreated cellulose was dispersed in anhydrous tetrahydrofuran and reacted with 2-bromoisobutyryl bromide and pyridine to prepare Cell-BiB. As shown in **Figure 6**, Cell-BiB could react with 4-hydroxy-2,2,6,6-tetramethylpiperidin-1-oxyl (TEMPO) in DMF in the presence of sodium hydride (NaH) to obtain functionalized cellulose (Cell-TEMPO). At first, PS was grafted from cellulose backbone with Cell-TEMPO as macroinitiator in the absence of any catalyst to produce Cell-g-PS. Cell-g-(PMMA-*b*-PS) copolymer was synthesized by chain extension of above Cell-g-PS via the second NMP. Such kind of cellulose graft block copolymers may be applied as reinforcing agents, packing materials, and membrane materials. More efforts can be

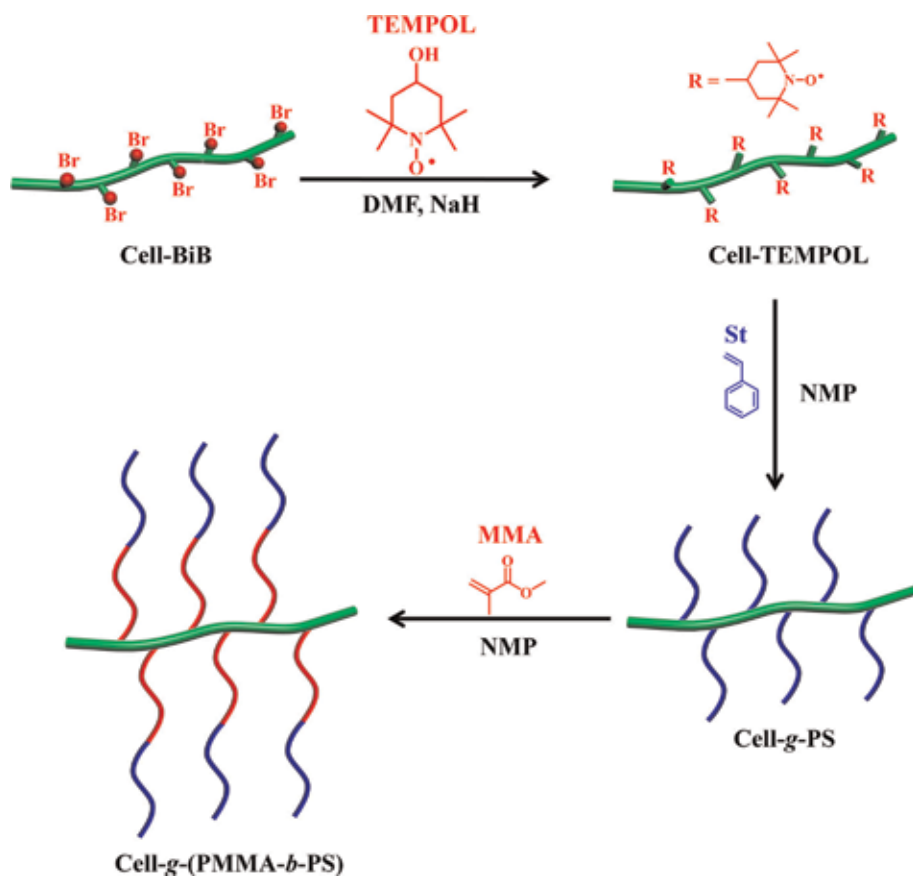


Figure 6. Schematic illustration for the synthesis of Cell-g-PS and Cell-g-(PMMA-b-PS) copolymers through NMP technique.

made in the future by grafting functional block polymers from cellulose via NMP to design novel stimuli-responsive hybrid materials with excellent macroscopic mechanical properties.

3. Perspective

CRPs are versatile and robust techniques to develop well-defined cellulose graft copolymers as novel thermoplastic and elastomers with desired properties for particular application demands. As the most adopted technique for cellulose graft copolymers, conventional ATRP suffers from the limitation of removing metal catalysts from the resultant products, which may cause undesired toxicity and coloration. Recently, new advances in ARTP have been reported, and metal-free ATRP has been developed to synthesize narrowly distributed polymers with well-defined structures by using photoredox organic catalysts under light irradiation instead of metal catalysts [84–86]. This new strategy can greatly promote the design and preparation of cellulose graft copolymers for different application fields. Cellulose graft copolymers show improved properties compared to the linear counterparts due to their unique molecular architectures, and the macroscopic performance of cellulose graft copolymers is affected by the degree of polymerization of cellulose

backbone, the grafting density (the average number of grafts per anhydroglucose unit), the degree of polymerization, and distribution of grafts. Various block and random copolymers have been grafted from cellulose via CRPs as described above. However, as exhibited in **Figure 7a**, heterograft and graft-on-graft architectures with cellulose as backbone remain unreported, and these interesting graft copolymers can be synthesized by the combination of RAFT polymerization and ATRP, ring-opening polymerization (ROP) and ATRP or ROP and RAFT polymerization.

Due to the increased attention paid on biomass-derived thermoplastics and elastomers, it becomes necessary and desirable to explore new monomers, which can be synthesized from bioresources, including lignins, terpenes, plant oils, rosin acids, and coumarins. For instance, bioresources, 7-hydroxyl-4-methylcoumarin, vanillin, guaiacol, and oleyl alcohol, can be used to synthesize sustainable monomers by reacting with acryloyl chloride, methacryloyl chloride or methacrylate anhydride as shown in **Figure 7b**. Among these monomers, 7-acryloyloxy-4-methylcoumarin (AMC), 7-methacryloyloxy-4-methylcoumarin (MMC), acrylated vanillin (AV), methacrylated vanillin (MV), acrylated guaiacol (AG), and methacrylated guaiacol (MG) can be utilized as rigid segments, while oleyl acrylate (OA) and oleyl methacrylate (OM) can be utilized as soft segments in the graft copolymers. Though there has been considerable progress, it is still challenging to

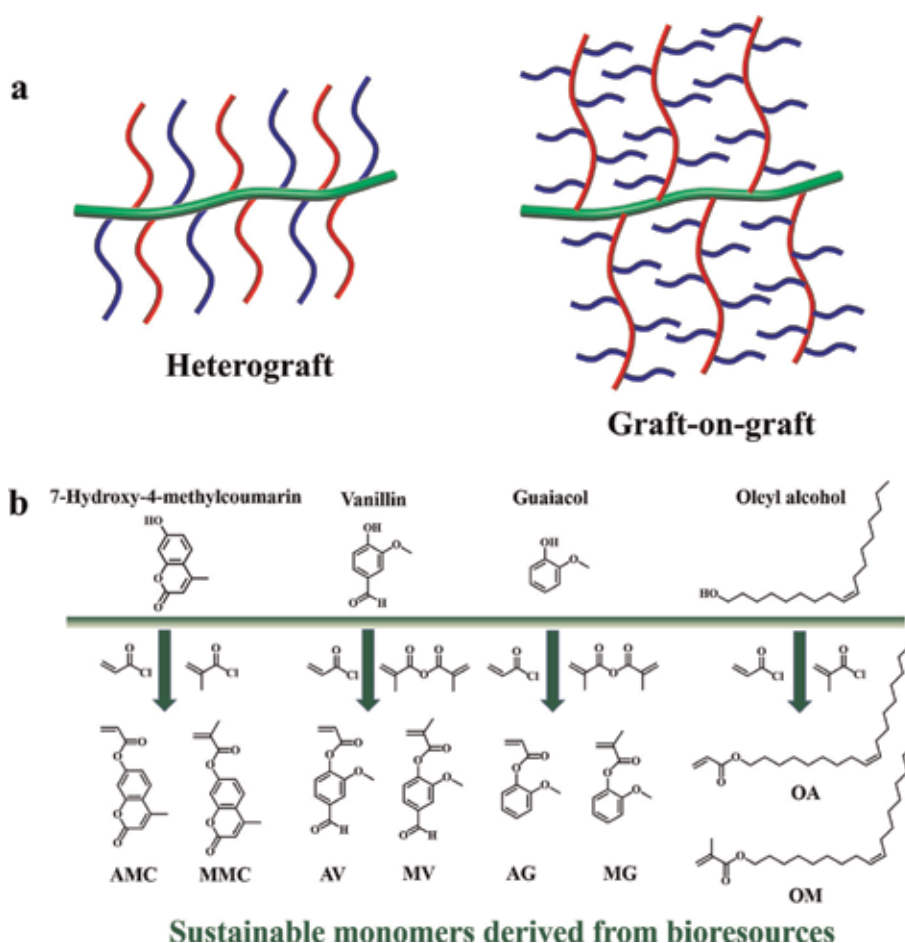


Figure 7. (a) Heterograft and graft-on-graft architectures of cellulose graft copolymers. (b) Sustainable monomers derived from different bioresources.

achieve breakthroughs for the development of cellulose graft copolymers with ultra-strong mechanical properties comparable to commercial petroleum-based products. The marriage of cellulose and novel bio-based monomers via CRPs can provide a variety of opportunities for sustainable materials ranging from thermoplastics to elastomers, and these fascinating materials can find a pyramid of applications in our daily life in the near future.

Acknowledgements

This work was supported by the National Natural Science Foundation of China (Grants 51603199 and 21776049) and China Postdoctoral Science Foundation (Grant 2017M622629).

Conflict of interest


The authors declare no conflict of interest.

Author details

Feng Jiang*, Fenfen Wang, Chenqian Pan and Yanxiong Fang*
School of Chemical Engineering and Light Industry, Guangdong University of Technology, Guangzhou, Guangdong, China

*Address all correspondence to: jiangf@gdut.edu.cn and fangyx@gdut.edu.cn

IntechOpen

© 2019 The Author(s). Licensee IntechOpen. This chapter is distributed under the terms of the Creative Commons Attribution License (<http://creativecommons.org/licenses/by/3.0>), which permits unrestricted use, distribution, and reproduction in any medium, provided the original work is properly cited. 

References

- [1] Spence KL, Venditti RA, Rojas OJ, Habibi Y, Pawlak JJ. The effect of chemical composition on microfibrillar cellulose films from wood pulps: Water interactions and physical properties for packaging applications. *Cellulose*. 2010; **17**:835-848. DOI: 10.1007/s10570-010-9424-8
- [2] Amin MCIM, Ahmad N, Halib N, Ahmad I. Synthesis and characterization of thermo- and pH-responsive bacterial cellulose/acrylic acid hydrogels for drug delivery. *Carbohydrate Polymers*. 2012; **88**:465-473. DOI: 10.1016/j.carbpol.2011.12.022
- [3] Ullah H, Santos HA, Khan T. Applications of bacterial cellulose in food, cosmetics and drug delivery. *Cellulose*. 2016; **23**:2291-2314. DOI: 10.1007/s10570-016-0986-y
- [4] Forsman N, Lozhechnikova A, Khakalo A, Johansson LS, Vartiainen J, Österberg M. Layer-by-layer assembled hydrophobic coatings for cellulose nanofibril films and textiles, made of polylysine and natural wax particles. *Carbohydrate Polymers*. 2017; **173**: 392-402. DOI: 10.1016/j.carbpol.2017.06.007
- [5] Livazovic S, Li Z, Behzad AR, Peinemann KV, Nunes SP. Cellulose multilayer membranes manufacture with ionic liquid. *Journal of Membrane Science*. 2015; **490**:282-293. DOI: 10.1016/j.memsci.2015.05.009
- [6] Zhang QL, Lin DQ, Yao SJ. Review on biomedical and bioengineering applications of cellulose sulfate. *Carbohydrate Polymers*. 2015; **132**: 311-322. DOI: 10.1016/j.carbpol.2015.06.041
- [7] Jung YH, Chang TH, Zhang HL, Yao CH, Zheng QF, Yang VW, et al. High-performance green flexible electronics based on biodegradable cellulose nanofibril paper. *Nature Communications*. 2015; **6**:7170. DOI: 10.1038/ncomms8170
- [8] Moon RJ, Martini A, Nairn J, Simonsen J, Youngblood J. Cellulose nanomaterials review: Structure, properties and nanocomposites. *Chemical Society Reviews*. 2011; **40**:3941-3994. DOI: 10.1039/c0cs00108b
- [9] Zhang X, Mao YM, Tyagi M, Jiang F, Henderson D, Jiang B, et al. Molecular partitioning in ternary solutions of cellulose. *Carbohydrate Polymers*. 2019; **220**:157-162. DOI: 10.1016/j.carbpol.2019.05.054
- [10] Araki J, Kataoka T, Katsuyama N, Teramoto A, Ito K, Abe K. A preliminary study for fiber spinning of mixed solutions of polyrotaxane and cellulose in a dimethylacetamide/lithium chloride (DMAC/LiCl) solvent system. *Polymer*. 2006; **47**:8241-8246. DOI: 10.1016/j.polymer.2006.09.060
- [11] Ostlund Å, Lundberg D, Nordstierna L, Holmberg K, Nydén M. Dissolution and gelation of cellulose in TBAF/DMSO solutions: The roles of fluoride ions and water. *Biomacromolecules*. 2009; **10**: 2401-2407. DOI: 10.1021/bm900667q
- [12] Philipp B, Nehls I, Wagenknecht W, Schnabelrauch M. ¹³C-NMR spectroscopic study of the homogeneous sulphation of cellulose and xylan in the N₂O₄-DMF system. *Carbohydrate Research*. 1987; **164**:107-116. DOI: 10.1016/0008-6215(87)80123-4
- [13] Rosenau T, Potthast A, Sixta H, Kosma P. The chemistry of side reactions and byproduct formation in the system NMMO/cellulose (Lyocell process). *Progress in Polymer Science*. 2001; **26**:1763-1837. DOI: 10.1016/S0079-6700(01)00023-5

- [14] Cai J, Zhang LN. Unique gelation behavior of cellulose in NaOH/urea aqueous solution. *Biomacromolecules*. 2006;7:183-189. DOI: 10.1021/bm0505585
- [15] Pinkert A, Marsh KN, Pang SS, Staiger MP. Ionic liquids and their interaction with cellulose. *Chemical Reviews*. 2009;109:6712-6728. DOI: 10.1021/cr9001947
- [16] Fox SC, Li B, Xu DQ, Edgar KJ. Regioselective esterification and etherification of cellulose: A review. *Biomacromolecules*. 2011;12:1956-1972. DOI: 10.1021/bm200260d
- [17] Satgé C, Verneuil B, Branland P, Granet R, Krausz P, Rozier J, et al. Rapid homogeneous esterification of cellulose induced by microwave irradiation. *Carbohydrate Polymers*. 2002;49:373-376. DOI: 10.1016/S0144-8617(02)00004-8
- [18] Yu TL, Liu SQ, Xu M, Peng J, Li JQ, Zhai ML. Synthesis of novel aminated cellulose microsphere adsorbent for efficient Cr(VI) removal. *Radiation Physics and Chemistry*. 2016;125:94-101. DOI: 10.1016/j.radphyschem.2016.03.019
- [19] Montanari S, Roumani M, Heux L, Vignon MR. Topochemistry of carboxylated cellulose nanocrystals resulting from TEMPO-mediated oxidation. *Macromolecules*. 2005;38:1665-1671. DOI: 10.1021/ma048396c
- [20] Barthel S, Heinze T. Acylation and carbanilation of cellulose in ionic liquids. *Green Chemistry*. 2006;8:301-306. DOI: 10.1039/B513157J
- [21] Wu J, Zhang J, Zhang H, He JS, Ren Q, Guo ML. Homogeneous acetylation of cellulose in a new ionic liquid. *Biomacromolecules*. 2004;5:266-268. DOI: 10.1021/bm034398d
- [22] Carlmark A, Larsson E, Malmström E. Grafting of cellulose by ring-opening polymerisation-a review. *European Polymer Journal*. 2012;48:1646-1659. DOI: 10.1016/j.eurpolymj.2012.06.013
- [23] Horikawa M, Fujiki T, Shiroasaki T, Ryu N, Sakurai H, Nagaoka S, et al. The development of a highly conductive PEDOT system by doping with partially crystalline sulfated cellulose and its electric conductivity. *Journal of Materials Chemistry C*. 2015;3:8881-8887. DOI: 10.1039/c5tc02074c
- [24] Zhang Z, Tingaut P, Rentsch D, Zimmermann T, Sèbe G. Controlled silylation of nanofibrillated cellulose in water: Reinforcement of a model polydimethylsiloxane network. *ChemSusChem*. 2015;8:2681-2690. DOI: 10.1002/cssc.201500525
- [25] Roy D, Semsarilar M, Guthrie JT, Perrier S. Cellulose modification by polymer grafting: A review. *Chemical Society Reviews*. 2009;38:2046-2064. DOI: 10.1039/b808639g
- [26] Matyjaszewski K. Atom transfer radical polymerization (ATRP): Current status and future perspectives. *Macromolecules*. 2012;45:4015-4039. DOI: 10.1021/ma3001719
- [27] Siegwart DJ, Oh JK, Matyjaszewski K. ATRP in the design of functional materials for biomedical applications. *Progress in Polymer Science*. 2012;37:18-37. DOI: 10.1016/j.progpolymsci.2011.08.001
- [28] Chiefari J, Chong YK, Ercole F, Krstina J, Jeffery J, Le TP, et al. Living free-radical polymerization by reversible addition-fragmentation chain transfer: The RAFT process. *Macromolecules*. 1998;31:5559-5562. DOI: 10.1021/ma9804951
- [29] Boyer C, Bulmus V, Davis TP, Ladmiral V, Liu JQ, Perrier S. Bioapplications of RAFT polymerization. *Chemical Reviews*.

2009;**109**:5402-5436. DOI: 10.1021/cr9001403

[30] Hawker CJ, Bosman AW, Harth E. New polymer synthesis by nitroxide mediated living radical polymerizations. *Chemical Reviews*. 2001;**101**:3661-3688. DOI: 10.1021/cr990119u

[31] Nicolas J, Guillauneuf Y, Lefay C, Bertin D, Gimes D, Charleux B. Nitroxide-mediated polymerization. *Progress in Polymer Science*. 2013;**38**: 63-235. DOI: 10.1016/j.progpolymsci.2012.06.002

[32] Yan LF, Ishihara K. Graft copolymerization of 2-methacryloyloxyethyl phosphorylcholine to cellulose in homogeneous media using atom transfer radical polymerization for providing new hemocompatible coating materials. *Journal of Polymer Science Part A: Polymer Chemistry*. 2008;**46**: 3306-3313. DOI: 10.1002/pola.22670

[33] Chang FX, Yamabuki K, Onimura K, Oishi T. Modification of cellulose by using atom transfer radical polymerization and ring-opening polymerization. *Polymer Journal*. 2008; **40**:1170. DOI: 10.1295/polymj. PJ2008136

[34] Sui XF, Yuan JY, Zhou M, Zhang J, Yang HJ, Yuan WZ, et al. Synthesis of cellulose-*graft*-poly(*N,N*-dimethylamino-2-ethyl methacrylate) copolymers via homogeneous ATRP and their aggregates in aqueous media. *Biomacromolecules*. 2008;**9**:2615-2620. DOI: 10.1021/bm800538d

[35] Meng T, Gao X, Zhang J, Yuan JY, Zhang YZ, He JS. Graft copolymers prepared by atom transfer radical polymerization (ATRP) from cellulose. *Polymer*. 2009;**50**:447-454. DOI: 10.1016/j.polymer.2008.11.011

[36] Wang ZK, Zhang YQ, Jiang F, Fang HG, Wang ZG. Synthesis and characterization of designed cellulose-

graft-polyisoprene copolymers. *Polymer Chemistry*. 2014;**5**:3379-3388. DOI: 10.1039/c3py01574b

[37] Lin CX, Zhan HY, Liu MH, Fu SY, Zhang JJ. Preparation of cellulose graft poly(methyl methacrylate) copolymers by atom transfer radical polymerization in an ionic liquid. *Carbohydrate Polymers*. 2009;**78**:432-438. DOI: 10.1016/j.carbpol.2009.04.032

[38] Wang HL, Fu YJ, Wang ZF, Shao ZY, Qin MH. Regioselectivity in the acylation of cellulose with 2-bromoisobutyryl bromide under homogeneous conditions. *Cellulose Chemistry and Technology*. 2017;**51**: 11-21

[39] Fu YJ, Li GB, Wang RR, Zhang FS, Qin MH. Effect of the molecular structure of acylating agents on the regioselectivity of cellulosic hydroxyl groups in ionic liquid. *BioResources*. 2017;**12**:992-1006. DOI: 10.15376/biores.12.1.992-1006

[40] Hiltunen MS, Raula J, Maunu SL. Tailoring of water-soluble cellulose-*g*-copolymers in homogeneous medium using single-electron-transfer living radical polymerization. *Polymer International*. 2011;**60**:1370-1379. DOI: 10.1002/pi.3090

[41] Xin TT, Yuan TQ, Xiao S, He J. Synthesis of cellulose-*graft*-poly(methyl methacrylate) via homogeneous ATRP. *BioResources*. 2011;**6**:2941-2953

[42] Raus V, Štěpánek M, Uchman M, Šlouf M, Látalová P, Čadová E, et al. Cellulose-based graft copolymers with controlled architecture prepared in a homogeneous phase. *Journal of Polymer Science Part A: Polymer Chemistry*. 2011;**49**:4353-4367. DOI: 10.1002/pola.24876

[43] Zhong JF, Chai XS, Fu SY. Homogeneous grafting poly(methyl methacrylate) on cellulose by atom transfer radical polymerization.

- Carbohydrate Polymers. 2012;**87**: 1869-1873. DOI: 10.1016/j.carbpol.2011.07.037
- [44] Jiang F, Wang ZK, Qiao YL, Wang ZG, Tang CB. A novel architecture toward third-generation thermoplastic elastomers by a grafting strategy. *Macromolecules*. 2013;**46**: 4772-4780. DOI: 10.1021/ma4007472
- [45] Ifuku S, Kadla JF. Preparation of a thermosensitive highly regioselective cellulose/*N*-isopropylacrylamide copolymer through atom transfer radical polymerization. *Biomacromolecules*. 2008;**9**:3308-3313. DOI: 10.1021/bm800911w
- [46] Cui GH, Li YH, Shi TT, Gao ZG, Qiu NN, Satoh T, et al. Synthesis and characterization of Eu(III) complexes of modified cellulose and poly(*N*-isopropylacrylamide). *Carbohydrate Polymers*. 2013;**94**:77-81. DOI: 10.1016/j.carbpol.2013.01.045
- [47] Yang LL, Zhang JM, He JS, Zhang J, Gan ZH. Synthesis and characterization of temperature-sensitive cellulose-*graft*-poly(*N*-isopropylacrylamide) copolymers. *Chinese Journal of Polymer Science*. 2015;**33**:1640-1649. DOI: 10.1007/s10118-015-1703-2
- [48] Liu YD, Huang GC, Pang YY, Han MM, Ji SX. One-pot synthesis of thermoresponsive cellulose-based miktoarm graft copolymer by simultaneous ATRP and ROP. *Journal of Renewable Materials*. 2015;**3**:113-119. DOI: 10.7569/JRM.2014.634141
- [49] Pang XC, He YJ, Jung J, Lin ZQ. 1d nanocrystals with precisely controlled dimensions, compositions, and architectures. *Science*. 2016;**353**: 1268-1272. DOI: 10.1126/science.aad8279
- [50] Chmielarz P. Cellulose-based graft copolymers prepared by simplified electrochemically mediated ATRP. *Express Polymer Letters*. 2017;**11**:140. DOI: 10.3144/expresspolymlett.2017.15
- [51] Du H, Han RT, Tang EJ, Zhou J, Liu SJ, Guo XF, et al. Synthesis of pH-responsive cellulose-*g*-P4VP by atom transfer radical polymerization in ionic liquid, loading, and controlled release of aspirin. *Journal of Polymer Research*. 2018;**25**:205. DOI: 10.1007/s10965-018-1601-8
- [52] Parviainen H, Hiltunen M, Maunu SL. Preparation and flocculation behavior of cellulose-*g*-PMOTAC copolymer. *Journal of Applied Polymer Science*. 2014;**131**:40448. DOI: 10.1002/app.40448
- [53] Hiltunen M, Siirilä J, Aseyev V, Maunu SL. Cellulose-*g*-PDMAam copolymers by controlled radical polymerization in homogeneous medium and their aqueous solution properties. *European Polymer Journal*. 2012;**48**:136-145. DOI: 10.1016/j.eurpolymj.2011.10.010
- [54] Hiltunen M, Siirilä J, Maunu SL. Effect of catalyst systems and reaction conditions on the synthesis of cellulose-*g*-PDMAam copolymers by controlled radical polymerization. *Journal of Polymer Science Part A: Polymer Chemistry*. 2012;**50**:3067-3076. DOI: 10.1002/pola.26092
- [55] Yan LF, Wei T. Graft copolymerization of *N,N*-dimethylacrylamide to cellulose in homogeneous media using atom transfer radical polymerization for hemocompatibility. *Journal of Biomedical Science and Engineering*. 2008;**1**:37. DOI: 10.4236/jbise.2008.11006
- [56] Tang EJ, Du KD, Feng XY, Yuan M, Liu SJ, Zhao DS. Controlled synthesis of cellulose-*graft*-poly[2-(diethylamino)-ethyl methacrylate] by ATRP in ionic liquid [AMIM]Cl and its pH-responsive property. *European Polymer Journal*.

2015;**66**:228-235. DOI: 10.1016/j.eurpolymj.2015.01.041

[57] Zhang YQ, Xu ZH, Wang ZK, Ding YS, Wang ZG. Strong enhancements of nucleation and spherulitic growth rates through amplified interfacial effects for immiscible linear polymer/comb-like copolymer double-layer films. RSC Advances. 2014;**4**:20582-20591. DOI: 10.1039/c4ra02167c

[58] Wang ZK, Jiang F, Zhang YQ, You YZ, Wang ZG, Guan ZB. Bioinspired design of nanostructured elastomers with cross-linked soft matrix grafting on the oriented rigid nanofibers to mimic mechanical properties of human skin. ACS Nano. 2015;**9**:271-278. DOI: 10.1021/nn506960f

[59] Wang ZK, Yuan L, Jiang F, Zhang YQ, Wang ZG, Tang CB. Bioinspired high resilient elastomers to mimic resilin. ACS Macro Letters. 2016;**5**:220-223. DOI: 10.1021/acsmacrolett.5b00843

[60] Zhou J, Tang EJ, Zhao L, Han RT, Liu SJ, Zhao DS. Adjustment of molecular weight for a cellulose-*graft*-poly(ethylene glycol dimethacrylate) polymer brush by atom transfer radical polymerization in an ionic liquid. Journal of Polymer Materials. 2018;**35**:245-256. DOI: 10.32381/JPM.2018.35.02.9

[61] Wu M, Zhang YQ, Peng Q, Song LZ, Hu ZG, Li Z, et al. Mechanically strong plant oil-derived thermoplastic polymers prepared via cellulose graft strategy. Applied Surface Science. 2018;**458**:495-502. DOI: 10.1016/j.apsusc.2018.07.072

[62] Liu YP, Yao KJ, Chen XM, Wang JF, Wang ZK, Ploehn HJ, et al. Sustainable thermoplastic elastomers derived from renewable cellulose, rosin and fatty acids. Polymer Chemistry. 2014;**5**:3170-3181. DOI: 10.1039/c3py01260c

[63] Puskas JE, Chen YH. Biomedical application of commercial polymers and novel polyisobutylene-based thermoplastic elastomers for soft tissue replacement. Biomacromolecules. 2004;**5**:1141-1154. DOI: 10.1021/bm034513k

[64] Adhikari B, Majumdar S. Polymers in sensor applications. Progress in Polymer Science. 2004;**29**:699-766. DOI: 10.1016/j.progpolymsci.2004.03.002

[65] Cheng YJ, Yang SH, Hsu CS. Synthesis of conjugated polymers for organic solar cell applications. Chemical Reviews. 2009;**109**:5868-5923. DOI: 10.1021/cr900182s

[66] Jiang F, Zhang YQ, Fang C, Wang ZK, Wang ZG. From soft to strong elastomers: The role of additional crosslinkings in copolymer-grafted multiwalled carbon nanotube composite thermoplastic elastomers. RSC Advances. 2014;**4**:60079-60085. DOI: 10.1039/c4ra11626g

[67] Jiang F, Zhang YQ, Wang ZK, Fang HG, Ding YS, Xu HX, et al. Synthesis and characterization of nanostructured copolymer-grafted multiwalled carbon nanotube composite thermoplastic elastomers toward unique morphology and strongly enhanced mechanical properties. Industrial and Engineering Chemistry Research. 2014;**53**:20154-20167. DOI: 10.1021/ie504005f

[68] Jiang F, Zhang YQ, Wang ZK, Wang WT, Xu ZH, Wang ZG. Combination of magnetic and enhanced mechanical properties for copolymer-grafted magnetite composite thermoplastic elastomers. ACS Applied Materials & Interfaces. 2015;**7**:10563-10575. DOI: 10.1021/acsami.5b02208

[69] Fang C, Zhang YQ, Wang WT, Wang ZK, Jiang F, Wang ZG. Fabrication of copolymer-grafted multiwalled carbon nanotube composite

- thermoplastic elastomers filled with unmodified MWCNTs as additional nanofillers to significantly improve both electrical conductivity and mechanical properties. *Industrial and Engineering Chemistry Research*. 2015;**54**:12597-12606. DOI: 10.1021/acs.iecr.5b03599
- [70] Jiang F, Fang C, Zhang J, Wang WT, Wang ZG. Triblock copolymer elastomers with enhanced mechanical properties synthesized by RAFT polymerization and subsequent quaternization through incorporation of a comonomer with imidazole groups of about 2.0 mass percentage. *Macromolecules*. 2017;**50**:6218-6226. DOI: 10.1021/acs.macromol.7b01414
- [71] Wang WT, Wang XH, Jiang F, Wang ZG. Synthesis, order-to-disorder transition, microphase morphology and mechanical properties of BAB triblock copolymer elastomers with hard middle block and soft outer blocks. *Polymer Chemistry*. 2018;**9**:3067-3079. DOI: 10.1039/C8PY00375K
- [72] Jiang F, Zhang X, Hwang W, Briber RM, Fang YX, Wang H. Supramolecular luminescent triblock copolymer thermoplastic elastomer via metal-ligand coordination. *Polymer Testing*. 2019;**78**:105956. DOI: 10.1016/j.polymertesting.2019.105956
- [73] Wang WT, Zhang J, Jiang F, Wang XH, Wang ZG. Reprocessable supramolecular thermoplastic BAB-type triblock copolymer elastomers with enhanced tensile strength and toughness via metal-ligand coordination. *ACS Applied Polymer Materials*. 2019;**1**:571-583. DOI: 10.1021/acscapm.8b00277
- [74] Wang ZK, Yuan L, Tang CB. Sustainable elastomers from renewable biomass. *Accounts of Chemical Research*. 2017;**50**:1762-1773. DOI: 10.1021/acs.accounts.7b00209
- [75] Wang WY, Lu W, Goodwin A, Wang HQ, Yin PC, Kang NG, et al. Recent advances in thermoplastic elastomers from living polymerizations: Macromolecular architectures and supramolecular chemistry. *Progress in Polymer Science*. 2019;**95**:1-31. DOI: 10.1016/j.progpolymsci.2019.04.002
- [76] Tschan MJ-L, Brulé E, Haquette P, Thomas CM. Synthesis of biodegradable polymers from renewable resources. *Polymer Chemistry*. 2012;**3**:836-851. DOI: 10.1039/C2PY00452F
- [77] Lee H, Pietrasik J, Sheiko SS, Matyjaszewski K. Stimuli-responsive molecular brushes. *Progress in Polymer Science*. 2010;**35**:24-44. DOI: 10.1016/j.progpolymsci.2009.11.002
- [78] Lin CX, Zhan HY, Liu MH, Habibi Y, Fu SY, Lucia LA. RAFT synthesis of cellulose-*g*-polymethylmethacrylate copolymer in an ionic liquid. *Journal of Applied Polymer Science*. 2013;**127**:4840-4849. DOI: 10.1002/app.38071
- [79] Hufendiek A, Trouillet V, Meier MA, Barner-Kowollik C. Temperature responsive cellulose-*graft*-copolymers via cellulose functionalization in an ionic liquid and RAFT polymerization. *Biomacromolecules*. 2014;**15**:2563-2572. DOI: 10.1021/bm500416m
- [80] Liu YD, Jin XS, Zhang XS, Han MM, Ji SX. Self-assembly and chiroptical property of poly(*N*-acryloyl-L-amino acid) grafted celluloses synthesized by raft polymerization. *Carbohydrate Polymers*. 2015;**117**:312-318. DOI: 10.1016/j.carbpol.2014.09.074
- [81] Ott MW, Herbert H, Graf M, Biesalski M. Cellulose-*graft*-polystyrene bottle-brush copolymers by homogeneous raft polymerization of soluble cellulose macro-ctas and “cta-shuttled” r-group approach. *Polymer*.

2016;**98**:505-515. DOI: 10.1016/j.
polymer.2016.05.006

[82] Jiang F, Pan CQ, Zhang YQ,
Fang YX. Cellulose graft copolymers
toward strong thermoplastic elastomers
via raft polymerization. *Applied Surface
Science*. 2019;**480**:162-171. DOI:
10.1016/j.apsusc.2019.02.210

[83] Karaj-Abad SG, Abbasian M,
Jaymand M. Grafting of poly[(methyl
methacrylate)-*block*-styrene] onto
cellulose via nitroxide-mediated
polymerization, and its polymer/clay
nanocomposite. *Carbohydrate
Polymers*. 2016;**152**:297-305. DOI:
10.1016/j.carbpol.2016.07.017

[84] Treat NJ, Sprafke H, Kramer JW,
Clark PG, Barton BE, Read de Alaniz J,
et al. Metal-free atom transfer radical
polymerization. *Journal of the American
Chemical Society*. 2014;**136**:
16096-16101. DOI: 10.1021/ja510389m

[85] Theriot JC, Lim C-H, Yang H,
Ryan MD, Musgrave CB, Miyake GM.
Organocatalyzed atom transfer radical
polymerization driven by visible light.
Science. 2016;**352**:1082-1086. DOI:
10.1126/science.aaf3935

[86] Lu CW, Wang CP, Yu J, Wang JF,
Chu FX. Metal-free ATRP “grafting
from” technique for renewable cellulose
graft copolymers. *Green Chemistry*.
2019;**21**:2759-2770. DOI: 10.1039/
C9GC00138G

Thermoplastic Recycling: Properties, Modifications, and Applications

Taofik Oladimeji Azeez

Abstract

The increasing rate of plastic waste generation coupled with undesirable disposal, especially in the urban areas, has resulted to environmental threat in the globe which has been attributed to legislation, poor biodegradability, economic growth, rural to urban migration, increase in consumption, and standard or cost of living. This chapter will focus on overview, properties of virgin and recycled thermoplastics, recycling techniques, and applications of different types of thermoplastic articles such as HDPE, LDPE, PVC, PET, and polypropylene (PP) with improved properties based on modifications using eco-friendly materials for sustainable applications in order to save human existence from the menace of environmental and economic issues.

Keywords: thermoplastics, recycling, modifications, properties, applications

1. Introduction

Globally, poor solid waste management remains an issue of concern in an environment due to inadequate policies, legislation, and public enlightenment on waste disposal [1]. The policies of the government on the environment are merely by mouth with poor implementation. The enlightenment programs remain poor with lack of needed coverage, intensity, and continuity so as to change the attitude toward the management of the waste disposal to the environment. However, the poor activities of government agencies for a safe environment may be attributed to improper funds, inadequate facilities and human resources, low technology know how, and taxation system [2]. Integrated solid waste management, 3R (i.e., reduce, reuse, and recycle) principles have contributed to minimization of waste in the environment. Successful means of solid waste management required an integration of technical, economic, and sociocultural involvement. The generation and disposal of plastic waste in environment have been undesirable activities that posed serious threat to humans' existence due to large quantities, low biodegradability, and its significant effect on economic growth [3]. In Japan, the waste quantities increased from 46 million tons in 2001 to 65 million tons in 2010 and are expected to have 0.7 kg/capita/day production in 2050 [4] and range from 0.44 to 0.66 kg/capita/day production in Nigeria [5]. The increase in solid waste generation in which plastics are included, in the urban area, is dependent on the increase in migration from rural to urban area, rate of consumption and standard of living, lifestyle, population density, and climatic changes [5, 6] (see **Table 1**).

S/N	Waste material	Percentage (%)	
		Japan (%)	Nigeria (%)
1	Paper and cardboard	34	4
2	Organics	32	78
3	Plastics	17	9
4	Metals	6	4
5	Glass	5	3
6	Inorganic	4	1
7	Special waste	2	1
	Total	100	100

Table 1.
Solid waste generated [4, 5].

Plastics		Japan (%)
1	Polyethylene	24.1
2	Polypropylene	23.1
3	Polyvinyl chloride	15.2
4	Polystyrene	7.0
5	PET	4.0
6	ABS	3.5
7	Others	13.3

Table 2.
Recycling and generation of thermoplastics [11].

In the USA, about 30 million tons of plastic wastes were produced in 2009 and only about 7% was recycled. Plastic wastes end up in landfills, beaches, rivers, and oceans, thereby causing environmental problems [7]. In the UK, about 5 billion of plastic wastes are generated every year [8]. In some developed countries like Japan, plastic waste is found to be the third major municipal and industrial waste [4] but second in developing countries like Nigeria [9, 10]. Based on production and utilization of plastics in Japan, about 90% of the plastics are thermoplastics (a type of plastic that undergoes a reversible chemical reaction for its curing and melting at high temperature) used for containers and packaging materials (films, sheets, bottles), daily necessities, household appliances, and automobiles as presented in **Table 2** and **Figure 1** [10, 11]. About 60–70% of thermoplastics are polyolefins, while PET, PS, and PVC make other compositions [12]. In Europe and developing countries, the incineration and landfill techniques used for management of plastics waste covered about 74%, despite advanced effect. Plastics are less expensive, weight saving, durable articles which can readily be molded into a variety of products and found useful in a wide range of applications [13], but its production and usage caused several environmental problems through disposal [14, 15]. Moreover, durability of thermoplastics is a consequence for disposal and accumulation in landfills.

Plastic recycling refers to a process of achieving useful products from waste plastics after its reprocessing or re-melting. Recycling is one of the most important actions currently available that provides a solution on environmental and ecological

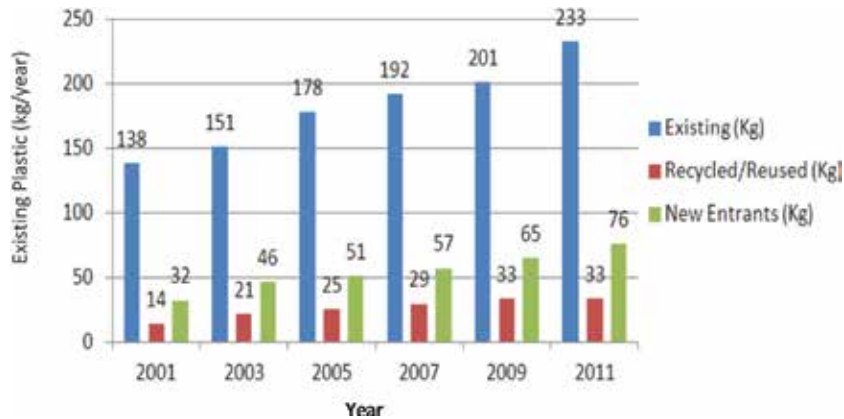


Figure 1.
 Existing, recycled, and new entrants of plastic wastes [10].

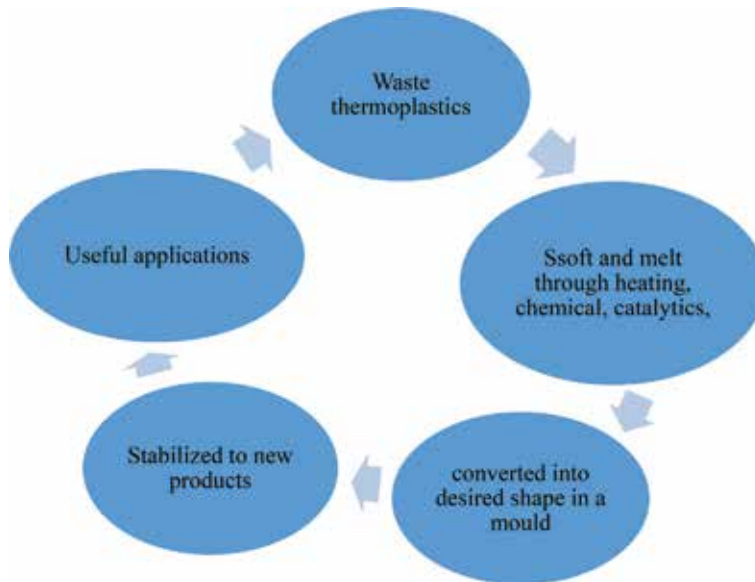


Figure 2.
 Thermoplastic recycling process chart.

threats posed by reduce oil usage, carbon dioxide emissions, and the quantities of waste requiring disposal [14, 16]. Despite plastic recycling remaining to be the best means of minimizing plastic waste, its quality is influenced by polymer cross-contamination, additives, non-polymer impurities, and degradation [17]. Recycling of thermoplastics posed many benefits such as provision of raw materials for manufacturing industry, reduced environmental threat to humans since it is non-biodegradable, minimized incineration and landfill issues, less energy consumption for sustenance, and it serving as a source of income and providing job opportunity [18]. However, economic factors that influenced the viability of thermoplastic recycling include the price, cost of recycling compared with forms of required disposal, suitability for specific applications, lack of information about the availability of recycled plastics, and quantity and quality of supply recycled thermoplastics compared with virgin thermoplastics [17, 18]. Thermoplastic recycling follows the pattern of **Figure 2**.

Waste polymer recycling can be carried out by four approaches in accordance with ISO 15270, namely:

1. Primary recycling refers to the recycling of the scrap material of controlled history. This process remaining to be the most popular as it ensures simplicity, low cost, and applicability to clean uncontaminated single-type waste. It involves melting with use of solvents and remolding of clean materials [19].
2. Mechanical recycling: waste plastic is recycled or reprocessed by mechanical process using melt extrusion, injection, blowing, vacuum, and inflation molding method after sorting [2, 20, 21]. This method utilizes a 100% utilization and conversion of waste plastic to produce the same or other valuable products but with reduced qualities which can be enhanced by the application of additives. It may or may not be necessarily separated depending on desired products and quality. It is applicable to reprocessing plastics that require pretreatment or decontamination.
3. Chemical or feedstock recycling: waste plastics serve as raw materials and convert into monomer or other products such as fuel oils and cooking gas through decomposition and depolymerization of feedstock with the use of thermal energy or catalyst [22, 23]. This method seems to be economical but reduced the yield of new products [24] and less than the yield of the mechanical recycling of thermoplastics due to no loss of materials and accumulation caused by pipeline blockage as a result of shutdown of the machine, thereby lowering melting points during solidification stages. Pipeline blockages or clogs may be difficult to remove. This method involves decomposition of waste polymers to lower-molecular-weight species for reuse with applications of solvents like benzene, chlorobenzene, trichloroethylene, toluene, and xylene called dissolution/precipitation (DR) or solubilization before pyrolysis (applied high temperature and pressure in the absence of oxygen) [25]. This provides an insight to the solution of clogged pipeline issues but at increased processing cost and time with high-energy consumption compared to mechanical recycling.
4. Energy recovery: This is an effective means to reduce the quantity of organic materials by incineration, with difficult environment pollution control from the waste plastics [24, 26]. It involves cement kiln and waste power generation.

This chapter focuses on modifications of thermoplastic materials (HDPE, LDPE, PVC, PET, and PP) and mechanical recycling for enhanced properties, performance, and quality of the products for sustainable applications.

2. Recycling of modified virgin and waste thermoplastics

The choice of recycling of waste thermoplastics depends on processing equipment such as injection, single-screw extruder and film blowing machine, and processing conditions (temperature, time, content of materials, and rheological behavior) and product uses [27–32]. The application of additives or modifiers like compatibilizer (nonreactive and reactive), fillers or fibers (inorganic and organic) have been attributed to ease processing and improvement in compatibility [28, 31]. More so, the recycling of waste thermoplastics is cheaper than virgin types, but its inferior properties [20, 21], contaminations, and poor suitability [33] remain an

issue of concern for effective applications. Blending technology remains a proffer solution due to low cost to produce, lower technical risk, and eco-friendly materials when compared to developing new polymers [28]. Sorting or separation before recycling through manual [34] application of principle of density and solubilization with the use of solvents (hexane, benzene, xylene, and toluene) provides solution to contamination [2] but not cost effect and risk. Techniques for modifications of thermoplastics may be due to the use of different waste or virgin thermoplastics and natural materials, thereby producing composites with enhanced properties and durability [35]. This can be influenced by processing, crystallization, and phase morphology as reported by Lin et al. [32]. The use of different waste or virgin thermoplastics seems to be uneconomical due to cost of blended and non-compatibility of the thermoplastics which may require a new compatibilizer. The use of natural materials for modification of virgin and waste thermoplastics remains a potential technique for thermoplastic recyclates. Therefore, the major reasons for modification of plastic resins in the industries include to meet specific processing and performance specification of a plastic product that is not satisfied by a single component, to upgrade the properties of postconsumer plastic wastes, for scientific research, for interest and development, and for financial optimization [31, 32]. However, degradation of thermoplastic materials by chemical processes is a function of reaction between the components and the environment. The reduction in photodegradation of thermoplastics by ultraviolet absorber as an antioxidant shows a retardation effect of oxidation [36]. Therefore, the aging process of thermoplastics can be influenced by the synergistic action of factors like electromagnetic radiation and thermal energy on the oxidation, favoring the initiation of degradation by excision of chain and radicals of thermoplastics [36].

2.1 Modifications and properties of recycling of virgin and waste HDPE

The incorporation of the carbon nanotube, zeolite, LDPE, PP, natural fillers, and fibers with treatment into the waste polymer for reuse has resulted to an improvement of the composite strength and enhancement of compatibility of blended components of composites as presented in **Table 3**. The improvement has been reported to be a function of compatibilizer types, size and particle shape, branching, and dimensions of polymeric chains as reported by [37]. In the case of natural fibers or fillers, it seems fibers or fillers containing compatibilizer which may or may not have been identified. Moreover, the melting flow rate of recycling of postconsumer or waste HDPE remains inconsistent with stabilization, and the consistency can be achieved with a mixture of phosphite and phenolic. This might be uneconomical. The enhancement in mechanical properties and performance of the HDPE matrix and composite product by additives (sodium hydroxide (NaOH), sodium lauryl sulfate (SLS), and acetic anhydride) have also been attributed to increased interfacial adhesion coupled with its improved water absorption [21], biodegradability, biocompatibility, antimicrobial activity, and non-toxicity with the use of chitosan compounds [38]. The density of recycled virgin and waste HDPE is within the range of 0.02–0.96 g/cm³ [36, 39]. Increase in density can be ascribed to chemocrystallization, annealing effects and changes in lamellar orientation, fiber loading, moisture absorption, and aging of HDPE products [35]. Annealing effect involves changes in spherulite size of HDPE material after heat effect, and aged surface shows loss of gloss observed as a result of environmental effect through oxidative stress and disappearance of crystalline molecule of the HDPE materials produced by a surface contraction. The surface contractions initiate micro-cracks and lead to embrittlement of ductile HDPE polymers [35].

Materials	Modification	Tensile strength (MPa)	Tensile modulus (MPa)	Flexural strength (MPa)	Flexural modulus (MPa)	Hardness	Impact strength (J/m^2)	References
Virgin HDPE	—	21	189	—	—	—	6.8	[33]
Virgin HDPE	Using LDPE	22.5	860	—	—	—	135	[28]
Virgin HDPE	3% Carbon nanotube and 2 cycles	36	1700	—	—	—	5	[40]
Waste HDPE	Natural zeolite, clinoptilolite (K_2, Na_2, Ca) $Al_6Si_3O_{17} \cdot 23H_2O$ of 1-2% with particle size $<40 \mu m$	21.8	218	—	—	—	25	[37]
Waste HDPE	—	24.619	836.25	27.114	1390.7	21	859.3	[20]
	<i>Combretum dolichopetalum</i> fiber	32.427	939.6	18.2	1568.1	28	496.0462	
	Acetic anhydride-treated <i>Combretum dolichopetalum</i> fiber	38.5153	1220	8.5111	1994.4.24	33	787.3806	
	NaOH-treated <i>Combretum dolichopetalum</i> fiber	34.9041	984.99	32.067	2277.15	39	469.5912	
Waste HDPE	—	27.628	792.59	34.519	1390.7	24	962.8	[21]
	<i>Cissus populnea</i> fiber	30.4827	839.022	36.1904	1425.89	30	155.795	
	<i>Cissus populnea</i> fiber treated with NaOH	29.6903	793.05	39.3962	1568.44	35	398.62	
	<i>Cissus populnea</i> fiber treated with SLS	31.8013	823.245	39.568	1455.68	38	394.683	

Table 3. Mechanical properties of modified virgin and waste HDPE materials.

2.2 Modifications and properties of recycling of virgin and waste LDPE

The high quantity of waste LDPE and its average mechanical properties coupled with influence of aging of the product have not motivated utilization in many packaging applications such as bags, film, and pallet covers, but modifications may improve the mechanical properties. Also, the qualities of LDPE composites have been linked with poor interfacial adhesion between both phases of individual constituents which explain weak mechanical properties. This interfacial adhesion has a direct relation to compatibility. The processing conditions of machine also influenced the compatibility of the polymers. Some modifications of LDPE are presented in **Table 4**. The use of virgin and waste or recycled PP to modify LDPE using twin and single-screw extruder has been reported by Sylvie and Jean-jacques [12]. In the report, PP increases some mechanical properties such as tensile strength and modulus with reduced impact strength of the LDPE for single extruding machine, although the twin extruding machine gave better mechanical properties due to improvement in homogeneity of the polymer. The use of compatibilizer such as EPDM, graft copolymer (PE-g-poly (2-methyl-1,3-butadiene), and

Thermoplastics	Modification	Tensile strength (MPa)	Tensile modulus (MPa)	Hardness	Impact strength (J/m ²)	References
Virgin LDPE	Starch grafted with maleic anhydride	16.34	520.16	—	—	[45]
Virgin LDPE	Virgin PP	25.1			5.5–6.5	[36]
Waste LDPE	Natural zeolite, clinoptilolite (K ₂ ,Na ₂ ,Ca)Al ₆ Si ₃ O ₇₂ . 23H ₂ O of 1–2% with particle size <40 μm	19.5–22.9	195.73–232.14		18–26	[37]
Waste LDPE	Waste 10% PP	8.7–12.1	241–336.1		23–37.2	[41]
Waste LDPE	Waste 10% PP + EPDM	7.6–8.5	211.1–236.1		46.4–53	[36]
Waste LDPE	—	30.33	240.7	2.3	583	[47]
Waste LDPE	Husk filler	31.58	565.7	13.15	600	[48]
	Okpa filler	35.14	861.2	17.53	583	[47]
Virgin LDPE	10% PP using single-screw extruder	9.4	205		15.2	[12]
Waste LDPE	10% PP	10.0	248		12.3	[12]
Virgin LDPE	10% PP using twin screw extruder	9.6	226		8.5	
Waste LDPE	10% PP using twin screw extruder	10.3	256		12.6	
Waste LDPE	10% PP + 5% graft copolymer using twin screw extruder	11.8	280		12.5	
Waste LDPE	10% PP + 5% EPDM using twin screw extruder	10.1	245		16.5	

Table 4. Mechanical properties of unmodified and modified virgin and waste LDPE.

ethylene-propylene copolymer enhanced the interaction between the polymers and resilience, thereby improving the mechanical properties of the LDPE/PP composites. The use of compatibilizer in virgin and recycled polyolefins influenced the quality of the composites based on technology and recycled waste of LDPE by the addition of EPDM compatibilizer [41]. The presence of ethylene-propylene diene monomer (EPDM) revealed the variation in properties such as wide-angle x-ray diffraction (WAXD), differential scanning calorimetry (DSC), and mechanical properties of virgin and recycled LDPE/PP [36]. The destruction of thermal and mechanical properties of virgin LDPE and PP as well as blended LDPE/PP was found to be greater than those from recycled polyolefins because of the absence of antiaging in the virgin products. The impact EPDM modifier have been reported on stability of LDPE/PP products based on natural and influenced ageing conditions with improved mechanical (tensile and impact strength) properties of the LDPE/PP with increase in modifier content. The impact EPDM modifier significantly improved the compatibility of recycled LDPE and PP and reduces the recrystallization of PP in the blends during aging and decreases the formation of the imperfect β polymorph crystal which depends on the presence of additives resulting in chain mobility retardation, presence of shear stress changing the chain structures, and fast cooling conditions at foil production as reported by Borovanska et al. [36]. Moreover, the significant improvement in rheological property such as viscosity, crystallinity index, and tensile properties of the recycled LDPE can be achieved by linear low-density polyethylene (LLDPE) blend with a ratio of 4:1 and applicably good for film products at 60% blended LLDPE [15]. The modification of recycled LDPE by PP using injection molding machine was also reported that the tensile properties increases with reduction in impact strength as increase in PP content as well as reduced processing temperature [42].

The effect of wood flour of *Pinus radiata* as fillers at a constant loading of 45 wt.% of recycled post-consumed plastic waste reported to be influenced by virgin PP [43]. In the report, the addition of virgin PP improved tensile and flexural moduli and flexural strength of wood plastic/LDPE composites (WPC). The highest mechanical properties of recycled LDPE composites have been reported for wood polymer composites with virgin PP (5%) and lower mechanical properties with higher virgin PP content of 55 and 71.5% compared to PE. The moisture absorption of WPC with virgin PP blend reported to be higher than without PP with adverse effect on the mechanical properties when immersed in water. More so, the use of virgin PP delay degradation and lower the thermal stability of WPC. This is also stay in agreement with report of Zhao et al. [44]. The decrease in tensile strength with increasing starch content in starch/LDPE composites attributed to incompatibility of the hydrophobic LDPE and hydrophilic starch and the increase in stiffness attributed to better dispersion of starch in LDPE matrix [45]. This incompatibility demands the use of compatibilizers such as styrene/ethylene-co-butylene/styrene grafted with maleic anhydride (SEBS-g-MA) and anhydride grafted polypropylene (PP-g-MA), Mixture Irganox 1098/Irganox 1078-Irgafos 168/Chimassorb 944 [44, 46].

The novel application of natural materials (filler or fibers) is to enhance undesirable properties and poor biodegradation of LDPE matrix. The use of rice husk, bambara, and mahogany fillers with improved tensile strength and modulus, flexural strength and modulus, and hardness with reduction in impact strength has been reported [47–49]. The increase in mechanical, thermal, and biodegradation behaviors of the composites was attributed to improved interfacial adhesion and compatibility. The reduction in impact strength is a result of fiber dispersion, uneven distribution, and micropore formation in the composites. It can be deduced that natural fillers or fibers contain a compatibilizer which has not been identified. There is also limited report on the modifications of fillers and fibers for enhancement of mechanical,

physical (water absorption, density, etc.), thermal, and electrical properties (conductivity, dielectric properties, etc.) of LDPE matrix. Chemical recycling (pyrolysis) had been a major technology for waste or postconsumer LDPE to save the environment, but not cost-effective; emissions of some constituents and required additives or modifiers (catalysts) for considerable yields of the products in many applications [24, 30]. Incorporation of natural zeolite, clinoptilolite ($(K_2, Na_2, Ca) Al_6 Si_3 O_{72}$), improved the strength of the filled composites, rheological behavior, thermal, compatibility of the individual polymeric components, morphology, and texture of the moldings from recycled polyolefins which strongly depends on the type of zeolite, size and shape, branching, dimensions, and types of polymeric chains [37].

Chemical materials have been used as catalysts in the pyrolysis of plastics to obtain liquid products with higher yield and selectivity. Hence, numerous experiments were performed to find out the best catalyst to produce the most desirable products, taking the economic factor into consideration. Pyrolysis of plastic waste to fuel involves many limitations that prohibit the industrial plastic recycling process including the difficulty in modifying it from batch process to continuous process. In industrial process, plastic waste is fed into the reactor directly through hopper for melting in pyrolysis reactor with high melting point (300°C and above, depending on the types of plastic). Therefore, any temperature lower than its melting point may result to solidification of the plastics in the process pipelines, hence causing blockage of the pipelines.

2.3 Modifications and properties of recycling of virgin and waste PVC

The increase in commercial vehicles and road usage with construction resulted to increase in demand of bitumen for pavement and road construction. Yet, the durability of the bitumen depends on appropriate binder for enhancement of performance of bitumen. The use of little quantity of virgin thermoplastics provides a reasonable performance with bitumen but is uneconomical compared with only bitumen. The utilization of waste PVC for effective performance as bitumen binder in pavement and road construction products seems to be interesting because of its low cost and because it is one of the abundant thermoplastics that causes environmental threat [50]. The applications of PVC have been reported to hinder and be not suitable for many applications because of incompatibility as a result of many factors [51]. PVC possesses high melting points which hindered the mixing, and it is impractical to make any further attempts to incorporate it in some applications like bitumen road construction. Recycled LDPE/PVC blends have been modified using EPDM as effective toughening, compatibilizer, and dispersant agent in applications. Recyclability of PVC waste can be achieved mechanically without modifications or use of new plasticizer since the separation of other mixed plastics is possible through triboelectrostatic technology [50, 52]. The technology of triboelectrostatics depends on the ability of polymer to the electron loses or gains because electrons gains and charges negatively may be as a result of higher affinity of polymers, whereas loss of electrons and positively charge may be attributed to polymer with the lower affinity. Because of high electronegativity of chloride ions, it can mix with many polymers such as PET, PP, PS, and PE with enhanced properties as reported by Hamad et al. [50]. The use of wood fillers or fibers as natural modifiers have been reported to improve mechanical properties of recycled PCV rather the recyclability [53], and slightly reduction in mechanical (tensile, flexural, hardness and impact) and structural properties (i.e., decrease in molecular weight due to molecular chain scission caused by shear stress involved in reprocessing) [54]. The reduction in properties exists because of incompatibility or poor intermolecular interaction which can be modified by surface techniques.

2.4 Modifications and properties of recycling of virgin and waste PET

Polyethylene terephthalate (PET) is a transparent semicrystalline, long-chain thermoplastic polyester which can be produced by a polymerization of terephthalic acid with ethylene glycol and remains the most used thermoplastics in many applications [55, 56]. It is characterized as easy to handle, durable, strong, thermally with low glass transition temperature, and chemically stable with low gas permeability [57]. It exhibits brittle behavior, good mechanical properties, and dimensional stability as well as good gas and chemical resistance which resulted to its wide applications [58]. Waste PET may be in bottles, foils, and cords from tire [57, 58]. Globally, the rate of generation of waste PET is about 20 million tonnes that amounted to about 15% which is alarming due to population growth, urbanization, standard of living, and cost of production, but the recycling rate of waste PET found to be 29.3% lower [56]. The issue with the reuse of waste PET may be associated with size, content, mixing process, type of mixer, temperature, time profile during mixing process, and contaminations or additives like stabilizers and pigments [58, 59]. In bitumen asphalt modification for the road construction, the mixing process may be wet or dry process. The wet process involves blending of thermoplastics and bitumen in a mixer and then mixing of thermoplastic modified bitumen to aggregates, while the latter involves incorporation of thermoplastics to very hot aggregates prior to mixing with bitumen [56]. Waste PET recycling employs dry process, and it can be modified to achieve better feasibility in terms of adhesion between the aggregates and binder, stability, and even mixing and minimizes the pore formation and moisture absorption. Appropriate recycling process conditions of waste PET make significant environmental and economy impacts through conservation of natural resources, environmental pollution, energy, and enhancement of engineering and physical properties of construction materials [58]. An increase in recycled PET content caused a decrease in melt flow index or rheological properties of the aggregate [29]. Recycled PET exhibits pseudo-plastic behavior, and it has been used to improve the rheological properties of asphalt as well as increased the viscosity and stiffness and enhanced the softening of stone mastic asphalt (SMA) [58].

Incorporation of recycled PET with appropriate content and size increased the compressive, tensile, and flexural strength/s and ductility of concrete, creates lightweight aggregate of development of building materials, or decreases the bulk density of the composites, thereby helping polymer concrete in saving energy and minimizing the problem of solid waste posed by PET as well as other thermoplastics provided the impurities were removed prior to reprocessing [58].

Synthetic thermoplastics such as HDPE and acrylonitrile butadiene styrene (ABS) blend nano silicon (IV) oxide (SiO_2), and polylactic acid (PLA) can modify PET waste to improve its performance using the extrusion process based on a different mixing ratio. The use of virgin HDPE has been reported to improve rheological and mechanical properties when compared to waste PET using a less than 5% virgin HDPE [60]. The mechanical properties of composites of recycled PET improved with increase in incorporated nano silicate (SiO_2) content blended with ABS [61]. Modification of PET waste by the addition of small amounts of virgin PLA using melt mixing technology also shows reduction in viscosity of the composites with higher thermal sensitivity and mechanical properties compared to recycled PET [50, 62]. It should be noted that the performance of recycling of waste PET was hindered due to the presence of impurities, decomposition, and degradation of polymer chains as reported by Imamura et al. [57]. The modifications by compatibilizer like ethylene glycidyl methacrylate (EGMA) modified PE copolymer significantly improved the miscibility of recycled PET with PP, PE,

and PS molecules, respectively, unlike linear low density polyethylene copolymer (LDPE) [57]. The use of natural materials to modify the properties of recycled PET such as fibers or fillers is not available in literature. The efficacy and performance of recycled PET applications required optimum conditions of modified process, PET size and content, and additive or modifier content.

2.5 Modifications and properties of recycling of virgin and waste polypropylene

Due to favorable qualities of PP like density, versatility, photodegradation, and cheapness in cost of production, it is replacing many materials used for artifacts such as packaging products and automobile bumpers. The increasing rate of use of polypropylene coupled with inherent incompatibility of polyester and polyolefins seeks for improvement in the performance of PP in many applications [63]. The improvement in PP performance has been achieved through modification techniques by incorporation of grafted maleic anhydride (PP-g-MAH), clay-based nano-fillers, inorganic nanoscale particles, and poly(trimethylene terephthalate) (PTT) blends using organically modified montmorillonite (Cloisite nanoclays) as compatibilizers for the purpose of improving compatibility, mechanical, crystallization, and melting behavior of PP composites [64–66]. PTT is an aromatic polyester with combined properties of PET and poly(butylene terephthalate) (PBT). The factors that influence the properties of the PP composites are mix or blend ratio, crystallization temperature, compatibility process time, and size [63]. There is loss of mechanical properties for composites of LDPE and HDPE modified with PP which is due to incompatibility of recycled PP/LDPE and PP/HDPE composites [39]. The modification of recycled PP with HDPE reveals a partial compatibility which caused an improvement in tensile strength and elongation with the use of EPDM compatibilizer [67]. The modification of recycled LDPE/PP with 1% montmorillonite nanoclay exhibits appreciable improvement in strength, physical properties, and stability of bitumen [68].

3. Microstructural behavior of recycled thermoplastic matrix and its modifications

The microstructural behavior in this content is limited to Fourier-transform infrared spectroscopy and scanning electron microscopy as discussed in subSection 3.1.

3.1 Fourier-transform infrared spectroscopy

FTIR analysis of recycled thermoplastics exhibits no extra peaks for the blends, neither any shifts nor changes in the absorption bands of the carbonyl, hydroxyl, and carboxylic groups of HDPE, LDPE, PET, PVC, and PP resins which indicates the absence of any specific interaction, entanglement, or chemical reaction between the polymers and modifiers as reported by Mamoor et al. (**Figure 3**) [29]. In the case of modification of recycled thermoplastics using untreated natural fiber, there exists a shift or change in the absorption peaks of the carbonyl, hydroxyl, and carboxylic groups of the fiber-reinforced recycled thermoplastics, thereby influencing the physical and mechanical properties of the matrix and interfacial between the fiber and HDPE as reported by researchers [21, 69]. This resulted in improved quality of the thermoplastic products. The shift, change, appearance, and disappearance of absorption peaks correspond to reaction of the functional groups. This

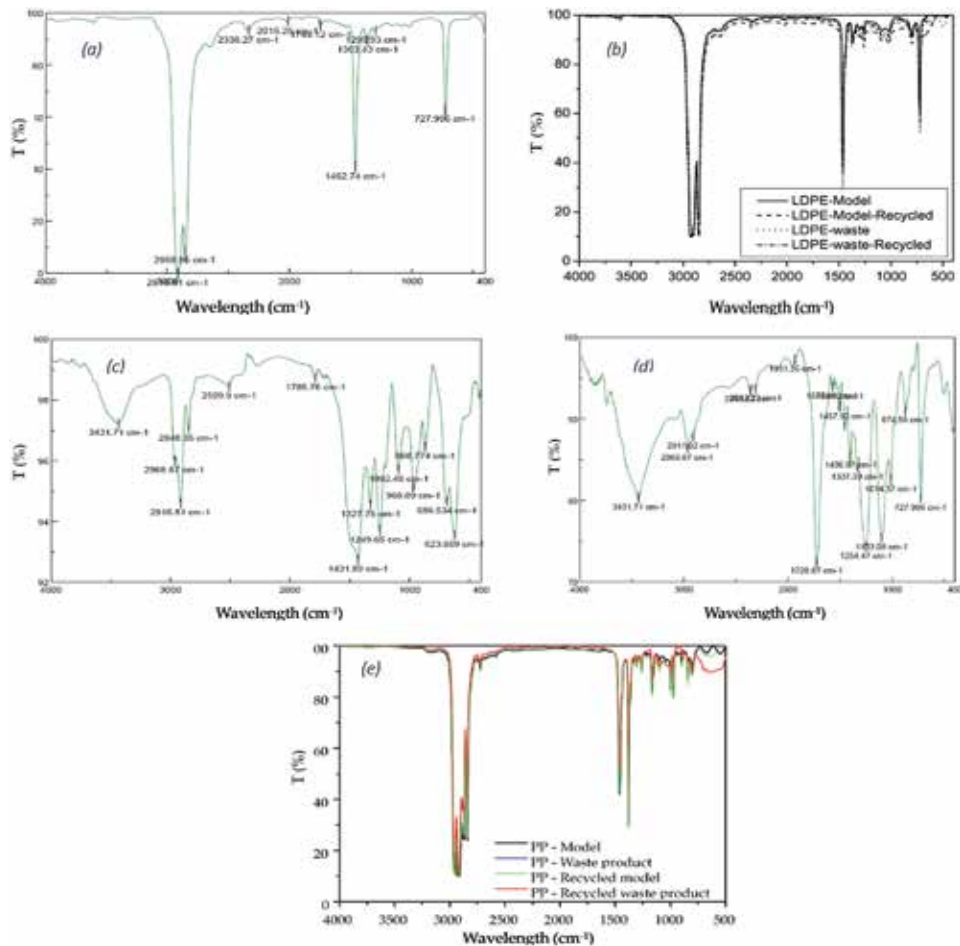


Figure 3. FTIR of recycled thermoplastics (a) HDPE [29], (b) LDPE [30], (c) PCV [29], (d) PET [29], and (e) PP [29].

functional group dictates chemical reaction between the polymers and modifier, resulted to change in absorption peak correlate change in strength and modulus of the thermoplastics.

3.2 Scanning electron microscopy

The scanning electron microscopy depicts the morphology of virgin and recycled thermoplastics at fracture surfaces when stressed and characterized the ductile, toughness, stiffness, and brittle nature of HDPE, LDPE, PCV, PET, and PP without modification [32], but improvement in compatibility using EPDM compatibilizer has been reported [2, 70]. The improvement in rheological morphology does not indicate an improvement in compatibility as well as mechanical properties [71]. Modification of recycled HDPE with treated natural fiber using NaOH, SLS, acetic anhydride, CaCO₃ filler, and zeolites as well as synthetic fibers is characterized with improvement in polymer dispersion, even distribution of fibers, interfacial adhesion, fiber tearing, micro-crack formation, modifier content and size, nature of the modifier, and reduction in void formation [20, 43, 72–75]. This indicated the enhanced compatibility which corroborates the improvement in physical, mechanical, and thermal properties of the modified recycled thermoplastics and dictates its applications.

4. Application of recycled thermoplastics

4.1 Applications of recycled HDPE

The application of the HDPE composites is a function of the favorable properties coupled with cost implication of the production, and it may be affected by additional modified agents such as fiber or filler, NaOH, acetic anhydride, zeolite, and sodium lauryl sulfate. The use of recycled HDPE composites has been reported for many applications such as packaging (food storage containers and bottles for milk jugs) [13, 28, 38], banners, swimming pool installation, corrosion protection for steel pipelines, folding chairs and tables, electrical and plumbing boxes, plastic surgery (skeletal and facial reconstruction) [27], modified asphalt for pavement and road construction [29, 59, 75], housewares, industrial wrapping and gas pipes [30], and storage sheds, enhancing the economic, health, and social values as well as minimizing environmental issues that might be posed by HDPE disposal [38]. Applications of recycled HDPE in the encapsulation of radioactive, hazardous, and mixed wastes have been reported by Lageraen and Kalb [76].

4.2 Applications of recycled LDPE

Incorporation of recycled LDPE at concentrations ranging from 2 to 5% by mass of bitumen possesses consistent desirable properties for bitumen asphalt applications [51, 69]. Utilization of LDPE for production of liquid milk packaging [16], bread packaging and sandwich bags, housewares, toys, buckets, wire and cable jacketing, and carpet [13, 38, 68] and use of recycled thermoplastics for encapsulation of hazardous, radioactive, and mixed waste disposal save the environment from economic, environmental, and health issues [76].

4.3 Applications of recycled PVC

Polyvinyl chloride waste has been used in plumbing pipes and fittings, but its utilization as a binder in bitumen applications has been found unsuccessful due to high melting points which hindered the mixing as a result of poor compatibility [51]. PVC sheets have been reported to be employed for making food trays, cling film and blister packages [13], household appliances, packaging, construction, medicine such as human rehabilitation, electronics, automotive and aerospace components [29], and building floor applications [52].

4.4 Applications of recycled PET

Recycled PET could be used for making waterproof [13] water and soft drink bottles, thermally stabilized films (e.g., capacitors, graphics, film base and recording tapes, etc.), electrical components, and textile products [58] if properly modified. The use of recycled waste PET as a modifier in bitumen road and pavement construction is hindered by mixing ratio and processing conditions due to high melting point [51]. It is widely used in making automobile part, electronics, food packaging, house ware, lighting product, power tools, sports tools, x-ray sheets, and photographic applications [55, 59].

4.5 Applications of recycled PP

Recycled polypropylene can be used for packaging articles, automobile bumper, foams, bottle tops, carpets, and household components [13] and in making straws

and sweet wrappings, PP powder, and PP mulch at concentrations ranging from 2 to 5% by mass of bitumen consistently desirable for bitumen asphalt applications [51]. The recycled PP is also applicable in 3D printing filament [77]. An application of recycled PP is dependent on good compatibility with modified materials with synergistic effects.

5. Conclusion

Globally, disposal of postconsumer or waste thermoplastics into the environment is alarming and posed a serious economic, environmental, health, and social burden. Employing appropriate technology, especially mechanical recycling with modifications of thermoplastics, can save the world from threat that might be posed by thermoplastic wastes. Appropriate additives such as natural fibers and fillers with eco-friendly, less expensive, available, and degradable potentials should encourage saving the world from this serious menace. The use of recycling technique with appropriate modification will not only exhibit conservation of the waste thermoplastics but altered the physical, rheological, mechanical, electrical, and thermal properties of the recycled thermoplastics for effective applications. An effective and sustainable application of recycled thermoplastics depends on optimization of process conditions, parameter, modifying agents and techniques, equipment, and time. Hence, the quality and performance of the recycled aggregates or composites are enhanced.

Conflict of interest

There is no conflict of interest.


Author details

Taofik Oladimeji Azeez

Department of Biomedical Technology, Federal University of Technology, Owerri, Nigeria

*Address all correspondence to: taofikoladimeji@gmail.com

IntechOpen

© 2019 The Author(s). Licensee IntechOpen. This chapter is distributed under the terms of the Creative Commons Attribution License (<http://creativecommons.org/licenses/by/3.0>), which permits unrestricted use, distribution, and reproduction in any medium, provided the original work is properly cited. 

References

- [1] Achilias DS, Andriotis L, Koutsidis IA, Louka DA, Nianias NP, Sifaka P, et al. Recent advances in the chemical recycling of polymers (PP, PS, LDPE, HDPE, PVC, PC, nylon, PMMA), material recycling. In: Achilias DD, editor. *Material Recycling-Trends and Perspectives*. Rijeka, Croatia: IntechOpen; 2012. pp. 3-64
- [2] Achilias DS, Roupakias C, Megalokonomos P, Lappas AA, Antonakou EV. Chemical recycling of plastic wastes made from polyethylene (LDPE and HDPE) and polypropylene (PP). *Journal of Hazardous Materials*. 2007;**149**(3):536-542. DOI: 10.1016/j.jhazmat.2007.06.076
- [3] Christine T. Recycling electronic wastes in Nigeria: Putting environmental and human rights at risk. *Northwestern Journal of International Human Rights*. 2012;**10**(3):154-172
- [4] El-newehy M. *Plastic Waste Management*. King Saud University; 2016. pp. 1-35
- [5] Igbinomwanhia DI. Status of waste management. In: *Integrated Waste Management*. Rijeka, Croatia: IntechOpen; 2011. pp. 11-34
- [6] Angaye TCN, Abowei JFN. Review on the environmental impacts of municipal solid waste in Nigeria: Challenges and prospects. *Greener Journal of Environmental Management and Public Safety*. 2017;**6**(2):018-033. DOI: 10.15580/GJEMPS.2017.2.062117079
- [7] Weber R, Gaius C, Tyskland M, Johnston P, Forter M, Hollerti H, et al. Dioxin- and POP- contaminated sites-contemporary and future relevance and challenges: Overview and background, aims and scope of the series. *Environmental Science and Pollution Research International*. 2008;**15**(5):363-393
- [8] European Commission (EC). *White Paper on Climate Change, SEC2009*. pp. 386-388
- [9] Nzeadibe TC, Iwuoha HC. Informal waste recycling in Lagos, Nigeria. *Communications in Waste and Resource Management*. 2008;**9**(1):24-31
- [10] Aderogba KA. Polymer wastes and management in cities and towns of Africa and sustainable environment: Nigeria and European experiences. *Social Sciences*. 2014;**3**(4-1):79-88. DOI: 10.11648/j.ss.s.2014030401.19
- [11] Plastic Waste Management Institute. *An Introduction to Plastic Recycling*. Tokyo, Japan: Plastic Waste Management Institute; 2016
- [12] Sylvie B, Jean-jacques R. Study and characterization of virgin and recycled LDPE/PP blends. *European Polymer Journal*. 2002;**38**:2255-2264
- [13] Zare Y. *Recycled Polymers: Properties and Applications*. Vol. 2. Rijeka, Croatia: IntechOpen; 2016. pp. 27-50
- [14] Edmonds N. *Plastics 101 Introduction*; Plast New Zeal Ind Assoc 2016. pp. 1-40
- [15] Fråne A, Stenmarck Å, Rüdénhausen M, Zu C, Gíslason S, Raadal HL, et al. *Nordic Improvements in Collection and Recycling of Plastic Waste* [Internet]. Norden, Denmark; 2015. Available from: www.norden.org/en/publications
- [16] Choudhury A, Mukherjee M, Adhikari B. Mixtures of recycled milk pouches with a virgin LDPE-LLDPE blend. *Progress in Rubber, Plastics and Recycling Technology*. 2005;**21**(3):219-230
- [17] Pivnenko K, Jakobsen LG, Eriksen MK, Damgaard A, Astrup TF.

- Challenges in plastics recycling. In: di Pula SM, editor. *Proceedings Sardinia 2015: Fifteenth International Waste Management and Landfill Symposium*. Cagliari, Italy: CISA Publisher; 2015. pp. 1-7
- [18] Hopewell J, Dvorak R, Kosior E. Plastics recycling: Challenges and opportunities. *Philosophical Transactions of the Royal Society B*. 2009;**364**:2115-2126
- [19] Grigore ME. Methods of recycling , properties and applications of recycled thermoplastic polymers. *Recycling*. 2017;**2**(24):1-11. DOI: 10.3390/recycling2040024
- [20] Azeez TO, Onukwuli OD, Walter PE, Menkiti MC. Influence of chemical surface modifications on mechanical properties of combretum dolichopetalum fibre—high density polyethylene (HDPE) composites. *Pakistan Journal of Scientific and Industrial Research Series A: Physical Sciences*. 2018;**61**(1):28-34
- [21] Azeez TO, Onukwuli DO. Effect of chemically modified cissus populnea fibers on mechanical, microstructural and physical properties of cissus populnea/ high density polyethylene composites. *Engineer Journal*. 2017;**21**(2):25-42. DOI: 10.4186/ej.2017.21.2.25
- [22] Garcia JM, Robertson ML. The future of plastics recycling. *Science*. 2017;**358**(6365):870-872. DOI: 10.1126/science.aaq0324
- [23] Ademiluyi T, Akpan C. Preliminary evaluation of fuel oil produced from pyrolysis of low density polyethylene water-sachet wastes. *Journal of Applied Sciences and Environmental Management*. 2007;**11**(3):15-19
- [24] Park JJ, Park K, Park J, Kim DC. Characteristics of LDPE pyrolysis. *Korean Journal of Chemical Engineering*. 2002;**19**(4):658-662
- [25] Wong SL, Ngadi N, TAT A. Solubilisation of low density polyethylene (LDPE) for pyrolysis. In: 4th International Graduate Conference on Engineering Science and Humanity. Johor Bahru, Malaysia: Universiti Teknologi Malaysia; 2013. pp. 1-7
- [26] Garcia JM. Catalyst: Design challenges for the future of plastics recycling. *Chem*. 2016;**1**:813-815
- [27] Miller P, Sbarski I, Iovenitti P, Masood S, Kosior E. Rheological properties of blends of recycled HDPE and virgin polyolefins. *Polymer Recycling*. 2001;**6**(4):181-186
- [28] Kukaleva N, Simon GP, Kosior E. Modification of recycled high-density polyethylene by low-density and linear-low-density polyethylenes. *Polymer Engineering and Science*. 2003;**43**(1):9-12
- [29] Mamoor GM, Shahid W, Mushtaq A, Amjad U, Mehmood U. Recycling of mixed plastics waste containing polyethylene, polyvinylchloride and polyethylene terephthalate. *Chemical Engineering Research Bulletin*. 2013;**16**:25-32
- [30] Achilias DS, Antonakou E, Roupakias C, Megalokonomos P, Lappas A. Recycling techniques of polyolefins from plastic wastes. *Global NEST Journal*. 2008;**10**(1):114-122
- [31] Jesmy J, Jyotishkumar P, Sajeev MG, Sabu T. Recycling of polymer blends. In: Grigoryeva O, Fainleib A, editors. *Recent Developments in Polymer Recycling*. Transworld Research Network: Kerala, India; 2011. pp. 187-214
- [32] Lin J, Pan Y, Liu C, Huang C, Hsieh C, Chen C-K, et al. Preparation and compatibility evaluation of polypropylene/high density polyethylene polyblends. *Materials*. 2015;**8**:8850-8859

- [33] Parmar H. Rheology of peroxide modified recycled high density polyethylene [thesis]. Melbourne, Australia: RMIT University; 2007
- [34] Stefan T. Recycling of mixed plastic waste—Is separation worthwhile? [thesis]. Stockholm, Sweden: Royal Institute of Technology; 2000
- [35] Luzuriaga S. Utilization of compatibilization and restabilization methods in the recycling of commingled municipal plastic waste [thesis]. Brunensis: Masaryk University in Brno; 2009
- [36] Borovanska I, Krastev R, Benavente R, Pradas MM, Lluch AV, Samichkov V, et al. Ageing effect on morphology, thermal and mechanical properties of impact modified LDPE/PP blends from virgin and recycled materials. *Journal of Elastomers and Plastics*. 2014;**46**(5):427-447
- [37] Borovanska I, Cerrada ML, Zipper P, Djoumaliisky S. Recycled polyolefin blends: Effect of modified natural zeolite on their properties and morphology. *Polymer-Plastics Technology and Engineering*. 2016;**55**(5):486-497
- [38] Lima PS, Brito RSF, Santos BFF, Tavares AA, Agrawal P, Andrade DLACS. Rheological properties of HDPE/chitosan composites modified with PE-g-MA. *Journal of Materials Research*. 2016;**32**(4):2017
- [39] Bonelli CMC, Martins AF, Mano EB, Beatty CL. Effect of recycled polypropylene on polypropylene/high-density polyethylene blends. *Journal of Applied Polymer Science*. 2001;**80**:1305-1311
- [40] Svensson S. Reprocessing and characterisation of high density polyethylene reinforced with carbon nanotubes [thesis]. Borås: University of Borås; 2017
- [41] Borovanska I, Dobрева T, Benavente R, Djoumaliisky S, Kotzev G. Quality assessment of recycled and modified LDPE/PP blends. *Journal of Elastomers and Plastics*. 2012;**44**:1-19
- [42] Strapasson R, Amico SC, Pereira MFR, Sydenstricker THD. Tensile and impact behavior of polypropylene/low density polyethylene blends. *Polymer Testing*. 2005;**24**:468-473
- [43] Arango C, Rodríguez-Illamazares S, Castaño J, Zuñiga A. Effect of virgin heterophasic pp copolymer content on moisture absorption, thermal and mechanical properties of recycled polyethylene wood flour composites. *Journal of the Chilean Chemical Society*. 2014;**59**(1):2373-2377
- [44] Zhao X, Luo X, Lin X, Qi X. Rheological and thermal properties of blends of recycled LDPE and virgin LDPE. *Advances in Materials Research*. 2013;**737**:2501-2504
- [45] Wojtowicz A, Janssen LPBM, Moscicki L. Blends of natural and synthetic polymers. In: Janssen LPBM, Moscicki L, editors. *Thermoplastic Starch: A Green Material for Various Industries*. Weinheim, Germany: University of Groningen; 2009. pp. 35-53
- [46] Jose J, Jyotishkumar P, George SM, Thomas S. 6. Recycling of polymer blends. In: Grigoryeva O, Fainleib A, editors. *Recent Developments in Polymer Recycling*. Transworld Research Network: Kerala, India; 2011. pp. 187-214
- [47] Azeez TO, Olaitan SA, Atuanya CU, Chukwudi DO, Akagu CC, et al. Effect of filler weight fraction on the mechanical properties of bambara groundnut (Okpa) husk polyethylene composite. *International Journal of Current Research*. 2013;**5**(7):1714-1717

- [48] Atuanya CU, Olaitan SA, Akagu CC, Onukwuli OD. Effect of rice husk filler on mechanical properties of polyethylene matrix composite. *International Journal of Current Research and Review*. 2013;**05**(15):111-118
- [49] Olaitan SA, Azeez TO, Atuanya CU, Onukwuli OD, Officha MC, Menkiti MC. Effect of mahogany filler on mechanical properties of reinforced polyethylene matrix. *Academic Research International*. 2013;**4**(4):284-292
- [50] Hamad K, Kaseem M, Deri F. Recycling of waste from polymer materials: An overview of the recent works. *Polymer Degradation and Stability*. 2013;**98**(12):2801-2812. DOI: 10.1016/j.polymdegradstab.2013.09.025
- [51] Casey D, McNally C, Gibney A, Gilchrist MD. Development of a recycled polymer modified binder for use in stone mastic asphalt. *Resources, Conservation and Recycling*. 2008;**52**(10):1167-1174
- [52] Yarahmadi N, Jakubowicz I, Martinsson L. PVC floorings as post-consumer products for mechanical recycling and energy recovery. *Polymer Degradation and Stability*. 2003;**79**:439-448
- [53] Augier L, Sperone G, Garcia C, Borredon M. Influence of the wood fibre filler on the internal recycling of poly(vinyl chloride)-based composites. *Polymer Degradation and Stability*. 2007;**92**:1169-1176
- [54] Petch-Wattana N, Covavisaruch S, Sanetuntikul J. Recycling of wood plastic composites prepared from poly(vinyl chloride) and wood flour. *Construction and Building Materials*. 2012;**28**:557-560
- [55] Ahmad AF, Razali AR, Razelan ISM. Utilization of polyethylene terephthalate (PET) in asphalt pavement: A review. In: *IOP Conference Series: Materials Science and Engineering*; IOP Publishing. 2017. pp. 1-7
- [56] Choudhary R, Kumar A, Murkute K. Properties of waste polyethylene terephthalate (PET) modified asphalt mixes: Dependence on PET size, PET content, and mixing process. *Periodica Polytechnica Civil Engineering*. 2018;**2**:1-9
- [57] Imamura N, Sakamoto H, Higuchi Y, Yamamoto H, Kawasaki S, Yamada K, et al. Effectiveness of compatibilizer on mechanical properties of recycled PET blends with PE, PP and PS. *Materials Sciences and Applications*. 2014;**5**:548-555
- [58] Sulyman M, Haponiuk J, Formela K. Utilization of recycled polyethylene terephthalate (PET) in engineering materials: A review. *International Journal of Environmental Science and Development*. 2016;**7**(2):100-108
- [59] Kalantar ZN, Karim MR, Mahrez A. A review of using waste and virgin polymer in pavement. *Construction and Building Materials*. 2012;**33**:55-62. DOI: 10.1016/j.conbuildmat.2012.01.009
- [60] Navarro R, Ferrandiz S, Lopez J, Segui VJ. The influence of polyethylene in the mechanical recycling of polyethylene terephthalate. *Journal of Materials Processing Technology*. 2008;**195**:110-116
- [61] Shi G, He L, Chen C, Liu J, Liu Q, Chen H. A novel nanocomposite based on recycled poly(ethylene terephthalate)/ABS blends and nano-SiO₂. *Advances in Materials Research*. 2011;**150-151**:857-860
- [62] Mantia FP, Botta L, Morreale M, Scaffaro R. Effect of small amounts of poly(lactic acid) on the recycling of poly(ethylene terephthalate) bottles.

Polymer Degradation and Stability.
2012;**97**:21-24

[63] Jafari SH, Kalati-vahid A, Khonakdar HA, Asadinezhad A, Wagenknecht U, Jehnichen D.

Crystallization and melting behavior of nanoclay-containing polypropylene/poly (trimethylene terephthalate) blends. *Express Polymer Letters*. 2012;**6**(2):148-158

[64] Dorscht BM, Tzoganakis C. Reactive extrusion of polypropylene with supercritical carbon dioxide: Free radical grafting of maleic anhydride. *Journal of Applied Polymer Science*. 2003;**87**: 1116-1122. DOI: 10.1002/app.11561

[65] Si M, Araki T, Ade H, Kilcoyne ALD, Fisher R, Sokolov JC, et al. Compatibilizing bulk polymer blends by using organoclays. *Macromolecules*. 2006;**39**:4793-4801. DOI: 10.1021/ma060125+

[66] Vo LT, Giannelis EP. Compatibilizing poly(vinylidene fluoride)/nylon-6 blends with nanoclay. *Macromolecules*. 2007;**40**:8271-8276. DOI: 10.1021/ma071508q

[67] Penava NV, Rek V, Houra IF. Effect of EPDM as a compatibilizer on mechanical properties and morphology of PP/LDPE blends. *Journal of Elastomers and Plastics*. 2012;**45**(4):391-403

[68] Sadeque M, Patil KA. Marshall properties of waste polymer and nanoclay modified bitumen. *The FACTA Universitatis, Series: Architecture and Civil Engineering*. 2014;**12**(1):1-9

[69] Ahmedzade P, Fainleib A, Gunay T, Grigoryeva O, Kultayev B, Starostenko O, et al. Use of maleic anhydride grafted recycled polyethylene treated by irradiation in bitumen modification. In: 6th Eurasphalt & Eurobitume Congress 2016; Prague, Czech Republic. 2016. pp. 1-9

[70] Clemons C. Elastomer modified polypropylene—polyethylene blends as matrices for wood flour—plastic composites. *Composites: Part A*. 2010;**41**(11):1559-1569. DOI: 10.1016/j.compositesa.2010.07.002

[71] Micic P, Bhattacharya SN, Field G. Melt strength and elastic behaviour of LLDPE/LDPE blends. *International Polymer Processing*. 1996;**11**(1):14-20

[72] Fávoro SL, Ganzerli TA, de Carvalho Neto AGV, da Silva ORRF, Radovanovic E. Chemical, morphological and mechanical analysis of sisal fiber-reinforced recycled high-density polyethylene composites. *Express Polymer Letters*. 2010;**4**(8):465-473

[73] Muhamed HE, Yehia MSE, Ashraf AM, Muhamed HZ. Composites from rice straw and high density polyethylene: Thermal and mechanical properties. *International Journal of Engineering Science*. 2015;**4**(4):57-64

[74] Cheraghi H, Ghasemi FA, Payganeh G. Morphology and mechanical properties of PP/LLDPE blends and ternary PP/LLDPE/nano-CaCO₃ composites. *Strength of Materials*. 2013;**45**(6):730-738

[75] Colbert BW. The performance and modification of recycled electronic waste plastics for the improvement of asphalt pavement materials [thesis]. Michigan: Michigan Technological University; 2012

[76] Lageraen PR, Kalb PD, Adams JW, Fuhrmann M, Milian L, Weber C, et al. Use of Recycled Polymers for Encapsulation of Radioactive, Hazardous and Mixed Wastes. United States: U.S. Department of Energy; 1997

[77] Iunolainen E. Suitability of recycled PP for 3D printing filament [MSc thesis, plastics technology]. 2017

Thermal Resistance Properties of Polyurethanes and Its Composites

Javier Carlos Quagliano Amado

Abstract

The nature of starting materials and the condition of polyurethane (PU) preparation are regarded as the main general parameters that determine PU thermal resistance. The effect of structure and presence of additives were identified as the major general factors on this regard. Structural factors include phase micro-structure, i.e., chemical structure, proportion, and segregation of soft and hard segments, polyol type (petrochemical or natural oil-based), isocyanate and chain extender type, and thermoplasticity of PU. In respect to the effect of additives, the incorporation of fillers is the most direct strategy to increase PU heat resistance. With respect to fiber additives, in general a positive effect is found on improving thermal resistance, although this generalization could not apply, considering the large number of different PU and environmental conditions of usage.

Keywords: polyurethane, thermal resistance, structure, additives, stability

1. Introduction

Polyurethanes (PUs) are characterized by excellent properties such as good resistance to abrasion and good oil and atmospheric resistance. Their main applications are very wide, as flexible foam in upholstered furniture and rigid foam in wall insulations, roofs, and appliances; thermoplastic PU resins in medical devices, automotive parts, and footwear industries; and last but not least their uses as coatings, adhesives, sealants, and elastomers (CASE) which are very important, for example, on floors and pipe protection and again in automotive parts.

It is not unusual that PU have to sustain very high temperatures in several uses, specially in applications such as defense [1]. For example, high-temperature resistant adhesives are required in advanced aircraft, space vehicles, missiles, and ground vehicles [2].

Thermal stability describes thermal durability as well as heat resistance. Polymers with higher thermal stability are characterized by higher melting points, softening and thermal decomposition, smaller mass loss during heating at high temperatures, and higher heat deflection temperature under load, without losing their basic properties which determine its functionality. In respect to analytical techniques, differential thermal analysis (DTA) and thermogravimetric analysis (TGA) were traditionally used to evaluate the thermal properties of several types of polyurethane and are still standard analytical techniques that are utilized. Thermal stability requirements can be summarized in the following statements: retention of mechanical properties (melting/softening point), high resistance to chemical attack, and high resistance to breakdown, specially under oxidative conditions.

The following figure introduces the general reactions involved in PU thermal decomposition:

The first reaction is fast. Flammable gases then react much faster with oxygen, producing more heat and small molecule gaseous degradation products (**Figure 1**). Finally, char reacts with oxygen but in a much slower rate, releasing heat but with a lesser rate. The first step of the degradation includes the scission of the urethane bonds to obtain the polyol and the isocyanate groups apart. In the second set reactions, dimerization gives off gaseous carbon dioxide and carbodiimide, and trimerization gives isocyanurates, while reactions with water render aromatic amines and carbon dioxide again. Heat is released in every reaction step, sustaining degradation until eventually a compact char is left.

PUs have unique properties derived from their two-phase microstructure composed of hard and soft segments. Soft segments (SS) are formed by polyols and have low glass transition temperatures, while hard segments (HS) are derived from diisocyanates and chain extenders and possess high glass transition temperature. PU can be considered as a block copolymer with alternating soft and hard segments along the macromolecule chain. The SS originates from the polyol and imparts extensibility to PU. The HS which is composed of urethane and aromatic rings aggregates into microdomains resulting from the hydrogen bonding, and the domains provide physical cross-linking points for materials [3].

Ingredients for manufacturing PU are polyisocyanate, polyester or polyether polyol, and a chain extender like a diol or diamine. The most reactive component is isocyanate due to its -NCO groups. The quality of PU obtained depends on the ratio of -NCO to -OH groups to obtain a good end product with the required properties. Insufficiency as well as an excess of -NCO groups will result in the formation of allophanate or biuret compounds, with different properties. On the other side, urea and isocyanurate linkages displayed higher thermal stability than polyurethanes [4].

Thermal stability of PU has been extensively studied for many decades. As introduced above, three general reactions can occur during the thermal degradation of polyurethane: (i) dissociation to the original polyol and isocyanate; (ii) formation of a primary amine, alkene, and carbon dioxide; and (iii) formation of a secondary amine and carbon dioxide [5]. The tendency for a particular mechanism depends on the chemical nature of the groups, adjacent to the urethane linkage, and the environmental conditions. Polyurethane degradation usually starts with dissociation of the urethane bonds and carbon dioxide and isocyanate evaporation [6]. The general consensus, however, is that decomposition occurs in three steps at the level

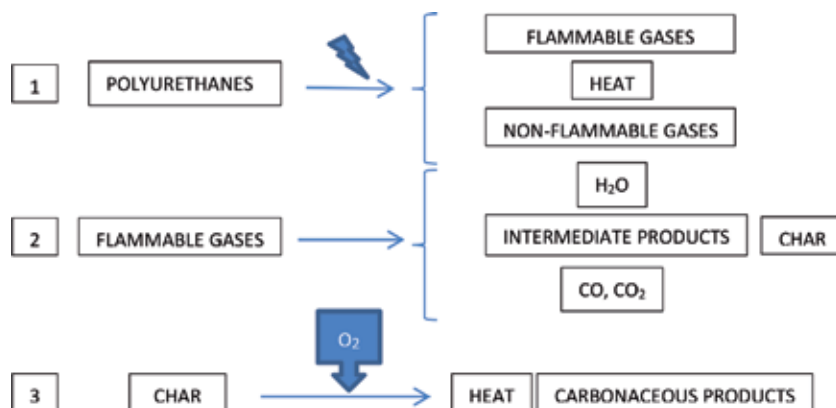


Figure 1.
General mechanism of thermal decomposition of PUs.

of the urethane group between 200 and 300°C [7]. The most important factors that determine thermal stability of PU are the nature of starting materials and the condition of polymer preparation [4].

When polyurethanes undergo thermal degradation, some potentially hazardous chemicals are released. These chemicals could not lead to visible warning. When PU is submitted to high temperatures, special health and safety precautions should be put in practice. It was early noticed that at temperatures above 600°C, cyanide is produced from PU decomposition and polyureas, giving off the so-called yellow smokes [8, 9] and emission of other toxic products [10]. The conditions of synthesis (polycondensation) and the nature of the reagents (initial prepolymers and monomers) influence the composition of the volatile compounds and residues arising from decomposition [7]. Health and safety, apart from material performance, is one of the reasons why it is important to establish heat stability ranges for materials with such a wide spectrum of utilization as PUs.

This review is intended to convey a brief compilation of research in the field of thermal resistance of non-foamed PUs and to identify strategies to augment stability to high temperatures of PUs and its composites. It is not focused in other aspects of PU which has been thoroughly covered by many other experts in reviews and books [6, 10–16]. We will concentrate on the effect of structural changes and on the effect of additives on PU thermal resistance. This contribution has in mind that the vast information about thermal properties of PU cannot be summarized in one single review but tries to present main factors that determine thermal resistance of these important polymeric materials.

2. Effect of structure on PU thermal resistance

The first structural factor that greatly influences thermal resistance is phase microstructure; this is the nature, proportion, and segregation of soft and hard segments (SS and HS, respectively). At the same time, microphase is determined by the chemical structure of PU (polyol, isocyanate, and chain extender type), so the effect of phase microstructure on thermal resistance often overlaps with chemical structure. Therefore, individual effects are rather complex to analyze. Thermal degradation is mainly initiated within the HS, which has normally the faster degradation stage. When it comes to SS, as this is composed by macrodiol, which is typically the weakest link in the oxidation of PU elastomers, using macrodiols that have high oxidative stability could give PUs with better thermo-oxidative stability. A lower flexibility in chains of SS domains produced a lower thermal resistance threshold (temperature where 5% sample weight is lost) as a result of lower crystallinity [17]. The structure of the HS has more influence on thermal stability rather than SS structure. Interurethane hydrogen bonding plays a significant role in the thermal stability of segmented PUs, which can be enhanced by a higher degree of phase separation between SS and HS [18]. The higher the concentration of the urethane group, the lower are both the activation energy for thermal decomposition and the thermal stability of the PU [19].

The polyester polyol-based PUs are more stable than the materials obtained with polyether macrodiols [4, 18]. For example, onset decomposition of polyether-polyurethane in air is about 245°C. This is anticipated to be about 13°C as compared with that in nitrogen atmosphere. Such anticipation suggested that polyester-polyurethane is more stable thermally than polyether-polyurethane. It also suggested that the different soft segments will influence the thermal stability of PU [20]. Polycarbonate diols, cured with MDI and chain extended with 1,4-butanediol, showed a drop-off in the weight of samples at around 290°C [21]. Krol and Pilch

Pitera [22] studied the effect of increasing polyol chain length on TDI-cured polyoxyethyleneglycols; the heat effect of endothermic processes within 260–420°C becomes lower and lower, while the effect at 360–440°C becomes more important. They correlated this effect with the increasing share of ether-type bonds or ester-type bonds with simultaneous reduction in the number of urethane groups; polyether PUs from polypropylenglycol (PPG), HDI, and BDO had melting temperatures of 223°C [23]. These few examples are representative of the general trend that polyester polyol-based PUs are more thermally stable than polyether macrodiol-based PUs. Hydroxy-terminated polybutadiene (HTPB) are a particular telechelic polyol in which PUs are utilized as liners for composite propellants in the manufacture of rockets. When reacted with TDI and cross-linked with small molecular weight diols as chain extenders, the final stage of decomposition was at 375°C [24].

The effect of isocyanate on thermal stability was seen early. The higher the symmetry of the isocyanate, the higher the thermal stability [25]. Aliphatic isocyanates give urethanes a higher thermal stability [4]. The decomposition of polymers made with 4,4'-diphenylmethane diisocyanate (MDI) occurred above 400°C and was at least a two-step process, while the decomposition of polymers containing toluene diisocyanate (TDI) occurred below 400°C and appeared to be a one-step reaction [26]. For PUs cured with 4,4'-dibenzyl diisocyanate (DBDI), based on polytetramethylene ether glycol (PTMEG) and chain extended with butylenglycol, three main degradation processes were seen: at approximately 340°C the decomposition of urethane groups occurred, at 420°C the destruction of ether groups took place, and at 560°C the destruction of carbon chains and rings began. In general, the DBDI material had a higher thermal oxidation stability than the similar polymer achieved with MDI [14]. Polyurethanes made from polyester-based PUs cured with MDI had a better thermal stability than those based on TDI, according to their higher degree of hard segment crystallinity [26].

Natural oil-based polyurethanes generally had better initial thermal stability (below 10% weight loss) in air than the polypropylene oxide-based PU, while the latter was more stable in nitrogen at the initial stage of degradation. If a higher weight loss (50%) is taken as the criterion of thermal stability, then oil-based polyurethanes appear to be more thermally stable material [27–30]. PU prepared from formiated soybean oil polyols and TDI with different OH functionalities showed an initial weight loss process at 210°C, while maximum weight loss was at 400°C [31]. An increase in NCO index of elastomeric PU samples prepared from soybean oil-derived polyol increased hydrogen bonds and consequently thermal stability [32]. PU from TDI, polycaprolactone, butanediol, and monoglyceride of sunflower oil had the first and second maximum peaks both linked to the degradation of urethane bonds in the rigid segment of PU. The third and fourth maximum peaks were the results of degradation of the ester bonds in the soft segments, which take place from 380°C, while the composition of the aromatic compounds begins at 480°C [33]. This findings support the fact that research on oil-based PUs is increasing, considering their natural origin and good thermal resistance properties.

PUs synthesized with the use of oligomeric α,ω -dihydroxy(ethylene-butylene adipate) (dHEBA) polyol, aliphatic 1,6-hexamethylene diisocyanate (HDI), and 1,4-butanediol (BDO) were stable until 428°C. Ten percent of initial mass was lost at 344°C [32] which is a higher temperature than TDI or other conventional polyether polyols such as polytetramethylene ether glycol-derived PUs [33]. A TPU made from polycaprolactone polyol cured with polymeric diphenyl diisocyanate prepolymer displayed a 5% weight loss at about 260°C [34]. The thermo-oxidative degradation of phosphorus-containing polyurethane based in polypropylene glycol, TDI, and 1,4-butanediol incorporating phenylbis(hydroxyethyl) phosphonate was studied by using TGA. The onset of thermal degradation is lowered to 360°C due

to the lower thermal stability of phosphorous chain extender [35]. Although being cured with TDI, thermal resistance is much higher than for other TDI-cured PUs. Phosphonate PU displayed high thermal resistance: during the thermal degradation, the phosphorous molecules form a protective layer on the polymer surface, increasing the polyurethane thermal stability [36].

Regarding chemical structure, biuret and allophanate linkages are the thermally weakest chemical entities in PU networks. Dissociation of both types generally takes place above about 110°C and is completed by about 170°C [37]. These linkages appear when unbalanced ratios of NCO and OH groups are present in reactants and are not normally desired regarding improvement of physical properties. An increase in cross-link density, type of cross-linking, and introduction of isocyanurate ring structures in the polymer chain backbone also has a strong beneficial effect on the thermal stability of polyurethanes [4].

Finally, thermoplastic polyurethanes (TPU) are a relatively novel group of the family of PUs and have high comparative thermal resistance [38] which allows them to be easily processed. TPU were introduced by DuPont in 1954 and developed through the 1950s and 1960 [39]. In general, polyurethanes have no pronounced melting point endothermic peak on differential thermograms, which is characteristic of noncrystalline polymers. On the other side, TPU have a distinct behavior compared to conventional PU, exhibiting thermal patterns like thermoplastics. For example, TPUs synthesized from novel fatty acid-based diisocyanates were reported to display considerable thermal stability without any significant loss of weight at temperatures below 235°C [40]. Significant thermal decomposition was observed only after 300°C [41].

3. Effect of additives on PU thermal resistance

In studying the complex structure and morphology of polymers modified by mineral fillers, some problems may arise concerning the character and extent of interaction at the polymer-filler interface, the homogeneity of filler distribution, the filler orientation in the case of filler anisometric particles, and the polymer-filler adhesion [42]. Polyurethanes do not get aside from this general rules. Thermal stability of PU has been reported to be improved via hybrid formation such as the incorporation of fillers, e.g., nanosilica, Fe₂O₃, and TiO₂, silica grafting, nanocomposite formation using organically modified layered silicates (nanoclays), incorporation of Si-O-Si cross-linked structures via sol-gel processes, and the incorporation of polyhedral oligomeric silsesquioxane (POSS) structures into the PU backbone or side chain [43].

Nanoclays confer high barrier performance and improved thermal stability in composites with plastics, which make these compounds suitable for many applications [44, 45]. In a PU made from HTPB, PTMEG, and TDI, TGA results revealed that the thermal stability of PU was improved by nanoclay sepiolite, and the onset decomposition temperature for PU nanocomposites with a sepiolite content of 3 wt% was about 20°C higher than that for pure PU. Initial degradation temperature for nanocomposites was around 300°C [46] and when Cloisite was utilized with PTMEG-TDI-BDO PU, an exotherm at 370–375°C in differential scanning calorimetry studies [47].

Small amounts of nanoclays as modifier to polyurethane matrix led to an increase in degradation temperature. The clay plates acted as barrier to oxygen transfer causing the degradation temperature to move to higher temperatures [48]. Stefanovic and coworkers [49] have shown that that polyurethane nanocomposite (PUNC) began to degrade at a temperature 20–40°C higher than pure PU copolymers. PUNC were

prepared from α,ω -dihydroxy-poly(propyleneoxide)-*b*-poly(dimethylsiloxane)-*b*-poly(propylene oxide) (PPO-PDMS-PPO) and organo-montmorillonite nanoclay (Cloisite 30B®) and cured with diphenylmethane diisocyanate.

Rubbery modulus for PU based on PTMEG as soft segment, isophorone diisocyanate as diisocyanate, and 1,4-butanediol as chain extender reinforced with nanosilica increased to higher temperatures, enhancing mechanical and thermal properties [50].

For thermoplastic PU composites filled with huntite and hydromagnesite mineral fillers, thermal decomposition occurred through double step with maximum rates at 347 and 411°C, and two shoulders are seen at 300 and 466°C, leaving 1.3 wt% carbonaceous char [51]. The TGA analysis of synthetic silico-metallic mineral particles (SSMMP) based on talc added to PU made from polycaprolactone and hexamethylene diisocyanate showed a significant increase in the onset temperature of the nanocomposites evidencing that the thermal resistance increased with the increase in the amount of filler added. The degradation temperature of the pure PU was the lowest, with a value of 301°C, and the degradation temperature for nanocomposites with 3 wt% of SSMMP was the highest, with values of 337–340°C [52]. Polyester-type PU filled with talc produced a 7°C increase in temperature for 5% weight loss [53].

Silsesquioxane cage structure-like hybrid molecules produce nanostructured organic-inorganic hybrid polymers called polyhedral oligomeric silsesquioxane. The POSS chains act like nanoscale reinforcing fibers, producing extraordinary gains in heat resistance. Octaaminophenyl POSS was used as a cross-linking agent together with 4,4'-methylenebis-(2-chloroaniline) to prepare PU networks containing POSS. TGA results showed the thermal stability was improved with incorporation of POSS into the system. The results can be ascribed to the significant nanoscale reinforcement effect of POSS cages on the polyurethane matrix [54].

Together with fillers, fibers generally impart heat resistance to PU, or at least do not produce a deterioration effect. Thermoplastic PU elastomer nanocomposites (TPUC) filled with 15% carbon nanofiber submitted to the torch of the oxyacetylene test resisted up to 210°C for 5 seconds, while non-filled TPU resisted only up to 175°C [55]. Composites of PU made from HTPB and TDI with coir and sisal fiber showed a principal degradation peak at around 400°C. PU from HTPB and TDI displayed the same general behavior [56]. However, there are reports that stated that fiber loading decreased thermal stability of composites with TPU: main temperature peak of complicated decomposition of a TPU was around 363°C. At the TPU/Kenaf 20% fiber loading, the first peak occurred between 246 and 369°C, with a threshold at 346°C [57]. TPUs have been reinforced with synthetic fibers such as glass [58], aramid [59], and carbon fiber [60].

Flame retardants delay decomposition temperature of PU. A study of the effect of ammonium polyphosphate (APP) on the thermal stability of some N-H and N-substituted polyurethanes showed that degradation mechanism could differ markedly [61]. Phosphorus flame retardants augment thermal resistance of PU. In pure PU, the specimen surface gradually degrades to volatile oligomers, monomer, and some molecules, whereas the presence of phosphorous flame retardant additive causes delay in degradation of polymer matrix. Phosphorus flame retardant additive compounds have low thermal stability, are decomposed earlier, and protect underlying PU matrix [20, 62]. Also, a range of stabilizers, including both organic and inorganic additives for better stability against different types of degradation, are available, with a focus on their efficacy and mechanisms of action [18].

Blending with other polymers is another strategy to augment thermal resistance of PU. Thermal decomposition of blends of a polyester urethane and polyether sulfone with or without poly(urethane sulfone), taken as a compatibilizing agent, was studied by TGA under dynamic conditions. Polyester-urethane has a temperature for

5% mass loss of 328°C and poly(ethersulfone) was 500°C, while among blends the one with 80/20 poly(ether sulfone)/polyester urethane had the higher value of 360°C [63]. Thermal resistance of styrene-butadiene-styrene rubber (SBS) was improved before and after thermal aging as the amount of added TPU was increased in rubber blends obtained via melt blending [64]. Thermal stability of a polyether-based TPU was found to be improved as a result of the incorporation of 5% polypropylene-graft-maleic anhydride (PP-g-MA) and 40% wollastonite: temperature for 50% weight loss increased from 380 to 416°C for composite compared to TPU [65]. From thermal degradation of polypropylene/TPU and ammonium polyphosphate blends, carbodiimide was generated, which, because of its instability, also reacted with water to give urea. These several cross-linking reactions stabilize the urethane bonds until 400°C [66]. PP/TPU blends with fire retardants formed an intumescent char residue protecting the matrix which prevented first peak of thermal degradation up to 200°C [67]. Thermoplastic elastomers can be prepared by creating blends of an elastic polymer with a dimensional stabilizing polymer [68] and enhance thermal/mechanical properties. Also stabilization of PU elastomers against thermal degradation by polymer modification could be achieved by introducing natural derived polymeric materials such as lignin in HTPB macrodiol [18].

Finally, the following figure is designed to summarize the main factors that affect thermal resistance of PU (**Figure 2**):

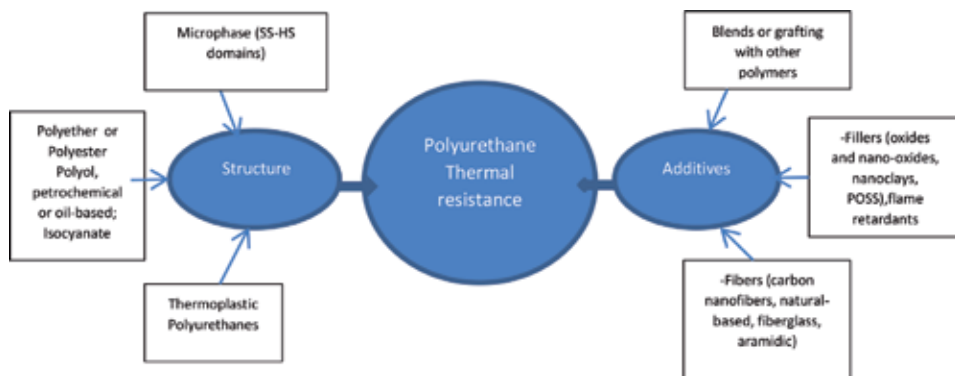


Figure 2.
Main factors that determine polyurethane thermal resistance.

4. Conclusion

As a result of this review compilation, it was concluded that the two main general factors that determine thermal resistance of PUs are its structure from one side and the presence of additives on the other side. The structural factors that influence thermal stability of PUs are the chemical nature and composition of hard (isocyanate plus chain extender) and soft (macrodiol) segments, its segregation, and PU thermoplasticity (derived from characteristic of TPU's stable linear structure). The additives that have a marked effect on augmenting thermal stability of PUs are mineral fillers (e.g., nano-oxides, nanoclays, talcs) and specific modifiers like POSS, flame retardants (both as additive and as polyol modifier), and fibers (natural or synthetic). Also, blending and grafting with other polymers are strategies that are utilized for increasing thermal resistance of PU, both for improving processing in manufacture and for high demanding applications. However, it is necessary to state that this review did not attempt to cover all particular factors that need to be taken into account when studying thermal stability of PU. Complex PU structures will

potentially have several weak chemical links, variable intermolecular forces, different relevant properties such as thermal conductivities, and even environmental factors that may cause decomposition (i.e., hydrolysis by moisture, acidity, oxidative or non-oxidative atmosphere) will contribute to only predict thermal stability in more or less broad temperature ranges.

Conflict of interest


The author declares no conflict of interest for this publication.

Author details

Javier Carlos Quagliano Amado
Applied Chemistry Department, Institute for Scientific and Technical Research for the Defense (CITEDEF), Buenos Aires, Argentina

*Address all correspondence to: jquagliano@citedef.gob.ar

IntechOpen

© 2019 The Author(s). Licensee IntechOpen. This chapter is distributed under the terms of the Creative Commons Attribution License (<http://creativecommons.org/licenses/by/3.0>), which permits unrestricted use, distribution, and reproduction in any medium, provided the original work is properly cited. 

References

- [1] Harvey J, Butler J, Chartoff R. Development of Isocyanurate Pour Foam Formulation for Space Shuttle External Tank Thermal Protection System. Ohio: University of Dayton, Research Institute; 1987
- [2] Rahman M, Kim H. Characterization of waterborne polyurethane adhesives containing different soft segments. *Journal of Adhesion Science and Technology*. 2007;**21**(1):81-96. DOI: 10.1163/156856107779976088
- [3] Prisacariu C, Scortanu E, Agapie B. In: Conference Proceedings 27th Meeting (Polymer Processing Society, Marakech); 2011
- [4] Barikali M. Thermally stable polyurethane elastomers: Their synthesis and properties. Loughborough University, Badminton Press; 1986. p. 322
- [5] Gaboriaud F, Vantelon JP. Mechanism of thermal degradation of polyurethane based on MDI and propoxylated trimethylol propane. *Journal of Polymer Science, Polymer Chemistry Edition*. 1982;**20**(8):2063-2071. DOI: 10.1002/pol.1982.170200809
- [6] Saunders JH, Frisch KC. *Polyurethane: Chemistry and Technology*. New York: Wiley-Interscience; 1962. p. 368
- [7] Ketata N, Sanglar C, Waton H, Alamercery S, Delolme F, Raffin G, et al. Thermal degradation of polyurethane bicomponent systems in controlled atmospheres. *Polymers & Polymer Composites*. 2005;**13**:1. DOI: 10.1177/096739110501300101
- [8] Chambers J, Jirickny J, Reese C. The thermal decomposition of polyurethanes and polyisocyanurates. *Fire and Materials*. 1981;**5**(4):133-141
- [9] Paabo M, Levin B. A review of the literature on the gaseous products and toxicity generated from the pyrolysis and combustion of rigid polyurethane foams. *Fire and Materials International Journal*. 1987;**11**(1):1-29. DOI: 10.1002/fam.810110102
- [10] Backus J, Bernard D, Darr W, Saunders J. Flammability and thermal stability of isocyanate-based polymers. *Journal of Applied Polymer Science*. 1968;**12**:1053-1074
- [11] Woods G. *ICI Polyurethanes Book (2nd Edition)*. Chichester, New York: John Wiley and Sons; p. 1990. ISBN-13:9780471926580
- [12] Randall D, Lee S. *The Polyurethanes Book*. New York: Wiley Ltd.; 2002
- [13] Zafar F, Eram Sharmin E. *Polyurethane: An Introduction*. Rijeka, Croatia: Intech; 2012. DOI: 10.5772/2416
- [14] Prisacariu C. *Polyurethane Elastomers. From Morphology to Mechanical Aspects*. Springer Verlag/Wein; 2011. p. 254. DOI: 10.1007/978-3-7091-0514-6
- [15] Szycher M. *Szycher's Handbook of Polyurethanes*. Boca Raton, Florida: CRC Press, Taylor and Francis; 2013. p. 1144. ISBN 9781138075733
- [16] Yilmaz F. *Aspects of Polyurethanes*. IntechOpen; 2017. DOI: 10.5772/65991
- [17] Lei W, Fang C, Zhou X, Li J, Yang R, Zhang Z, et al. Thermal properties of polyurethane elastomers with different flexible molecular chain based on p-phenylene diisocyanate. *Journal of Materials Science and Technology*. 2017;**33**(1):1424-1432. DOI: 10.1016/j.jmst.2017.05.014
- [18] Xie F, Zhang T, Bryant P, Kurusingal V, Colwell J, Laycock B. Degradation and stabilization of polyurethane elastomers. *Progress in Polymer Science*. 2019;**90**:211-268. DOI: 10.1016/j.progpolymsci.2018.12.003

- [19] Chang W. Decomposition behavior of polyurethanes via mathematical simulation. *Journal of Applied Polymer Science*. 1994;**53**(13):1759-1769. DOI: 10.1002/app.1994.070531306
- [20] Shufen L, Zhi J, Kaijun Y, Shuqin Y, Chow W. Studies on the thermal behavior of polyurethanes. *Polymer-Plastics Technology and Engineering*. 2006;**45**(1):95-108. DOI: 10.1080/03602550500373634
- [21] Eceiza A, Martin M, De la Caba G, Kortaberria G, Gabilondo N. Thermoplastic polyurethane elastomers based on polycarbonate diols with different soft segment molecular weight and chemical structure: Mechanical and thermal properties. *Polymer Engineering & Science*. 2008;**48**(2):297-306. DOI: 10.1002/pen.20905
- [22] Krol P, Pilch PB. Phase structure and thermal stability of crosslinked polyurethane elastomers based on well-defined prepolymers. *Journal of Applied Polymer Science*. 2007;**104**(3): 1464-1474. DOI: 10.1002/app.25011
- [23] Almeida C, Ramos M, Gonçalves D, Akcelrud L. Synthesis and characterization of segmented polyurethanes with controlled molecular weight blocks. Part 2: Correlations between morphology, thermal and mechanical properties. *Polímeros: Ciência e Tecnologia*. 2000;**10**(4):22. DOI: 10.1590/S0104-14282000000400006
- [24] Mahanta A, Patak D. HTPB-polyurethane: A versatile fuel binder for composite solid propellants. In: Zafar F, Sharmin E, editors. *Polyurethane: An Introduction*. Rijeka, Croatia: Intech; 2012. DOI: 10.5772/2416
- [25] Britain J. *The Polymer's Chemistry of Synthetic Elastomers*. Saunders JH. Chapter VII-A, J.P. Kennedy and Tornquist, ed. Interscience; 1969
- [26] Slade P, Jenkins L. Thermal analysis of polyurethane elastomers. *Journal of Polymer Science Part C: Polymer Symposia*. 1964;**6**(1):23-32
- [27] Yong Y, Chen W, Yu T, Linliu K, Tseng Y. Effect of isocyanates on the crystallinity and thermal stability of polyurethanes. *Journal of Applied Polymer Science*. 1996;**62**(5): 827-834. DOI: 10.1002/(SICI)1097-4628(19961031)62:5<827:AID-APP15>3.0.CO;2-P
- [28] Javni I, Zoran S, Petrović Z, Guo A, Fuller R. Thermal stability of polyurethanes based on vegetable oils. *Journal of Applied Polymer Science*. 2000;**77**(8):1723-1734. DOI: 10.1002/1097-4628(20000822)77:8<1723::AID-APP9>3.0.CO;2-K
- [29] Monteavaro L, Riegel Vidotti IC, Petzhold CL, Samios D. Thermal stability of soy-based polyurethanes. *Polímeros*. 2005;**15**(2):151-155
- [30] Mizera K, Ryszkowska J. Thermal properties of polyurethane elastomers from soybean oil-based polyol with a different isocyanate index. *Journal of Elastomers & Plastics*. 2018:1-18
- [31] Das B, Konwar U, Mandal M, Karak N. Sunflower oil based biodegradable hyperbranched polyurethane as a thin film material. *Industrial Crops and Products*. 2013;**44**:396-404. DOI: 10.1016/j.indcrop.2012.11.028
- [32] Kucinska-Lipka J, Gubanska I, Sienkiewicz M. Thermal and mechanical properties of polyurethanes modified with L-ascorbic acid. *Journal of Thermal Analysis and Calorimetry*. 2017;**127**:1631
- [33] Bocchio J, Wittemberg V, Quagliano J. Synthesis and characterization of polyurethane/bentonite nanoclay based nanocomposites using different diisocyanates: relation between

- mechanical and thermal properties. In: 3rd. International Conference on Structural Nanocomposites (Nanostruc 2016), IOP Publishing; DOI: 10.1088/1757-899X/195/1/012001
- [34] Huang S, Xiao J, Zhu Y, Qu J. Synthesis and properties of spray-applied high solid content two component polyurethane coatings based on polycaprolactone polyols. *Progress in Organic Coatings*. 2017; **106**:60-68. DOI: 10.1016/j.porgcoat.2017.02.011
- [35] Chang T, Zheng W, Chiu Y, Ho S. Thermo-oxidative degradation of phosphorus containing polyurethane. *Polymer Degradation and Stability*. 1995; **49**:353-360
- [36] Spirckel M, Regnier N, Mortaigne B, Youssef B, Bunel C. Thermal degradation and fire performance of new phosphonate polyurethanes. *Polymer Degradation and Stability*. 2002; **78**(2):211-218. DOI: 10.1016/s0141-3910(02)00135-0
- [37] Levchik S, Weil E. Thermal decomposition, combustion and fire-retardancy of polyurethanes—A review of the recent literature. *Polymer International*. 2004; **53**:1585-1610. DOI: 10.1002/pi.1314
- [38] Wu J, Li C, Wu Y, Leu M, Tsai Y. Thermal resistance and dynamic damping properties of poly (styrene-butadiene-styrene)/thermoplastic polyurethane composites elastomer material. *Composites Science and Technology*. 2010; **70**(8):1258-1264. DOI: 10.1016/j.compscitech.2010.03.014
- [39] Drobny J. A brief history of thermoplastic elastomers. In: *Handbook of Thermoplastic Elastomers*. Rijeka, Croatia: Intech; 2007. pp. 9-11. DOI: 10.1016/b978-081551549-4.50003-7
- [40] Akindoyo J, Beg M, Ghazali S, Islam M, Jeyaratnama N, Yuvaraj A. Polyurethane types, synthesis and applications—A review. *RSC Advances*. 2016; **6**(115):114453-114482. DOI: 10.1039/c6ra14525f
- [41] More AS, Lebarbe T, Maisonneuve L, Gadenne B, Alfos C, Cramail H. Novel fatty acid based diisocyanates towards the synthesis of thermoplastic polyurethanes. *European Polymer Journal*. 2013; **49**:823-833
- [42] Fujiyama M, Wakino T. Crystal orientation in injection molding of talc-filled polypropylene. *Journal of Applied Polymer Science*. 1991; **42**(1):9-20
- [43] Chattopadhyay D, Webster D. Thermal stability and flame retardancy of polyurethanes. *Progress in Polymer Science*. 2009; **34**:1068-1133
- [44] Ray S, East A. Advances in polymer-filler composites: Macro to nano. *Materials and Manufacturing Processes*. 2007; **22**(6):741-749
- [45] Alexandre M, Dubois P. Polymer-layered silicate nanocomposites: Preparation, properties and uses of a new class of materials. *Materials Science & Engineering R: Reports*. 2000; **28**:1-2, 163. DOI: 10.1016/s0927-796x(00)00012-7
- [46] Chen H, Huizhen L, Zhou Y, Zheng M, Ke C, Zeng D. Study on thermal properties of polyurethane nanocomposites based on organosepiolite. *Polymer Degradation and Stability*. 2012; **97**:242-247
- [47] Quagliano J, Bocchio J. Effect of nanoclay loading on the thermal decomposition of nanoclay polyurethane elastomers obtained by bulk polymerization. *IOP Conference Series: Materials Science and Engineering*. 2014; **64**(1):012035
- [48] Reza RM, Barikani M, Barmar M, Honarkar H. An investigation into the effects of different nanoclays on polyurethane nanocomposites

properties. *Plastics-Polymer-Plastics Technology and Engineering*. 2014;**53**(8):801-810

[49] Stefanović I, Spirkova M, Ostojić S, Pavlović P, Pergal M. Montmorillonite/poly(urethane-siloxane) nanocomposites: Morphological, thermal, mechanical and surface properties. *Applied Clay Science*. 2007;**149**(1):136-146

[50] Seo J, Kim B. Preparations and properties of waterborne polyurethane/nanosilica composites. *Polymer Bulletin*. 2005;**54**(1-2):123-128

[51] Guler T, Tayfun U, Bayramli E, Dogan M. Effect of expandable graphite on flame retardant, thermal and mechanical properties of thermoplastic polyurethane composites filled with huntite and hydromagnesite mineral. *Thermochimica Acta*. 2017;**647**:70-80

[52] Dias G, Argenton Prado M, Carone C, Ligabue R, Dumas A, Martin F, et al. Synthetic silico-metallic mineral particles (SSMMP) as nanofillers: Comparing the effect of different hydrothermal treatments on the PU/SSMMP nanocomposites properties. *Polymer Bulletin*. 2015;**72**:2991

[53] Bajsi E, Rek V, Sosi I. Preparation and characterization of talc filled thermoplastic polyurethane/polypropylene blends. *Journal of Polymers*. 2014:289283, 8 p

[54] Liu H, Zhen S. Polyurethane networks nanoreinforced by polyhedral oligomeric silsesquioxane. *Macromolecular Rapid Communications*. 2005;**26**(3):196-200

[55] Allcorn E, Natali M, Koo J. Ablation performance and characterization of thermoplastic polyurethane elastomer nanocomposites. *Composites Part A: Applied Science and Manufacturing*.

2013;**45**:109-118. DOI: 10.1016/j.compositesa.2012.08.017

[56] Mothe C, De Araujo C. Properties of polyurethane elastomers and composites by thermal analysis. *Thermochimica Acta*. 2000;**357-358**:321-325

[57] El-Shekeil Y, Sapuan S. Influence of fiber content on the mechanical and thermal properties of Kenaf fiber reinforced thermoplastic polyurethane composites. *Materials & Design*. 2012;**40**:299-303

[58] Wilberforce S, Hashemi S. Effect of fibre concentration, strain rate and weldline on mechanical properties of injection-moulded short glass fibre reinforced thermoplastic polyurethane. *Journal of Materials Science*. 2009;**44**:1333-1343

[59] Vajrasthira C, Amornsakchai T, Bualek-Limcharo E. Fiber-matrix interactions in aramid-short-fiber-reinforced thermoplastic polyurethane composites. *Journal of Applied Polymer Science*. 2003;**87**:1059-1067

[60] Correa R, Nunes R, Filho W. Short fiber reinforced thermoplastic polyurethane elastomer composites. *Polymer Composites*. 1998;**19**:152-155

[61] Montaudo G, Puglisi C, Scamporrino E, Vitalini D. Mechanism of thermal degradation of polyurethanes. Effect of ammonium polyphosphate. *Macromolecules*. 1984;**17**(8):1605-1614. DOI: 10.1021/ma00138a032

[62] Aslzadeh M, Abdouss M, Sadeghi G. Preparation and characterization of new flame retardant polyurethane composite and nanocomposite. *Journal of Applied Polymer Science*. 2012;**127**(3):16831690. DOI: 10.1002/app.37809

[63] Filip D, Macocinschi D. Thermogravimetric analysis of polyurethane-polysulfone

blends. *Polymer International*.
2002;**51**:699-706

[64] Wu Li C, Wu Y, Leu M, Tsai Y. Thermal resistance and dynamic damping properties of poly (styrene-butadiene-styrene)/thermoplastic polyurethane composites elastomer material. *Composites Science and Technology*. 2010;**70**:8:1258-1264

[65] Chuayjuljit S, Ketthongmongkol S. Properties and morphology of injection and compression-molded thermoplastic polyurethane/polypropylene-graft-maleic anhydride/wollastonite composites. *Journal of Thermoplastic Composite Materials*. 2012;**26**(7):923-935

[66] Bugajny M, Le Bras M, Bourbigot S. Thermoplastic polyurethanes as carbonization agents in intumescent blends. Part 2: Thermal behavior of polypropylene/thermoplastic polyurethane/ammonium polyphosphate blends. *Journal of Fire Sciences*. 2000;**18**(1):7-27. DOI: 10.1177/073490410001800102

[67] Jiao Y, Wang X, Wang Y, Wang D, Zhai Y, Lin J. Thermal degradation and combustion behaviors of flame-retardant polypropylene/thermoplastic polyurethane blends. *Journal of Macromolecular Science, Part B*. 2009;**48**(5):889-909. DOI: 10.1080/00222340903028969

[68] Shanks R, Kong I. Thermoplastic elastomers. In: El-Sonbati A, editor. *Thermoplastic Elastomers*. Intech; 2012. pp. 137-154. 416 p. ISBN: 978-953-51-0346-2

Recycled Polypropylene-Coffee Husk and Coir Coconut Biocomposites: Morphological, Mechanical, Thermal and Environmental Studies

Miguel Ángel Hidalgo-Salazar, Juan Pablo Correa-Aguirre, Juan Manuel Montalvo-Navarrete, Diego Fernando Lopez-Rodriguez and Andrés Felipe Rojas-González

Abstract

In this work, biocomposites based on recycled polypropylene (r-PP) and two different natural fibers (coffee husk-CHF and coconut coir-CCF fibers) were prepared using extrusion and injection molding processes. Also, the addition of maleated polypropylene (MAPP) as a coupling agent on the biocomposites was explored. Recycled polypropylene and its biocomposites were tested following ASTM standards in order to evaluate tensile and flexural mechanical properties. Also, thermal behavior and the morphology of these materials have been studied by differential scanning calorimetry (DSC), thermogravimetric analysis (TGA), and scanning electronic microscopy (SEM). The experimental results showed that the addition of CHF and CCF to the r-PP resulted in an increase in the flexural modulus and thermal properties of the composites but resulted in poor impact properties. Thermal characterization showed that CHF possesses a better thermal stability compared to CCF. However, both fibers act as nucleating agents and generate an increase in the thermal stability of the r-PP phase. Finally, it was observed that addition of 4% of MAPP significantly improved the mechanical strength and impact behavior of the biocomposites. Regarding environmental issues, a cradle to gate life cycle assessment was made in order to define the carbon footprint of the materials.

Keywords: coconut coir, coffee husk, recycled polypropylene, biocomposites, MAPP

1. Introduction

Residual biomass is defined as a compound that contains mainly nonedible vegetal material called lignocellulose. Lignocellulose is the most important component found in plant tissues and is composed of three different polymers: cellulose,

hemicellulose, and lignin. Each of these components can be found on different parts of the biological structure of the plant, being the hemicellulose is the matrix that covers the cellulose skeleton and the lignin is the encrusting material or protective layer [1].

On the other hand, a plastic waste is defined as the material recovered by the final users after having complied with the use for which it was produced [2, 3]. This type of waste is classified in two categories: postconsumer plastic and postindustrial. The first one refers to residual plastics that have been previously used by people. In contrast, postindustrial or preconsumer plastics are defined as the industrial reject material (cuts of materials and damaged pieces, among others) that is not returned to the production line. These are recycled to a great extent, due to the high availability that exists and its relative degree of purity.

Around 140 billion tons/year of biomass wastes are generated in the world as a result of agricultural activities [4] and 230 million tons/year of plastic wastes [5] related to the production of these materials. In the case of Colombia, an estimated production of 72 million tons/year of residual biomass is reported [6]. Crops such as coffee, bananas, coconut, corn, and sugar cane contribute a large proportion to this production. Waste generated by the coconut processing industry includes its shell, water, and coir. Shell and coir represent 35% in weight of the entire fruit. In Colombia, about 4100 tons/year of this type of waste are produced that is the reason why some studies are being carried out in the biotechnology and construction fields to give them an adequate use [7]. There are two types of coir, the brown coir which is obtained from mature coconuts and the white coir which is extracted from green coconuts. Generally, this type of fiber has a length of 350 mm, a diameter between 0.12 and 0.25 mm, and a density of 1250 kg/m³. It is a material resistant to microbial degradation and salt water. It has a high content of lignin and is defined as a strong material with a high tensile strength [8]. On the other hand, one of the wastes generated in large quantities during the process of the coffee bean transformation is the coffee husk. This material represents 4.5% of the grain composition, and about 33.000 tons/year is produced in Colombia [9]. The proposed uses for this waste are fermentation in order to obtain enzymes, organic acids, or bioethanol. Also, it is used as a substrate for the growth of fungi and other microorganisms [10]. This type of vegetable fiber has an average diameter of 1.2 mm, a high content of holocellulose, as well as a significant proportion of lignin [11].

On the other hand, the national demand for plastic resins is close to 1.2 million ton/year [12], of which about 27.5% are recovered [13]. The rest of the material is disposed in landfills or inadequately in open dumps. **Tables 1** and **2** show the waste generation of the main agricultural crops and plastic resins in Colombia, respectively.

There are different studies from different areas related to the use of biomass waste. A great number of treatments have been proposed to add value to this type of material or simply to change its characteristics and make its final disposition simpler [15]. The main areas for the use of biomass waste are animal and human nutrition, energy generation, biotechnology industry, and the production of biocomposites (natural fiber reinforced polymers or NFRP).

Since several decades, biocomposites have emerged as an option aimed to solve several issues within the composite materials science. In most of published cases in literature, the use of natural fibers combined with polymers is carried out to achieve some degree of reinforcement from the fibers to the polymer. Many studies report the use of natural fibers such as flax, hemp, jute, sisal, coconut fiber, banana, and fique, among many others [16], using an extensive variety of polymer matrices like polyethylene [17, 18], polypropylene (PP) [19] polystyrene (PS) [20], epoxy resin (EP) [21], natural rubber [22], and recycled polypropylene (r-PP) [2]. Clear effects have been seen in the improvement of mechanical and thermal performance.

Crop	Production (Ton/year) [6]	Waste	Waste factor (Ton _{waste} /Ton _{product}) [6]	Waste mass (Ton/year)
Oil Palm	3.039.637	Coarse Leaves	0.22	401.232
		Fiber	0.63	1.148.982
		Palm Coir	1.06	1.933.209
Sugarcane	24.811.681	Leaves	3.26	10.110.760
		Bagasse	2.68	8.311.913
Coffee	850.500	Pulp	2.13	1.811.565
		Husk	0.21	178.605
		Stem	3.02	2.568.510
Corn	1.293.975	Leaves and stems	0.93	1.203.396
		Cob	0.27	349.373
		Fibers	0.21	271.734
Rice	2.243.981	Straw	2.35	5.273.355
		Husk	0.2	448.796
Banana	2.026.828	Coir	1	2.026.828
		Stem	5	10.134.140
		Discard fruit	0.15	304.024
		Skin	0.3	608.048
Coconut	129.956	Coir	0.35 [14]	45484.6

Table 1.
 Generation of lignocellulosic waste in Colombia.

Polymer	National demand (Ton/year) [12]	Waste mass (Ton/year)
PVC	220.000	159.500
PS	78.000	56.550
LDPE	119.000	86.275
HDPE	160.000	116.000
PP	240.000	174.000
PET	163.000	118.175

Table 2.
 Generation of plastic waste in Colombia.

These materials have the potential to be used in different industrial areas, mostly on automotive, industrial, construction, and decoration applications [23]. Due to its renewable nature, research and development of biocomposites have been constantly increasing, and its applications are spreading to multiple areas, being its main attractive is the combination between low price, biodegradability, availability, and their capability to substitute other compounds that use regular reinforcements as glass or carbon fibers [24, 25]. Characteristics as the ones mentioned before contribute to lower the environmental burden of these kinds of materials throughout their life cycle. When compared to traditional plastic products, the substitution of the polymeric material with a natural fiber fraction on the composite can reduce

environmental impacts derived from raw material acquisition, operation life of the product, and end of life processes. Since natural fibers are in most cases residues from agricultural practices, their incorporation on an industrial process serves as a waste management alternative where the fibers are recycled as reinforcement for plastic materials, helping to minimize environmental burdens from their primary process in agriculture where they are treated as conventional waste. Also, the reincorporation of these residues contributes to assess environmental impacts of raw material transportation at a local scale. Furthermore, this material fraction substitution reduces the amount of plastic material needed to fabricate one product, and as a consequence, less quantity of polymers are demanded for production, and less extraction of fossil resources has to be made in order to supply this productive sector. Regarding processing, biocomposites offer a wide amount of advantages related to processing techniques. These materials not only can reduce the melting temperatures on the process, contributing to lower the embodied energy of the product and consequently the carbon emissions of the product, but also can be processed with existing tools and procedures, which means that the producer does not have to make major adjustments on his production line to work with them.

Nevertheless, not every composite is easy to process, and so traditional material may have a favored position related to biocomposites due to its advanced and well-studied processing techniques, and as direct result, fewer residues can be achieved during the fabrication process. Still some experiences with biocomposites have led to significant reduction of Greenhouse Gases during processing and transformation stages [26]. In the case of thermoformed trays, it was found that by replacing talc fillers with starch fibers, the carbon footprint for this product was reduced around a 20% regarding gas emissions from processing [27].

Other outstanding characteristic of biocomposites compared to their traditional counterparts is the reduction of weight for the final product. For automotive applications, this characteristic could allow savings of carbon emissions by reducing the total weight of the vehicle and thus consuming less fuel without compromising the integrity of the material properties and the security guidelines of the automotive industry. Materials that possess high specific stiffness and specific strength are often very valuable in applications in which weight will be a critical factor [25], which makes biocomposites ideal candidates for automobile design and spare parts production. Different automakers believe that all advanced composite car bodywork could be around 50–67% lighter than current similarly sized steel auto-body, 40–55% lighter than an aluminum auto-body, and 25–30% lighter than a steel auto-body. Nevertheless, there are not bio-based materials on commercial use or development that can be fully considered sustainable [28]. It is a fact that products derived from renewable resources tend to be competitive in the market if they prove to be similar or better than other products regarding performance and price. In fact, Reinders et al. [29] said that full bio-based brands usually have stronger purchase intentions than other brands, including those that are partially composed by bio-based products. However, the fact that a product has a renewable origin does not mean that its environmental performance is better when comparing it to traditional products in the market. A case-based evaluation is necessary to define the environmental aspects of a product and thus the sustainable nature of the product [30]. Virtually, biocomposites can be considered sustainable materials compared to traditional composites or fossil-based polymeric materials. The renewable provenance of these materials and the availability of the resource can suggest better environmental performance among its life cycle, easing pressures over the natural systems. However, critical aspects of the elaboration process during the materials life cycle can lead to different types of environmental impacts, which in turn, may be worse than the ones derived from traditional composite elaboration.

Manufacturing techniques should be strongly studied and refined in order to make them mainstream and reduce concerns and impacts regarding their development degree. Therefore, as mentioned before, this is the main reason why every case of composite material has to be reported on a case-based scenario in order to objectively define the sustainable nature of products developed with these kinds of materials. In this book chapter, biocomposites based on recycled polypropylene (r-PP) and two different natural fibers (coffee husk and coconut coir fibers) with maleated polypropylene (MAPP) as a coupling agent were prepared through extrusion and injection molding processes. Morphological, mechanical, and thermal properties of the biocomposites were investigated with the aim to understand the effect of fiber type and MAPP addition on the r-PP matrix properties. Also, the environmental performance of the materials was studied through a carbon footprint evaluation on a cradle to gate life cycle assessment.

2. Materials and methods

2.1 Materials

Coconut coir (CCF) was obtained from “Kiero Coco” S.A (Manizales-Colombia), and coffee husk fiber (CHF) was obtained from a local coffee mill located in Tuluá-Colombia. Recycled polypropylene (rPP) was a postindustrial waste collected from extrusion and injection processes carried out in the materials laboratory of the Autónoma de Occidente University (Cali, Colombia). Maleic anhydride grafted polypropylene (Licocene MAPP 6452 by Clariant) was used as coupling agent.

2.2 Natural fibers characterization

The time between the generation of the different fiber waste and its storage (at -20°C) was less than 8 hours, in order to minimize biochemical changes in the fibers. After separation, the fibers were dried in an oven at 45°C until reaching constant weight. Drying process was carried out at this temperature in order to avoid the elimination of volatile compounds and degradation of the lignocellulosic composition. After drying, the samples were milled (particle size <1 mm) in an impact mill (Retsch SR200). The milling time was 15 minutes for CHF and 30 minutes for CCF. Finally, fibers samples were stored in polyethylene bags with a hermetic seal at room temperature. After the characterization, the fibers were sieved in ASTM sieves, with the purpose of reaching a 60 mesh particle size, established by the ASTM standards for the analysis of solid samples.

The fibers (CHF and CCF) were characterized by proximate and elemental analysis, calorific power, and structural composition. These analyzes were performed in triplicate. Through the proximate analysis, the percentage of moisture content (M), volatile matter (VM), ash (A), and fixed carbon (FC) was determined according to ASTM D7582-12 [31]. These analyzes were performed using approximately 1.0 g of sample in a Leco brand thermogravimetric analyzer, TGA-601. **Table 3** shows the equations used in the determination of the proximate analysis of CHF and CCF. The calorific value was calculated using 1.0 g of sample in a Leco AC-350 calorimeter pump, following the ASTM 5865-13 standard. The calorific value establishes the amount of energy per unit mass that the waste can deliver when it is completely oxidized. This property was calculated using the equation also presented in **Table 3**.

Parameter	Equation
Moisture content at 105°C	$\%M_{105} = \frac{SW-DSW}{SW} \times 100$ (1)
Ash	$\%A = \frac{ACW-CW}{DSW} \times 100$ (2)
Volatile matter	$\%VM = \frac{DSW-VSW}{DSW} \times 100$ (3)
Fixed carbon	$\%FC = 100 - \%M_{105} - \%A - \%VM$ (4)
Superior calorific power	$SCP = 20.7999 - 0.3214 \frac{VM}{FC} + 0.0051 \left(\frac{VM}{FC} \right)^2$ $- 11.2277 \frac{A}{VM} + 4.4953 \left(\frac{A}{VM} \right)^2 - 0.7223 \left(\frac{A}{VM} \right)^3$ $+ 0.0383 \left(\frac{A}{VM} \right)^4 + 0.0076 \frac{FC}{A}$

SW: sample weight (gr), DSW: dry sample weight (gr), ACW: crucible weight + ashes (gr), CW: crucible weight, VSW: devolatilized sample weight (gr).

Table 3.
Equations used in the proximate analysis of lignocellulosic residues.

The elemental analysis was carried out in a Leco CHN-628 analyzer to determine the content of carbon (C), hydrogen (H), and nitrogen (N) according to ASTM D 5373-14 and in a Leco S-632 to quantify the sulfur content (S) according to ASTM D 4239-14. A weight sample of 0.1 g was used on both equipments.

The structural composition of the fibers was determined by the quantification of extractive compounds (EXT), lignin (LGN), cellulose (CEL), hemicellulose (HMC), and inorganic compounds (ashes). The preparation of the fibers was carried out following the standard NREL/TP-510-42620. In order to obtain the percentages of CEL, HMC, and LGN, it is necessary to perform two Soxhlet extractions to the fibers using water and ethanol as solvent, as indicated in the NREL/TP-510-42619 standard. The insoluble acid lignin percentage (LGN) or Klason lignin was calculated according to the standard NREL/TP-510-42618. The holocellulose percentage (HCL) was determined by following the ASTM D1104 standard, while the cellulose percentage was determined following the Han and Rowell methods [32]. **Table 4** shows the equations used for structural composition calculation of CHF and CCF.

Equation	Reference
$\%EXT_{water} = \frac{PEXT_{water}}{PR \times \%MS} \times 100$ (6)	[33]
$\%EXT_{ethanol} = \frac{PEXT_{ethanol}}{PR \times \%MS} \times 100$ (7)	
$\%EXT = \%EXT_{water} + \%EXT_{ethanol}$ (8)	
$\%LGN = \frac{PLGN}{PR_{EXT} \times \%MS} \times (100 - \%EXT)$ (9)	
$\%HCL = \frac{PHCL}{PR_{EXT} \times \%MS} \times (100 - \%EXT)$ (10)	[32, 33]
$\%CEL = \frac{PCEL}{PHCL} \times \%HCL$ (11)	[32]
$\%HMC = \%HCL - \%CEL$ (12)	

Where, % EXT: proportion of total extractives, % EXT_{water}: proportion of extractives in water, % EXT_{ethanol}: proportion of extractives in ethanol, PEXT_{water}: weight of extractives in water (gr), PEXT_{ethanol}: weight of extractives in ethanol (gr), PR: dry sample weight (gr), % MS: percentage of dry matter, % LGN: proportion of lignin, PLGN: weight of lignin (gr), PR_{EXT}: weight of the sample free of extractives (gr), % HCL: proportion of holocellulose, PHCL: weight of holocellulose (gr), % CEL: percentage of cellulose, PCEL: weight of cellulose (gr), % HMC: proportion of hemicellulose.

Table 4.
Equations used in the determination of the structural composition of lignocellulosic residues.

2.3 Preparation of the biocomposites

r-PP and its biocomposites were compounded in a co-rotating twin screw extruder (Harden Industries Ltd., China). For each case, MAPP, CCF, and CHF fibers were physically premixed with r-PP pellets in a plastic bag using 30% of fibers and 4% of MAPP in weight. A temperature gradient from 140 to 170°C from the feeder zone to the die was used. The rotation speed of the twin-screw was 50 rpm. The outcoming cord of r-PP and its biocomposites from the extruder were pelletized using a mill which produced pellets of about 5 mm long. After the pelletization process, the r-PP and its biocomposites samples were dried in an oven at 85°C followed by an injection molding process. A BOY XS (BOY Machines, Inc., USA) microinjection molding machine was used to prepare samples for flexural and impact tests. **Table 5** summarizes the injection-molding processing parameters used. **Figure 1** shows the injected specimens of neat PP, r-PP, r-PP-CHF, and r-PP-CCF biocomposites.

2.4 Characterization of the biocomposites

2.4.1 Flexural properties

Three point bending flexural tests were performed with an INSTRON universal testing machine model 3366 according to the ASTM D 790-17 as shown in **Figure 2**.

Parameter	Value
Barrel temperature(°C)	185
Nozzle temperature (°C)	180
Injection time (s)	3.8
Cycle time (s)	37.5
Screw travel (mm)	18.7
Back pressure (bar)	60
Injection pressure (bar)	80

Table 5.
Injection molding parameters used.

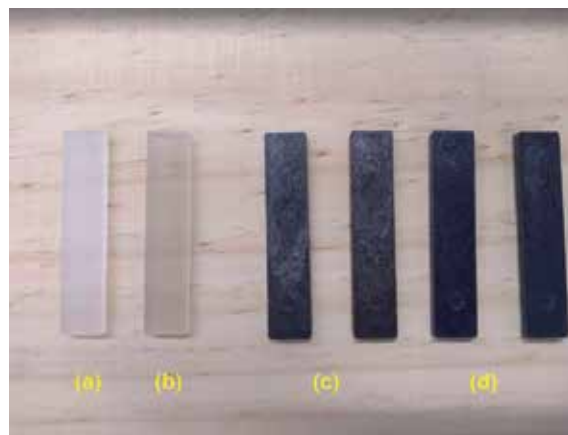


Figure 1.
Injected specimens of: (a) neat PP, (b) r-PP, (c) r-PP-CHF and (d) r-PP-CCF biocomposites.



Figure 2.
Assembly used for flexural test (according to ASTM D790).

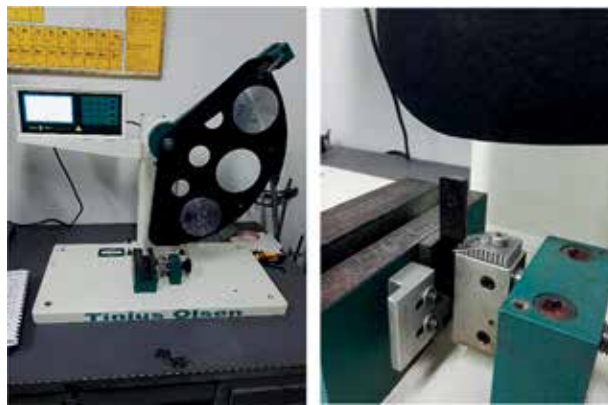


Figure 3.
Pendulum type impact test machine used for the notched IZOD impact measurements.

The tests were carried out on bars of rectangular cross section at 23°C and at a rate of crosshead motion between 1.34 and 1.44 mm/min. This rate was determined based on the dimensions of the specimens. Also, the distance between the supports was 50 mm and the tests were conducted up to 5% strain. All the results were taken as the average value of five samples.

2.4.2 Impact properties

The impact strength of PP and biocomposites was determined with an Izod Tinius Olsen impact pendulum equipped with a 4.53 N pendulum. Prior to the test, the materials were subjected to conditioning for 48 hours at 50% relative humidity and a temperature of 25°C. The specimens were made following the standard ASTM D256, and the starting angle of the test was 150° as shown in **Figure 3**. All the results were taken as the average value of five samples.

2.4.3 Thermal characterization

DSC test was carried out using a TA Q2000 differential scanning calorimeter under nitrogen atmosphere at a scanning rate of 10°C/min, with a sample of 10 mg in aluminum pans. The thermal history of the samples was erased by a preliminary heating cycle at 10°C/min from 20 to 200°C and maintaining it at that temperature for 10 min to melting residual crystals, cooling at 10°C/min to 0°C, and finally, they

were heated at °C/min from 0 to 200°C. The crystallization temperatures (T_c) and melting temperatures (T_m) were determined from cooling and second heating scans. The melting enthalpies values were normalized according to the proportion of the components in the samples. The crystallinity (χ_c) was determined from the Eq. (13):

$$\chi_c = \left(\frac{\Delta H_m}{[\Delta H_m^0 * (1 - w_{\text{Fiber}})]} \right) * 100 \quad (13)$$

where w_{Fiber} is the CHF or CCF fiber mass fraction, ΔH is the melting enthalpy of the sample, and ΔH_m^0 is the specific enthalpy of melting for 100% crystalline PP. This value was reported in literature as 293 J/g [34].

2.4.4 Morphology

Scanning electronic microscopy (SEM) of the biocomposites was carried out on the cryogenic fracture surfaces of the specimens using a Quanta FEG 250 microscope operating at a voltage of 10 kV. The samples were previously sputter coated with gold to increase their electric conductivity. Determinations were performed in different areas of the SEM micrograph.

2.4.5 Statistical analysis

Flexural and impact properties of the materials were subjected to analysis of variance (ANOVA), and the Tukey's test was applied at the 0.05 level of significance. All statistical analyses were performed using Minitab Statistical Software Release 12 (Pennsylvania, United States).

2.5 Environmental characterization of the materials

The environmental characterization of the materials was made through a cradle to gate Life Cycle Assessment based on the ISO 14041 parameters. The only indicator used for this evaluation was the carbon footprint, and the information for the emission factors was taken from secondary information found in literature.

3. Results and discussion

3.1 Natural fibers characterization

The proximate analysis of CCF and CHF is presented in **Table 6**. Comparing the obtained values, it is observed that the fiber with the highest moisture content is the

Natural fiber	%M ₁₀₅	%A	%VM	%FC	SCP (MJ/Kg)	References
CHF	11.61 ± 0.08	1.65 ± 0.05	83.08 ± 0.08	3.66	15.93	Obtained values
	9.22 – 25.3	1.71 – 2.5	68.2 – 81.87	16.42 – 18.5	19.8 – 21.41	[35–37]
CCF	12.15 ± 0.11	3.57 ± 0.08	73.07 ± 0.04	11.21	18.41	Obtained values
	9.65 – 10.1	3.2 – 5.56	69.35 – 75.5	11.2 – 15.44	14.67 -18.74	[38]

Table 6.
 Proximate analysis of the natural fibers.

CCF. This parameter is directly related to the dispersion of the fibers in a polymer matrix during the melting processing [39]. Higher moisture content causes lower dispersion of a lignocellulosic material in a polymer matrix. This effect can be related with the final properties of the obtained biocomposites. Also, CHF presented the highest volatile matter value. Volatile matter is related to the cellulose and hemicellulose percentage in the fibers. It is reported that hemicellulose influences the distance of interfibrillary cellulose, impacting fiber stiffness [40]. For that reason, a higher content of volatile matter represents a significant proportion of holocellulose in the fiber and represents higher toughness and a better fatigue behavior in the fiber [40]. Therefore, better results can be expected in the mechanical properties of a biocomposite obtained from CHF compared to a CCF-based biocomposite. The results show that the moisture content value in CCF is higher than the data presented by several authors [38, 41–43]. Also, CHF volatile matter content is higher in comparison with the values reported in literature [35–37]. On the other hand, ash, fixed carbon percentages, and calorific value lower of CHF are lower than the values reported in literature [35–37, 41, 43–45].

The elemental analysis values of the fibers are presented in **Table 7**. The results show that the carbon content in the CCF (53.88%) was higher in comparison with the reported values in literature, while the oxygen content was lower. On the other hand, CHF elemental analysis values are within the ranges established by other authors. Atomic ratios O/C and H/C obtained for CHF and CCF were 0.61, 0.54, 1.63, and 1.45, respectively. These results are in accordance with the values of biomass established in the Van Krevelen diagram [31]. The values of the O/C ratio obtained can be attributed to a high content of cellulose and hemicellulose in the biomass [3, 47]. This O/C relationship can be used as a parameter to evaluate the polarity of fibers in the production of biocomposites materials, being related to the content of hydroxyl groups. These groups are reactive centers of high polarity, which influence the formation of hydrogen bonds and the compatibility between fibers and a polymer [48]. For this reason, the O/C ratio allows to estimate the interaction degree between the lignocellulosic reinforcement and the polar polymeric matrix used [3], and its value is higher for CHF compared to CCF.

The structural compositions of the fibers are presented in **Table 8**. CHF presented a higher cellulose content (33.38%) compared to CCF (22.24%). Cellulose is considered as a semicrystalline biopolymer with a fibrous and rigid structure, which positively affects the stiffness in biocomposites materials [52]. Also, a greater amount of cellulose is related to better compatibility between the fibers and the polymeric matrix and a better mechanical performance of the biocomposite [53]. Regarding the lignin content, CCF shows a greater quantity (25.42%) compared to CHF (17.31%). This type of compound is considered as an amorphous polymer with chemical heterogeneity and a low physical consistency. Bajwa et al. [48] mentioned that increase in the lignin content decreases the mechanical resistance of thermoset biocomposites.

Natural Fiber	C (%)	H (%)	N (%)	O (%)	S (%)	Reference
CHF	50.72	6.88	1.07	41.27	0.06	Obtained values
	40.1–52.56	4.9–7.08	0–5.2	39.54–49.1	0–0.35	[35–37, 46]
CCF	53.88	6.51	0.68	38.84	0.08	Obtained values
	47.25–48.58	5.7–6.74	0–3.04	43.74–45.6	0	[38, 46]

Table 7.
Elemental analysis of the natural fibers.

Natural Fiber	Cellulose (%)	Hemicellulose (%)	Lignin (%)	Ashes (%)	Extractives (%)	References
CHF	33.38 ± 0.89	13.06 ± 0.60	17.31 ± 0.68	1.84 ± 0.06	34.42 ± 0.94	Obtained values
	29.17 – 35.4	18.2 – 28.96	22.35 – 23.2	1.4 – 4.6	17.67 – 21.8	[49, 50]
CCF	22.24 ± 1.46	15.62 ± 1.25	25.42 ± 0.81	3.71 ± 0.08	33.00 ± 0.28	Obtained values
	30.22 – 47.7	21.9 – 25.9	17.8 – 39.66	0.8 – 5.56	6.8 – 18.66	[8, 38, 51]

Table 8.
 Structural analysis of the natural fibers.

3.2 Characterization of the biocomposites

3.2.1 Mechanical properties

The influence of CHF, CCF fibers, and MAPP addition on the r-PP flexural and impact properties was evaluated. The tensile behavior of the materials is shown in **Figure 4**. **Table 9** presents flexural modulus, flexural strength, and impact strength values of the materials.

The results show that CHF and CCF fibers incorporation induce a significant improvement of flexural properties of r-PP. r-PP-CHF and r-PP-CCF biocomposites flexural modulus (FM) increased 97 and 13%, respectively, in comparison with r-PP. Although the FM values were improved in both biocomposites, the effect was sharper for r-PP-CHF. This can be explained with the structural analysis of the fibers (Section 3.1). The cellulose content is related to the oxygen proportion and is associated with the resistance degree of the fiber. In this sense, lignocellulosic materials with a higher oxygen content or a higher value in the O/C ratio will have a better mechanical performance [54–57]. CHF presented a higher cellulose content

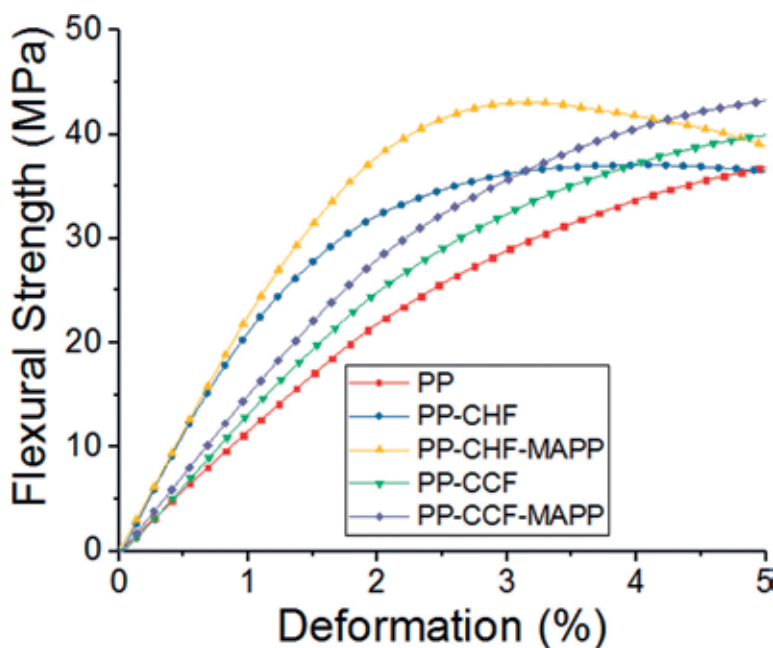


Figure 4.
 Average flexural stress vs. deformation of r-PP and r-PP biocomposites.

Sample	Flexural and impact properties [*]		
	Flexural properties		Impact properties
	Modulus (MPa)	Strength (MPa)	Impact strength (kJ/m ²)
r-PP	1193 ± 50 ^a	37.1 ± 1.7 ^a	11.5 ± 1.8 ^a
r-PP-CHF	2350 ± 71 ^b	37.2 ± 0.3 ^a	7.3 ± 0.4 ^b
r-PP-CHF-MAPP	2309 ± 114 ^b	43.1 ± 0.9 ^b	15.5 ± 1.3 ^c
r-PP-CCF	1349 ± 10 ^c	40.1 ± 0.7 ^c	10.7 ± 1.2 ^a
r-PP-CCF-MAPP	1351 ± 12 ^c	43.3 ± 0.4 ^b	16.5 ± 0.7 ^c

*a-c Different letters in the same column indicate significant differences ($p < 0.05$).
^{*}Mean of five replications ± standard deviation.*

Table 9.
Flexural and impact properties of r-PP and r-PP-natural fiber biocomposites.

in comparison with CCF (33.38 and 22.24%, respectively), which could explain the greater improvement in FM values with this fiber. It was also observed that MAPP addition did not generate significant differences ($p \geq 0.05$) on the FM values compared to r-PP-Fiber biocomposites.

On the other hand, CHF and CCF fibers addition generate slight improvements (1 and 8%) on the flexural strength (FS) compared to neat r-PP. These results agree with previous studies found in literature [58–60]. However, for both r-PP-fiber biocomposites, MAPP addition causes an increase in FS of 16% in comparison with r-PP.

Impact test results shows that CHF and CCF addition cause a decrease on the impact strength of 37 and 6%, respectively, in comparison with the r-PP. Similar results were reported by several studies about the morphology and mechanical properties of PP-natural fiber biocomposites [60–63]. However, for r-PP-CHF and r-PP-CCF, an increase on the impact strength of 35 and 44% was observed. This result shows that MAPP addition increases the capacity of r-PP to absorb energy. This phenomenon can be explained by a possible energy absorption promoted by fracture mechanisms, which involve detachment, slippage, and fragmentation of the fiber. Mechanisms are not present on the r-PP and r-PP biocomposites without MAPP.

The improvements in FS and impact strength with MAPP can be explained with the improved interfacial adhesion that MAPP caused. MAPP addition influences the chemical interaction between the hydrophobic matrix and the hydrophilic fiber through the formation of covalent bonds between the maleic anhydride groups and the hydroxyl groups present on the surface of the cellulosic fiber [57, 60]. In addition, Migneault et al. [55] mentioned that esterification reactions produced by the interaction between the natural fiber and the compatibility agent increase with the oxygen content of the fiber. Oxygen is directly related to the proportion of carbohydrates present in the surface of the fiber, creating a greater number of polar sites (hydroxyl groups) to react.

3.2.2 Thermal characterization

3.2.2.1 Differential scanning calorimetry (DSC)

DSC curves for r-PP and their biocomposites with CHF and CCF are shown in **Figure 5**. Numerical values of the thermal events are shown in **Table 10**.

The DSC cooling curve of r-PP (**Figure 5a**) shows a main exothermic peak located around 116°C corresponding to the crystallization of PP chains. When CHF, CCF, and MAPP were added into r-PP, a 3–6°C shift in the crystallization

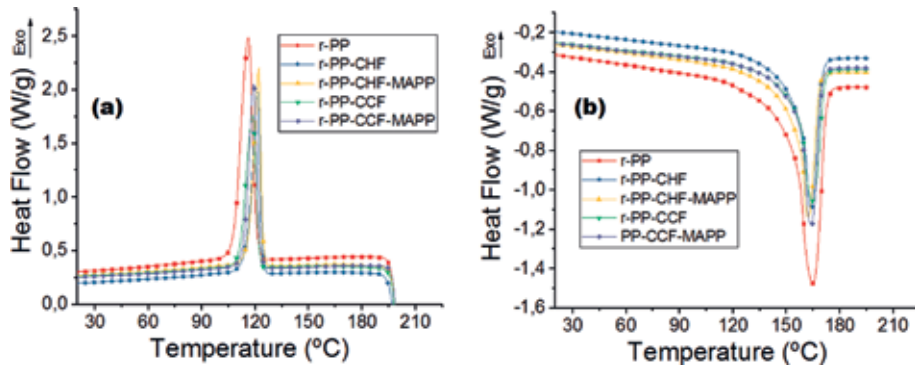


Figure 5.
 (a) Cooling and (b) second heating DSC curves for r-PP and r-PP biocomposites.

Sample	Cooling		Second heating	
	Tc* (°C)	Tm* (°C)	ΔHm (J/g)	χ (%)
r-PP	116	165	82	40
r-PP-CHF	121	164	64	44
r-PP-CHF-MAPP	122	162	63	44
r-PP-CCF	118	165	61	42
r-PP-CCF-MAPP	119	164	63	44

*Tc and Tm were taken at the maximum peak of crystallization and melting peaks.

Table 10.
 Thermal properties on cooling and second heating DSC scans of the samples.

temperature of r-PP was observed. This decrease indicates that natural fibers in biocomposites can act as a nucleation agent. The second heating runs of r-PP and r-PP biocomposites were shown in **Figure 5b**. All samples exhibit an endothermic peak between 162 and 165°C corresponding to the melting of the PP matrix. These results indicate that the addition of the CHF and CCF fibers does not disturb the melting processes of the PP matrix. Also, it is observed that PP crystallinity fraction melted during heating was 40%. For r-PP biocomposites, the crystalline phase content increases slightly up to 44%. These results show that CHF and CCF fibers promote the formation of crystalline phases in the r-PP present in the biocomposites. Some reports that were related to fiber-reinforced composites have found that the fibers act as nucleation points that increase the crystallinity of the polymer phase [64].

3.2.2.2 Thermogravimetric analysis (TGA)

TG and DTG curves were used to determine the thermal stability of coffee husk (CHF) and coir coconut fibers (CCF). The results are shown in **Figure 6**. Also, main thermal parameters obtained from these curves are summarized in **Table 11**.

As shown in TG curve (**Figure 6a**), fibers present three weight loss regions which are located around 60–100°C, 240–350°C, and 350–600°C. The first weight loss region below 100°C can be attributed to the evaporation of superficial water present in the sample, while the other regions might be associated with the decomposition of the fiber constituents. DTG curves (**Figure 6b**) show a first decomposition peaks at 299 and 284°C for CHF and CCF, respectively. These peaks correspond

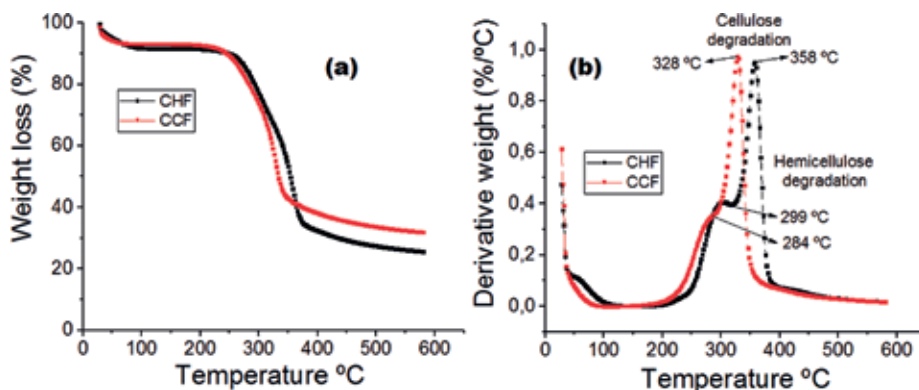


Figure 6.
(a) TG and (b) DTG curves of CHF and CCF fibers at heating rates of $10^{\circ}\text{C}/\text{min}$.

Sample	Degradation stage	To ($^{\circ}\text{C}$)	Tmax ($^{\circ}\text{C}$)	Residual Char (%)
Coffee husk fiber (CHF)	1	266	299	25
	2	336	358	
Coir coconut fiber (CCF)	1	245	284	31
	2	314	328	

Table 11.
Thermal degradation data of the fibers at $10^{\circ}\text{C}/\text{min}$ in nitrogen atmosphere.

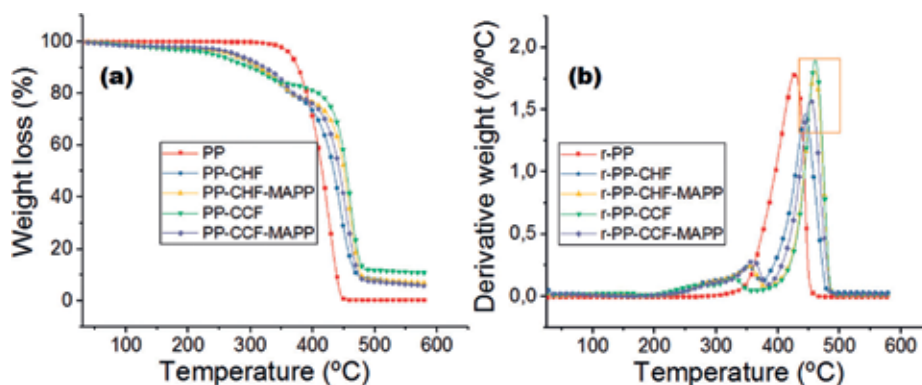


Figure 7.
(a) TG and (b) DTG curves of r-PP and r-PP biocomposites at heating rates of $10^{\circ}\text{C}/\text{min}$.

to the temperature of maximum weight loss rate (Tmax) of hemicellulose, while the second peaks located at 358°C and 328°C (for CHF and CCF) are related to the Tmax of α -cellulose. The residual weights of CHF and CCF have also been measured and are equal to 25 and 31% for CHF and CCF at 600°C . This results show that CHF possesses a better thermal stability compared to CCF.

TG and DTG curves for r-PP and r-PP biocomposites are shown in **Figure 7**. Also, main thermal parameters obtained from these curves are summarized in **Table 12**.

Recycled PP degradation occurs in a single step process with an onset temperature (To) located at 368°C and a Tmax of 428°C . The residue after final degradation was 0.4%. Regarding biocomposites, TG and DTG show that the addition of coffee husk and coir coconut fibers produces an increase in the thermal stability of the

Sample	Degradation stage	Tonset (°C)	Tmax (°C)	Residual Char (%)
r-PP	1	368	428	0.4
r-PP-CHF	1	260	354	8.4
	2	402	445	
r-PP-CHF-MAPP	1	264	355	8.2
	2	428	460	
r-PP-CCF	1	243	327	11.9
	2	427	460	
r-PP-CCF-MAPP	1	259	360	7.4
	2	411	453	

Table 12.
 Thermal degradation data of r-PP and r-PP biocomposites.

r-PP phase. As shown in **Table 12**, T_o increases between 34 and 60°C. Also, T_{max} increases between 33 and 28°C in comparison to r-PP (as indicates in the orange area). This increment in the thermal stability of the biocomposites has been previously observed in different studies, indicating that the incorporation of fibers in the material induces spherulite nucleation points, increasing the crystallinity of the polymer and improving its thermal properties [64].

3.2.3 Morphology

Figure 8a and **b** shows SEM images of the fractured surfaces of r-PP-CHF and r-PP-CCF, respectively. In these images, gaps between the fibers and the surrounding r-PP matrix can be clearly observed, which indicate a poor interfacial adhesion between the r-PP matrix and the natural fibers [65]. For **Figure 9a** and **b**, with the MAPP addition, gaps between natural fibers and r-PP were significantly reduced, and as a consequence, an improvement over the interface for the composite can be appreciated. This result confirms that MAPP addition improved the interfacial property of the hydrophobic PP matrix and the hydrophilic natural fibers. Also, this can be related with mechanical properties enhancement observed in the biocomposites after the MAPP addition.

3.2.4 Environmental characterization of the materials

When assessing the carbon footprint of the material, the stages of the life cycle were limited to raw material acquisition, transport, and processing. Since the

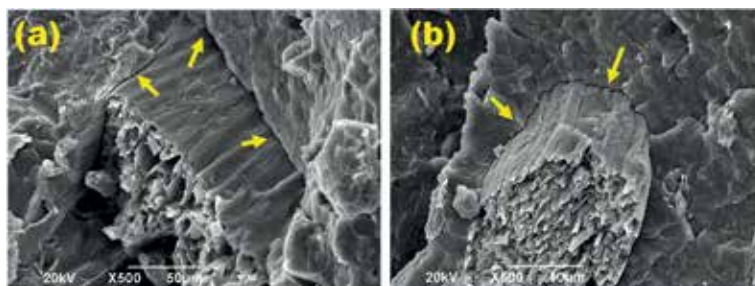


Figure 8.
 SEM pictures for rPP-CHF and rPP-CCF biocomposites.

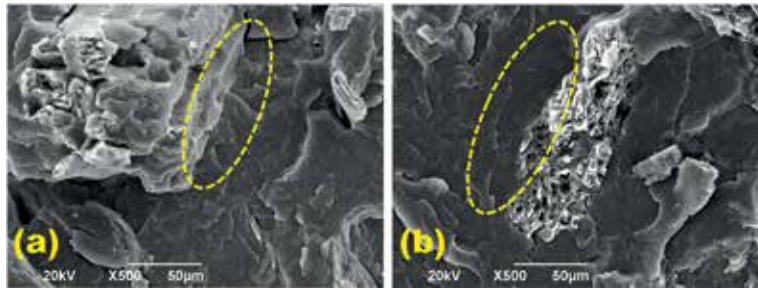


Figure 9.
SEM pictures for rPP-CHF-MAPP and rPP-CCF-MAPP biocomposites.

material was not transformed into a product, the functional unit was determined as the 1 kg of manufactured material and the carbon footprint was determined on a cradle to gate life cycle. The comparison was made between the biocomposite materials, recycled polypropylene, and neat polypropylene. Neat polypropylene was brought from Medellín 412 km away from the final user's location. Coffee husk was delivered from Tuluá (104 km) and coconut coir from Manizales (270 km). All the materials were transported on a diesel-powered truck to the final user location. Fibers were blended with the rPP matrix through an extrusion process and subsequently pelletized with a 1.5 kW mill.

Emissions were determined through emission factors for every activity involved on the elaboration of the material using the Eq. (14). For each emission factor, there is one activity related in order to calculate the emissions for the product elaboration. The results of those emissions are listed for each biocomposite on **Table 13**.

$$Emission = Emission\ factor * activity \quad (14)$$

From **Figure 10** emission accounting for each category, it could be noted that transport is the largest contributor to the overall emissions. Emissions on this stage are directly proportional to the amount of fuel used to transport the materials, and so, the further away the place, the greater the associated emissions. In order to achieve a more sustainable product, materials should be taken from regional suppliers to lower the footprint from transporting activities. Since rPP is produced inside the processing site, there is no emission associated to the transport of this material as stated on the life cycle boundaries for this particular case. Regarding raw material acquisition, the incorporation of natural fiber seems to improve the impact of the material compared to neat PP and recycled PP. For the coffee husk composite case, the carbon footprint on this stage for the 10 kg of material corresponds to 4.84 kg CO₂ eq, and for coconut coir biocomposite, it corresponds to 4.29 kg CO₂ eq. When compared to neat PP, a reduction in terms of carbon emissions of 76.93 and 73.78%, respectively, for rPP-CFH and rPP-CCH biocomposites. Also when compared to recycled polypropylene, it could be noted that emissions of rPP-CHF composite were slightly lower, reducing emissions on a 1.98%. Nevertheless, for rPP-CCF composite, the emissions raised on this stage on an 11.26% compared to rPP. In order to elaborate the composite, the fibers had to be blended with the recycled material, and so an extra process is needed as mentioned before. This extrusion and grinding process generates emissions of 4.54 kg CO₂ eq for both biocomposites, adding emissions to the overall score. For this scenario, the carbon footprint for the finished materials is shown on **Table 14**. This table shows the carbon footprint in terms of a functional unit defined as 1 kg of processed material.

rPP-CHF Biocomposite					
Stage	Material	Sub-stage	Emission factor	Activity	Emission
Raw material	Coffee husk	Production	0.52 kg CO ₂ /kg [66]	3 kg	1,56 kg CO ₂
		Grinding	0.374 kgCO ₂ /kWh [67]	0.55 kWh	0.21 kg CO ₂
		Transport	2.61 kgCO ₂ /L [68]	36.4 L	95.01 kg CO ₂
Processing	Biocomposite	Extrusion	0.374 KgCO ₂ /kWh [67]	10.6 kWh	3.98 kg CO ₂
		Grinding	0.374 KgCO ₂ /kWh [67]	1.5 kWh	0.56 kg CO ₂
Total					104.4 kg CO ₂
rPP-CCF Biocomposite					
Stage	Material	Sub-stage	Emission factor	Activity	Emission
Raw material	Coconut coir	Production	0.27 Kg CO ₂ /kg [70]	3 kg	0.81 kg CO ₂
		Grinding	0.374 kg CO ₂ /kWh [67]	1.1 kWh	0.41 kg CO ₂
		Transport	2.61 kg CO ₂ /L [68]	94.7 L	246.65 kg CO ₂
Processing	Biocomposite	Extrusion	0.374 kg CO ₂ /kWh [67]	10.6 kWh	3.98 kg CO ₂
		Grinding	0.374 kg CO ₂ /kWh [67]	1.5 kWh	0.56 kg CO ₂
Total					255.49 kg CO ₂
Recycled PP					
Stage	Material	Sub-stage	Emission factor	Activity	Emission
Raw material	Recycled PP	Process	0.38 kg CO ₂ /kg [68]	10 kg	3.80 kg CO ₂
		Grinding	0.374 kg CO ₂ /kWh [67]	1.5 kWh	0.56 kg CO ₂
Total					4.36 kg CO ₂
Neat PP					
Stage	Material	Sub-stage	Emission factor	Activity	Emission
Raw material	Neat PP	Process	1.86 kg CO ₂ /kg [71]	10 kg	18.60 kg CO ₂
		Transport	2.61 kg CO ₂ /L [68]	146.95 L	382.76 kg CO ₂
Total					401.36 kg CO ₂

Table 13.
 Results of the emissions for the compared materials.

3.3 Conclusions

Biocomposites based on recycled PP (r-PP) and two different natural fibers (coffee husk-CHF and coconut coir-CCF fibers) were prepared by a melt extrusion and injection processes. Proximate, elemental, and structural analysis performed to the natural fibers show that CHF contains a higher cellulose percentage and a higher ratio O/C in comparison to CCF. This condition makes CHF more attractive for biocomposites production. The effects of natural fibers and MAPP addition on the properties of the biocomposites were explored. Flexural characterization showed that MAPP incorporation induces a significant improvement of flexural properties

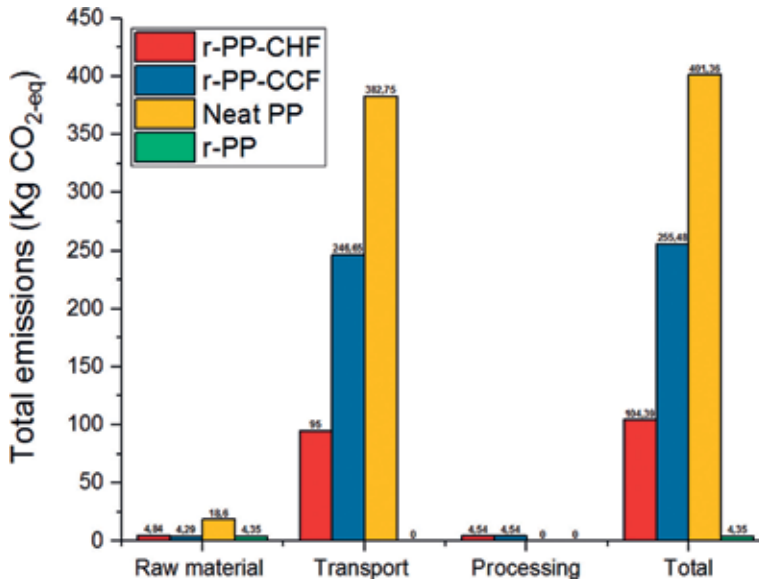


Figure 10.
Carbon emissions comparison for neat PP, r-PP, and r-PP biocomposites.

Material	Carbon footprint (kg CO ₂ eq/kg)
Neat Polypropylene	40.14
rPP-CHF	10.44
rPP-CCF	25.55
Recycled polypropylene	0.44

Table 14.
Carbon footprint of the compared materials.

of r-PP biocomposites. Also, the impact tests showed that the addition of MAPP increases the capacity of r-PP biocomposites to absorb energy. Thermal studies show that CHF and CCF fibers addition did not disturb the melting process and improves the thermal stability of the PP matrix. Despite that for this case scenario, the values of the carbon footprint for both biocomposites is considerably high compared to the recycled polypropylene, it is important to keep in mind that the evaluation was made on a cradle to gate analysis, this means that the benefits of the mechanical and thermal enhancements are not taken into account on this evaluation among the use and operational phases. Depending on the application, the use of these biocomposites has the potential to reduce the carbon footprint over the lifespan of a product made with it, saving emissions derived from usage and disposal. Regarding the performance of both biocomposites, it can be noted that rPP-CHF has a better operation regarding environmental issues due to the saved emissions from raw material transportation. This means that in order to elaborate more sustainable biocomposites, raw material should be delivered on a local extent. Also in order to lower the environmental impacts of the material, the fiber fraction is an important issue due to the replacement of polymer fraction over the composite and thus saving emissions from polymer primary elaboration process.

Acknowledgements

The authors acknowledge to the Universidad Autónoma de Occidente, Cali-Colombia and Universidad Nacional de Colombia, Manizales-Colombia for the technical and financial support.

Conflict of interest

The authors of this manuscript declare that do not hold any conflicts of interest that might have any bearing on research reported in their submitted manuscript.

Author details


Miguel Ángel Hidalgo-Salazar^{1*}, Juan Pablo Correa-Aguirre¹,
Juan Manuel Montalvo-Navarrete¹, Diego Fernando Lopez-Rodriguez² and
Andrés Felipe Rojas-González²

1 Research Group for Manufacturing Technologies GITEM, Universidad Autónoma de Occidente, Cali, Colombia

2 Investigation Group on Waste Recovery GIAR, Universidad Nacional de Colombia, Manizales, Colombia

*Address all correspondence to: mahidalgo@uao.edu.co

IntechOpen

© 2018 The Author(s). Licensee IntechOpen. This chapter is distributed under the terms of the Creative Commons Attribution License (<http://creativecommons.org/licenses/by/3.0>), which permits unrestricted use, distribution, and reproduction in any medium, provided the original work is properly cited. 

References

- [1] Amin FR, Khalid H, Zhang H, Rahman SU, Zhang R, Liu G, et al. Pretreatment methods of lignocellulosic biomass for anaerobic digestion. *AMB Express*. 2017;**7**(1):72. Available from: <http://www.ncbi.nlm.nih.gov/pubmed/28353158>
- [2] Leão RM, da Luz SM, Araújo JA, Christoforo AL, Leão RM, da Luz SM, et al. The recycling of sugarcane fiber/polypropylene composites. *Materials Research*. 2015;**18**(4):690-697. Available from: http://www.scielo.br/scielo.php?script=sci_arttext&pid=S1516-14392015000400690&lng=en&tlng=en
- [3] Sarasini F, Tirillò J, Zuorro A, Maffei G, Lavecchia R, Puglia D, et al. Recycling coffee silverskin in sustainable composites based on a poly(butylene adipate-co-terephthalate)/poly(3-hydroxybutyrate-co-3-hydroxyvalerate) matrix. *Industrial Crops and Products*. 2018;**118**:311-320. Available from: <https://www.sciencedirect.com/science/article/pii/S0926669018303005>
- [4] Abba HA, Nur IZ, Salit SM. Review of agro waste plastic composites production. *Journal of Minerals and Materials Characterization and Engineering*. 2013;**1**(05):271-279. Available from: <http://www.scirp.org/journal/doi.aspx?DOI=10.4236/jmmce.2013.15041>
- [5] Berto D, Rampazzo F, Gion C, Noventa S, Ronchi F, Traldi U, et al. Preliminary study to characterize plastic polymers using elemental analyser/isotope ratio mass spectrometry (EA/IRMS). *Chemosphere*. 2017;**176**:47-56. Available from: <https://www.sciencedirect.com/science/article/pii/S0045653517302783?via%3Dihub>
- [6] Ambientales UI de SC de E e I, Energética U de PMi, Instituto de Hidrología M y EAI. Atlas del potencial energético de la biomasa residual en Colombia. 2011; Available from: <https://bdigital.upme.gov.co/handle/001/1058>
- [7] Ebrahimi M, Caparanga AR, Ordonez EE, Villaflores OB. Evaluation of organosolv pretreatment on the enzymatic digestibility of coconut coir fibers and bioethanol production via simultaneous saccharification and fermentation. *Renewable Energy*. 2017;**109**:41-48. Available from: <https://www.sciencedirect.com/science/article/pii/S0960148117301933>
- [8] Lertwattanaruk P, Suntijitto A. Properties of natural fiber cement materials containing coconut coir and oil palm fibers for residential building applications. *Construction and Building Materials*. 2015;**94**:664-669. Available from: <https://www.sciencedirect.com/science/article/pii/S0950061815301823>
- [9] Conesa JA, Sánchez NE, Garrido MA, Casas JC. Semivolatile and volatile compound evolution during pyrolysis and combustion of Colombian coffee husk. *Energy & Fuels*. 2016;**30**(10):7827-7833. Available from: <http://pubs.acs.org/doi/10.1021/acs.energyfuels.6b00791>
- [10] de Carvalho Oliveira F, Srinivas K, Helms GL, Isern NG, Cort JR, Gonçalves AR, et al. Characterization of coffee (*Coffea arabica*) husk lignin and degradation products obtained after oxygen and alkali addition. *Bioresource Technology*. 2018;**257**:172-180. Available from: <https://www.sciencedirect.com/science/article/pii/S0960852418300488?via%3Dihub>
- [11] Manals-Cutiño EM, Salas-Tort D, Penedo-Medina M. *Tecnología Química*. Vol. 38. *Tecnología Química*. [publisher not identified]; 2018. pp. 169-181. Available from: <http://scielo.sld.cu/>

scielo.php?script=sci_arttext&pid=2224-61852018000100013

[12] ACOPLASTICOS. Plastics in Colombia [Internet]. 2018. Available from: <http://www.acoplasticos.org/index.php/mnu-nos/mnu-pyr/pec>

[13] CEMPRE-Colombia. National Study of Recycling and Recyclers: Approach to the Market of Recyclers and Experiences [Internet]. 2011. Available from: <https://cempre.org.co/documentos/>

[14] Alvarado K, Blanco A, Taquechel A. Fibra de coco: Una alternativa ecológica como sustrato agrícola. [Internet]. 2008; 3:30-31. Available from: http://www.actaf.co.cu/revistas/revista_ao_95-2010/Rev2008-3/

[15] Jaramillo Henao G, Zapata Márquez LM. Aprovechamiento de los residuos sólidos orgánicos en Colombia. instname Univ Antioquia [Internet]. 2008; Available from: <http://bibliotecadigital.udea.edu.co/dspace/handle/10495/45>

[16] Joseph K, Thomas S, Pavithran C. Effect of chemical treatment on the tensile properties of short sisal fibre-reinforced polyethylene composites. *Polymer (Guildf)*. 1996;**37**(23): 5139-5149. Available from: <https://www.sciencedirect.com/science/article/pii/S0032386196001449>

[17] Lin B-J, Chen W-H. Sugarcane bagasse pyrolysis in a carbon dioxide atmosphere with conventional and microwave-assisted heating. *Frontiers in Energy Research*. 2015

[18] Coutinho FMB, Costa THS, Carvalho DL. Polypropylene-wood fiber composites: Effect of treatment and mixing conditions on mechanical properties. *Journal of Applied Polymer Science*. 1997;**65**(6):1227-1235. Available from: <http://doi.wiley.com/10.1002/>

28SICI%291097-4628%2819970808%2965%3A6%3C1227%3A%3AAID-APP18%3E3.0.CO%3B2-Q

[19] La Mantia FP, Morreale M. Improving the properties of polypropylene-wood flour composites by utilization of maleated adhesion promoters. *Composite Interfaces*. 2007; **14**(7-9):685-698. Available from: <https://www.tandfonline.com/doi/full/10.1163/156855407782106500>

[20] Khalil HPSA, Rozman HD, Ahmad MN, Ismail H. Acetylated plant-fiber-reinforced polyester composites: A study of mechanical, hygrothermal, and aging characteristics. *Polymer - Plastics Technology and Engineering*. 2000; **39**(4):757-781. Available from: <http://www.tandfonline.com/doi/abs/10.1081/PPT-100100057>

[21] Hidalgo-Salazar MA, Correa JP. Mechanical and thermal properties of biocomposites from nonwoven industrial fique fiber mats with epoxy resin and linear low density polyethylene. *Results in Physics*. 2018;**8**: 461-467. Available from: <https://www.sciencedirect.com/science/article/pii/S2211379717322829>

[22] La Mantia FP, Morreale M. Green composites: A brief review. *Composites. Part A, Applied Science and Manufacturing*. 2011;**42**(6):579-588. Available from: <https://www.sciencedirect.com/science/article/pii/S1359835X11000406>

[23] AL-Oqla FM, Salit MS. *Materials Selection for Natural Fiber Composites*. London: Woodhead Publishing; 2017. 278 p

[24] Ashik KP, Sharma RS. A review on mechanical properties of natural fiber reinforced hybrid polymer composites. *Journal of Minerals and Materials Characterization and Engineering*. 2015; **3**(05):420-426. Available from: <http://>

www.scrip.org/journal/PaperDownload.aspx?DOI=10.4236/jmmce.2015.35044

[25] Väisänen T, Das O, Tomppo L. A review on new bio-based constituents for natural fiber-polymer composites. *Journal of Cleaner Production*. 2017; **149**:582-596. Available from: <https://www.sciencedirect.com/science/article/pii/S095965261730358X>

[26] Cheung WM, Leong JT, Vichare P. Incorporating lean thinking and life cycle assessment to reduce environmental impacts of plastic injection moulded products. *Journal of Cleaner Production*. 2017; **167**:759-775. Available from: <https://www.sciencedirect.com/science/article/pii/S0959652617319492>

[27] Pang M-M, Pun M-Y, Chow W-S, Ishak ZAM. Carbon footprint calculation for thermoformed starch-filled polypropylene biobased materials. *Journal of Cleaner Production*. 2014; **64**: 602-608. Available from: <https://www.sciencedirect.com/science/article/pii/S0959652613004873>

[28] Korol J, Burchart-Korol D, Pichlak M. Expansion of environmental impact assessment for eco-efficiency evaluation of biocomposites for industrial application. *Journal of Cleaner Production*. 2016; **113**:144-152. Available from: <https://www.sciencedirect.com/science/article/pii/S0959652615018338>

[29] Reinders MJ, Onwezen MC, Meeusen MJG. Can bio-based attributes upgrade a brand? How partial and full use of bio-based materials affects the purchase intention of brands. *Journal of Cleaner Production*. 2017; **162**:1169-1179. Available from: <https://www.sciencedirect.com/science/article/pii/S0959652617312969>

[30] Wall-Markowski CA, Kicherer A, Saling P. Using eco-efficiency analysis to

assess renewable-resource-based technologies. *Environmental Progress*. 2004; **23**(4):329-333. Available from: <http://doi.wiley.com/10.1002/ep.10051>

[31] Rojas González AF, Ruales Salcedo ÁV. Características energéticas de combustibles densificados de residuos de la uva isabella (*Viti labrusca* L.). *Rev Mutis*. 2016; **5**(2):5-15. Available from: <https://revistas.utadeo.edu.co/index.php/mutis/article/view/1069>

[32] Rowell RM, Young RA, Rowell JK. *Paper and Composites from Agro-Based Resources*. New York: CRC/Lewis Publishers; 1997. 446 p

[33] Sluiter A, Hames B, Ruiz CS, Sluiter J, Templeton D, DC. Determination of Structural Carbohydrates and Lignin in Biomass: Laboratory Analytical Procedure (LAP); Issue Date: April 2008; Revision Date: July 2011 (Version 07-08-2011) - 42618.pdf. Tech Rep NREL/TP -510-42618. 2008;(January): 1-15. Available from: <https://searchworks.stanford.edu/view/7616741>

[34] Wang Y, Fu Q, Li Q, Zhang G, Shen K, Wang Y-Z. Ductile-brittle-transition phenomenon in polypropylene/ethylene-propylene-diene rubber blends obtained by dynamic packing injection molding: A new understanding of the rubber-toughening mechanism. *Journal of Polymer Science Part B: Polymer Physics*. 2002; **40**(18):2086-2097. Available from: <http://doi.wiley.com/10.1002/polb.10260>

[35] Vassilev SV, Baxter D, Andersen LK, Vassileva CG. An overview of the chemical composition of biomass. *Fuel*. 2010; **89**(5):913-933. Available from: <https://www.sciencedirect.com/science/article/pii/S0016236109004967>

[36] de Oliveira JL, da Silva JN, Graciosa Pereira E, Oliveira Filho D, Rizzo CD. Characterization and mapping of waste from coffee and eucalyptus production in Brazil for

thermochemical conversion of energy via gasification. *Renewable and Sustainable Energy Reviews*. 2013;**21**: 52-58. Available from: <https://www.sciencedirect.com/science/article/pii/S1364032112007289>

[37] Ismail TM, Abd El-Salam M, Monteiro E, Rouboa A. Eulerian – Eulerian CFD model on fluidized bed gasifier using coffee husks as fuel. *Applied Thermal Engineering*. 2016; **106**:1391-1402. Available from: <https://www.sciencedirect.com/science/article/pii/S135943111631016X>

[38] Mythili R, Venkatachalam P, Subramanian P, Uma D. Characterization of bioresidues for biooil production through pyrolysis. *Bioresource Technology*. 2013;**138**:71-78. Available from: <https://www.sciencedirect.com/science/article/pii/S0960852413005543>

[39] Hietala M, Oksman K. Pelletized cellulose fibres used in twin-screw extrusion for biocomposite manufacturing: Fibre breakage and dispersion. *Composites. Part A, Applied Science and Manufacturing*. 2018;**109**: 538-545. Available from: <https://www.sciencedirect.com/science/article/pii/S1359835X18301453>

[40] Castellani R, Di Giuseppe E, Beaugrand J, Dobosz S, Berzin F, Vergnes B, et al. Lignocellulosic fiber breakage in a molten polymer. Part 1. Qualitative analysis using rheo-optical observations. *Composites. Part A, Applied Science and Manufacturing*. 2016;**91**:229-237. Available from: <https://www.sciencedirect.com/science/article/pii/S1359835X16303426>

[41] Jung S-H, Cho M-H, Kang B-S, Kim J-S. Pyrolysis of a fraction of waste polypropylene and polyethylene for the recovery of BTX aromatics using a fluidized bed reactor. *Fuel Processing Technology*. 2010;**91**(3):277-284.

Available from: <https://www.sciencedirect.com/science/article/pii/S037838200900321X>

[42] Kunwar B, Moser BR, Chandrasekaran SR, Rajagopalan N, Sharma BK. Catalytic and thermal depolymerization of low value post-consumer high density polyethylene plastic. *Energy*. 2016;**111**:884-892. Available from: <https://www.sciencedirect.com/science/article/pii/S0360544216307976>

[43] Li Q, Long Y, Zhou H, Meng A, Tan Z, Zhang Y. Prediction of higher heating values of combustible solid wastes by pseudo-components and thermal mass coefficients. *Thermochimica Acta*. 2017; **658**:93-100. Available from: <https://www.sciencedirect.com/science/article/pii/S004060311730268X>

[44] Azizi K, Keshavarz Moraveji M, Abedini NH. Simultaneous pyrolysis of microalgae *C. vulgaris*, wood and polymer: The effect of third component addition. *Bioresource Technology*. 2018; **247**:66-72. Available from: <https://www.sciencedirect.com/science/article/pii/S0960852417316085>

[45] Uzun BB, Yaman E. Pyrolysis kinetics of walnut shell and waste polyolefins using thermogravimetric analysis. *Journal of the Energy Institute*. 2017;**90**(6):825-837. Available from: <https://www.sciencedirect.com/science/article/pii/S1743967116301337>

[46] Galhano dos Santos R, Bordado JC, Mateus MM. Estimation of HHV of lignocellulosic biomass towards hierarchical cluster analysis by Euclidean's distance method. *Fuel*. 2018; **221**:72-77. Available from: <https://www.sciencedirect.com/science/article/pii/S0016236118302515>

[47] Jeguirim M, Limousy L, Fossard E. Characterization of coffee residues pellets and their performance in a residential combustor. *International*

Journal of Green Energy. 2016;**13**(6): 608-615. Available from: <http://www.tandfonline.com/doi/full/10.1080/15435075.2014.888664>

[48] Bajwa DS, Wang X, Sitz E, Loll T, Bhattacharjee S. Application of bioethanol derived lignin for improving physico-mechanical properties of thermoset biocomposites. *International Journal of Biological Macromolecules*. 2016;**89**:265-272. Available from: <https://www.sciencedirect.com/science/article/pii/S0141813016303944?via%3Dihub>

[49] Collazo-Bigliardi S, Ortega-Toro R, Chiralt BA. Isolation and characterisation of microcrystalline cellulose and cellulose nanocrystals from coffee husk and comparative study with rice husk. *Carbohydrate Polymers*. 2018;**191**:205-215. Available from: <https://www.sciencedirect.com/science/article/pii/S0144861718302789>

[50] Baêta BEL, Cordeiro PH de M, Passos F, Gurgel LVA, de Aquino SF, Fdz-Polanco F. Steam explosion pretreatment improved the biomethanization of coffee husks. *Bioresource Technology*. 2017;**245**: 66-72. Available from: <https://www.sciencedirect.com/science/article/pii/S0960852417314244>

[51] Dhyani V, Bhaskar T. A comprehensive review on the pyrolysis of lignocellulosic biomass. *Renewable Energy*. 2018;**129**:695-716. Available from: <https://www.sciencedirect.com/science/article/pii/S0960148117303427>

[52] Agustin-Salazar S, Cerruti P, Medina-Juárez LÁ, Scarinzi G, Malinconico M, Soto-Valdez H, et al. Lignin and holocellulose from pecan nutshell as reinforcing fillers in poly (lactic acid) biocomposites. *International Journal of Biological*

Macromolecules. 2018;**115**:727-736. Available from: <https://www.sciencedirect.com/science/article/pii/S014181301735064X>

[53] Tran D-T, Lee HR, Jung S, Park MS, Yang J-W. Lipid-extracted algal biomass based biocomposites fabrication with poly(vinyl alcohol). *Algal Research*. 2018;**31**:525-533. Available from: <https://www.sciencedirect.com/science/article/pii/S2211926416302995>

[54] Ayrilmis N, Kaymakci A, Güleç T. Potential use of decayed wood in production of wood plastic composite. *Industrial Crops and Products*. 2015;**74**: 279-284. Available from: <https://www.sciencedirect.com/science/article/pii/S0926669015300352>

[55] Migneault S, Koubaa A, Perré P, Riedl B. Effects of wood fiber surface chemistry on strength of wood-plastic composites. *Applied Surface Science*. 2015;**343**:11-18. Available from: <https://www.sciencedirect.com/science/article/pii/S0169433215005462>

[56] Arjmandi R, Ismail A, Hassan A, Abu BA. Effects of ammonium polyphosphate content on mechanical, thermal and flammability properties of kenaf/polypropylene and rice husk/polypropylene composites. *Construction and Building Materials*. 2017;**152**: 484-493. Available from: <https://www.sciencedirect.com/science/article/pii/S0950061817313880>

[57] Huang L, Mu B, Yi X, Li S, Wang Q. Sustainable use of coffee husks for reinforcing polyethylene composites. *Journal of Polymers and the Environment*. 2018;**26**(1):48-58. Available from: <http://link.springer.com/10.1007/s10924-016-0917-x>

[58] Lisperguer J, Bustos X, Saravia Y, Escobar C, Venegas H. Efecto de las características de harina de madera en

las propiedades físico-mecánicas y térmicas de polipropileno reciclado. *Maderas. Ciencia y tecnología*. 2013;**15** (ahead). Available from: http://www.scielo.cl/scielo.php?script=sci_arttext&pid=S0718-221X2013005000025&lng=en&nrm=iso&tlng=en

[59] Bledzki AK, Franciszczak P, Osman Z, Elbadawi M. Polypropylene biocomposites reinforced with softwood, abaca, jute, and kenaf fibers. *Industrial Crops and Products*. 2015;**70**: 91-99. Available from: <https://www.sciencedirect.com/science/article/pii/S0926669015001880>

[60] Nunes SG, da Silva LV, Amico SC, Viana JD, Amado FDR. Study of composites produced with recovered polypropylene and piassava Fiber. *Materials Research*. 2016;**20**(1):144-150. Available from: http://www.scielo.br/scielo.php?script=sci_arttext&pid=S1516-14392017000100144&lng=en&tlng=en

[61] Nourbakhsh A, Baghlani FF, Ashori A. Nano-SiO₂ filled rice husk/polypropylene composites: Physico-mechanical properties. *Industrial Crops and Products*. 2011;**33**(1):183-187. Available from: <https://www.sciencedirect.com/science/article/pii/S0926669010002554>

[62] Yang H-S, Kim H-J, Park H-J, Lee B-J, Hwang T-S. Effect of compatibilizing agents on rice-husk flour reinforced polypropylene composites. *Composite Structures*. 2007;**77**(1):45-55. Available from: <https://www.sciencedirect.com/science/article/pii/S0263822305001522>

[63] Yang H-S, Kim H-J, Son J, Park H-J, Lee B-J, Hwang T-S. Rice-husk flour filled polypropylene composites; mechanical and morphological study. *Composite Structures*. 2004;**63**(3-4): 305-312. Available from: <https://www>.

[sciencedirect.com/science/article/pii/S026382230300179X](http://www.sciencedirect.com/science/article/pii/S026382230300179X)

[64] Hidalgo-Salazar MA, Munõz MF, Mina JH. Influence of incorporation of natural fibers on the physical, mechanical, and thermal properties of composites LDPE-Al reinforced with fique fibers. *International Journal of Polymer Science*. 2015;**2015**:12-18

[65] Hidalgo-Salazar MA, Mina JH, Herrera-Franco PJ. The effect of interfacial adhesion on the creep behaviour of LDPE-Al-fique composite materials. *Composites. Part B, Engineering*. 2013;**55**:345-351. Available from: <https://www.sciencedirect.com/science/article/pii/S1359836813003430>

[66] Audsley E, Brander M, Chatterton JC, Murphy-Bokern D, Webster C, Williams AG. How low can we go? An assessment of greenhouse gas emissions from the UK foodsystem and the scope reduction by 2050. Report for the WWF and Food ClimateResearch Network. 2010; Available from: <https://dspace.lib.cranfield.ac.uk/handle/1826/6503>

[67] Factor marginal de emisión de gases de efecto invernadero del Sistema Interconectado Nacional para proyectos aplicables al Mecanismo de Desarrollo Limpio (MDL). 2014. Available from: https://www.icbf.gov.co/cargues/avance/docs/resolucion_minminas_91304_2014.htm

[68] Guía de cálculo de emisiones de GEI. Inicio. Generalitat de Catalunya [Internet]. 2017. Available from: http://canviclimatic.gencat.cat/es/reduex_emissions/com-calcular-emissions-de-geh/guia_de_calcul_demissions_de_co2/

[69] Turner DA, Williams ID, Kemp S. Greenhouse gas emission factors for recycling of source-segregated waste materials. *Resources, Conservation and Recycling*. 2015;**105**:186-197. Available

from: <https://www.sciencedirect.com/science/article/pii/S0921344915301245>

[70] Noponen MRA, Edwards-Jones G, Hagggar JP, Soto G, Attarzadeh N, Healey JR. Greenhouse gas emissions in coffee grown with differing input levels under conventional and organic management. *Agriculture, Ecosystems and Environment*. 2012;**151**:6-15. Available from: <https://www.sciencedirect.com/science/article/pii/S0167880912000345>

[71] Franklin associates. Cradle-to-Gate Life Cycle Inventory (LCI) of Nine Plastics Resins and Four Polyurethane Precursors - August 2011 [Internet]. 2011. Available from: <http://www.fal.com/projects.html>

*Edited by Gülşen Akın Evingür,
Önder Pekcan and Dimitris S. Achilias*

Thermosoftening Plastics are polymers that can be manipulated into different shapes when they are hot, and the shape sets when it cools. If we were to reheat the polymer again, we could re-shape it once again. Modern thermosoftening plastics soften at temperatures anywhere between 65 °C and 200 °C. In this state, they can be moulded in a number of ways. They differ from thermoset plastics in that they can be returned to this plastic state by reheating. They are then fully recyclable because thermosoftening plastics do not have covalent bonds between neighbouring polymer molecules. Methods of shaping the softened plastic include: injection moulding, rotational moulding, extrusion, vacuum forming, and compression moulding. The scope of this book covers three areas of thermosoftening plastics, thermoplastic materials, and their characterization. The following tests are covered in the book:

- thermal analysis (differential scanning calorimetry, heat deflection temperature test)
 - optical properties tests (fluorescence spectroscopy, UV spectroscopy)
- mechanical properties tests (thermogravimetry, rheometry, short term tensile test)

Published in London, UK

© 2020 IntechOpen

© Irina Vodneva / iStock

IntechOpen

ISBN 978-1-83880-614-9



9 781838 806149